UDK YU ISSN 0350-2368

Journal
for

TECHNOLOGY OF PLASTICITY

Volume 22 Number 1-2

Novi Sad, 1997

JTP, Vol.22 (1997), Number 1-2

Journal for Technology of Plasticity, Vol.22 (1997), Number 1-2

Publisher: Faculty of Technical Sciences
Institute for Production Engineering
Novi Sad - Yugoslavia

Editor: V. Vujović, Novi Sad, Yugoslavia

Editorial board:
A. Shabaik, Los Angeles, USA
P.I. Denisov, Russia
K. Novotny, Brno, Czech Republic
E. Wessely, Kosice, Slovakia
A. PLewinsky, Poznan, Poland
P. Popović, Niš, Yugoslavia
B. Devedžić, Kragujevac, Yugoslavia
V. Domazetović, Podgorica,Yugoslavia
D. Mandić, Beograd, Yugoslavia
M. Plančak, Novi Sad, Yugoslavia

Publishing of this journal has been financially supported by Ministry for Sciences and Technology of Republic of Serbia

CONTENTS

1. **ON THE PLASTIC PROPERTIES OF DAMAGED SHEETS**
Fülüp T., Tisza M. 1

2. **LUBRICATION AND THE CHOICE OF LUBRICANTS FOR DEEP-DRAWING**
Stefanović M., Aleksandrović S., Samardžić M 13

3. **THE ANALYTICAL METHOD OF DEFINING THE INFLUENCE OF MACHINING THE SURFACE OF THE WIRE UPON THE MINIMUM THICKNESS OF THE COATING OF THE WIRE AT DRAWING**
Ogarkov N.N., Nalimova M.V. 23

4. **HOT FORGING PROCESS ANALYSIS OF BRASS NUTS**
Stoiljković V., Randjelović S., Mijailović, V. 31

5. **AXISYMMETRICAL ELEMENT CONTOUR MODELLING AT DIE FORGING**
Janjić M., Vukčević M., Domazetović V., ... 39

6. **MATHEMATICAL MODELLING OF CALIBRATION PROCESS OF BARS FROM FREE CUTTING STEEL**
Denisov P.I., Zuev D.B., Beliaev A.I, Nekit R.V. 49

7. **COMPUTER SIMULATION SYSTEM OF HEAT PRODUCTION DURING EXTRUSION OF ALUMINIUM ALLOYS**
Petzov G., Markov V., Arsenov R. 57

8. **CONTACT STRESSES AND DEFORMATION LOAD IN UPSETTING OF CYLINDER BETWEEN SPHERICAL AND FLAT DIES**
Vilotić D., Plančak M., Vujović V., Milutinović M., Skakun P. 67

9. APPLICATION OF WORKABILITY DIAGRAM AND DISCONTINUOUS VELOCITY FIELDS TO FRACTURE ANALYSIS DURING METAL FORMING PROCESSES
Alexandrov S. 75

10. THE APPLICATION OF HILL'S METHOD TO THE ANALYSIS OF FORMING PROCESSES WITH DAMAGE EVOLUTION MODELS
Chikanova N. 93

Journal for Technology of Plasticity, Vol.22 (1997), Number 1-2

ON THE PLASTIC PROPERTIES OF DAMAGED SHEETS

Tibor Fülöp - Miklós Tisza
University of Miskolc, Department of Mechanical Engineering, Miskolc, Hungary
H3515 Miskolc - Egyetemváros

ABSTRACT

In this work an application of the yield functions determined by the PONTE CASTAÑEDA's variational principles will be presented. The yield constants for a general second order yield surface and for an orthotropic approximation will be calculated. This makes possible the study of the effect of void volume fraction and void shape on the formability of damaged sheets using existing finite element codes. Finally some of these new yield surfaces made for porous solids will be used to calculate the forming limit diagrams (FLD) of damaged materials. The results can be compared with the FEM models to evaluate the effect of the porosity – void volume fraction – and of the void shape on the formability of sheets.

1. INTRODUCTION

The prediction of the overall plastic properties of composite materials has been a problem of central interest for the last years. In order to analise the effect of the damage on the formability of heterogenous sheet materials, mainly two different approaches can be used. The first, known as Katchanov method [1], consists on the elaboration of a global criterion. Due to its limitations, recently considerable research was done on local approaches, like the continuum damage mechanisms.

By now, more knowledge is available on the characterisation of the effective properties of linear composite materials. Various homogenisation methods have been developed, like the variational principle of HASHIN and SHTRIKMAN, one of the most accepted linear model. A detailed review of other linear theories has been done by HASHIN [2]. As the materials having non-linear constitutive behaviour, for periodic microstructures the effective potentials can be bounded using some linear estimations, or, like the well-known GURSON model [3], a dilute estimate for porous materials can be calculated by generalisation of a self-consistent procedure. In the last six years a completely new way has been proposed by PONTE CASTAÑEDA [4] and WILLIS, based on new variational principles. A class of applications of these variational principles has been done to estimate limits for non-linear composites.

In the last three years models for composit materials having evolving microstructure have been also eladorated.

These new limits are generally based on the so called J_2 theory of the plasticity [5]. Their result is a second order yield surface. The prior variational statements were under the assumption of anisotropy for the constituent phases, however there are various possible anisotropic extensions of these non-linear constitutive models. Finally a class of the yield surfaces has been developed for different composites (materials having periodic or packed microstructures, containing voids, rigid or deformable inclusions). In order to use these models in the practical calculations (for example in the FEM applications) a generalisation of these yield functions seems to be adequate.

In this work the concept of this "*general*" yield criterion will be presented. As the application, the study of formability of damaged sheet metals will be done. The calculations are based on some of the new limits elaborated in the last five years for porous solids.

The FEM modelisation is a next practical application for the yield functions. In order to use the existing FEM codes without any modifications, an orthotropic approximation for the proposed "general" yield criterion will be presented. With this approximation the drawability of a cup will be evaluated.

Some of these new yield surfaces will be further used to calculate the forming limit diagrams (FLD) for materials containing microvoids. The formability of damaged materials has been recently evaluated by JEONG and PAN [6] for pressure sensitive matrix. Unfortunately their results are very complex to use, thus the earlier NEALE-CHATER [7] necking band bifurcation analysis seems to be a reasonable choice. This is based on the original Marciniak – Kuzy(ski model, and makes possible to calculate the effect of the porosity – void volume fraction – and of the void shape on the form of the FLD curve.

2. THE GENERAL YIELD SURFACE

2.1 Basic concepts

From a mathematical point of view, a yield function calculated by the new variational principles can be considered as a scalar function of the second order, symmetric stress tenzor □. The plasticity criteria must also satisfy the symmetry of material properties, and some further conditions may be the incompressibility or the insensitivity to the reverse loading (Baushinger effect). As it will be mentioned above, the new yield criteria based on the PONTE CASTAÑEDA's variational principles are originated from the so called J_2 theory [5], thus they can be described by a general quadratic yield equation. The basic properties of the yield criteria valid for porous solids are the sensitivity to the hydrostatic pressure, due to the presence of the micro-voids. Thus the quadratic yield functions elaborated for "classic", incompressible materials, can not be used in this case.

Mathematically, all of these new criteria can be described by a second order hyper-surface, in a 6 dimension stress space given by:

$$F(s,\sigma_y) = A_1\sigma_{11}^2 + A_2\sigma_{22}^2 + A_3\sigma_{33}^2 + A_4\sigma_{11}\sigma_{22} + A_5\sigma_{22}\sigma_{33} + A_6\sigma_{11}\sigma_{33} + A_7\sigma_{12}^2 + A_8\sigma_{23}^2 + A_9\sigma_{31}^2 = \sigma_y^2, \quad (1)$$

where $_y$ is the yield point of the material, and the A_i constants will be calculated for the special cases.

Some relation can be made between the constants A_i, required by the convexity of the above criterion. However in this part it will be used in the most general form, given by the following tensorial representation:

$$F(s,\sigma_0) = s : L : s \tag{2}$$

where L is a fourth order tensor, exhibiting the same symmetries as the Hook tensor, that is $L_{ijkl} = L_{klij} = L_{jikl} = L_{ijkl}$. The above equation gives an anisotropic material behaviour. The sensitivity on the hydrostatic pressure is also incorporated in the case of voided materials.

In our work an application of this concept of general yield surface will be presented for damaged materials having a periodic microstructure. The yield criteria calculated for different void shapes are presented in the APPENDIX.

The different yield constants can be evaluated by these yield criteria for different void shapes and void volume fraction (f). A graphical plot for these criteria is given in the **figure 1**. The most important behaviour of these yields functions is the dependence on the hydrostatic pressure, and the decrease of the yield point increasing the porosity.

2.2 Orthotropic approximation

The general form of the second order yield surface given above is valid for a great classe of composites. In the last five years different functions have been elaborated for damaged materials [4], for composites containing rigid inclusions [9] or grains with different orientartion [11]. Unfortunally it can not be used directly in the existing numerical codes. Hovewer their form is very similar to the form of the classical anisotropic yield function, elaborated by HILL in 1948. This yield criterion respect some conditions of symmetry, i.e. it have been elaborated for materials having an orthotropic symmetry. Actually this quadratic anisotropic yield criterion is one of the most generally inserted and used in the existing FEM codes. This gives the idea to use it for approximating the general yield function.

As it has been shown by DARRIEULAT and MONTHEILLET [12], the L yield tenzor, presented above can be uniquely decomposed in any coordinate system into the sum of an orthotropic and a symmetric tenzor:

$$L = L_o + L_{sym}, \tag{3}$$

Where L_0 is associated with orthotropic behaviour:

$$L_o = \begin{bmatrix} g+h & -2h & -2g & 0 & 0 & 0 \\ -2h & f+h & -2f & 0 & 0 & 0 \\ -2g & -2f & f+g & 0 & 0 & 0 \\ 0 & 0 & 0 & l & 0 & 0 \\ 0 & 0 & 0 & 0 & m & 0 \\ 0 & 0 & 0 & 0 & 0 & n \end{bmatrix} \tag{4}$$

and the constants are identified as the Hill's yield constants in the *48's* yield criterion:

$$F(s,\sigma_0) = f(\sigma_{22}-\sigma_{33})^2 + g(\sigma_{33}-\sigma_{11})^2 + h(\sigma_{11}-\sigma_{22})^2 + 2l\sigma_{23}^2 + 2m\sigma_{13}^2 + 2n\sigma_{12}^2 = \sigma_0^2 \tag{5}$$

Supposing, that the axes of the orthotropy are parallel with the axes of the principal stresses and comparing (5) with (1) it can easily be shown, that A_i are overdetermined. There are mainly two possibilities to calculate the values of the appropriate Hill constants using the A_i parameters. In fact, this approximation can be based on the values of $A_{5,6,7}$, or on $A_{1,2,3}$. It can be easily shown, than in our case the first approach is more adequate, and generally gives lower error. With this assumption the approximation will be the following:

Considering the equations:

$A_4 = -2h$; $A_5 = -2g$; $A_6 = -2f$,

one may obtained:

$$\begin{aligned} h+g &= -\frac{A_4}{2} - \frac{A_5}{2}; \\ f+h &= -\frac{A_4}{2} - \frac{A_6}{2}; \\ f+g &= -\frac{A_6}{2} - \frac{A_5}{2}. \end{aligned} \tag{6}$$

Finally, the equation (3) can be expressed in the next form:

$$L = L_o + L_{sym}\,, \tag{7}$$

where the two tensors are given in [15].

The approximation will be tested in the next part.

2.3 Validity of the approximation

In the equation (7) the first matrix gives the orthotropic approximation of L and the second one is the deviation from the orthotropic behaviour.

The matrix material - without micro-voids - is supposed to be orthotrop. Before continuing to evaluate the properties of damaged sheets using the proposed approximation, we must verify, that the material, in the domain of validity of yield criterion - for small porosities - is nearly orthotrop.

As first example the relative deviation in the spherical and cylindrical case have been calculated. We have supposed a porosity between zero and *0.2*, a value generally observed in conventional forming technologies [13]. The **figure 2** shows the relative deviation, defined by:

$$\omega_n = \frac{\|L_o\| - \|L_{sym}\|}{\|L_o\|} \tag{8}$$

where $\|\mathbf{L}\|$ is the norm of L. It can be shown, that the deviation is less than 5% for this porosities, whitch is sufficiently small to be accepted the orthotropic approximation.

Regarding the third yield criteria, we must verify the validity of approximation for different w void aspect ratios (defined on the **figure A1** in the APPENDIX). As it is shown at the **figure 3**, for $w \geq 0.5$, the approximation can be accepted, but it is not satisfied for smaller aspect ratios.

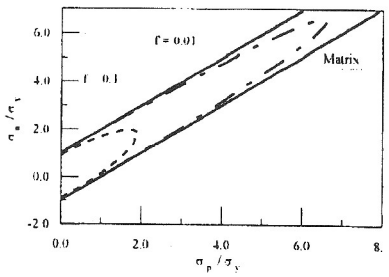


Figure 1
Effect of the porosity on the yield surfaces of damaged materials – spherical case

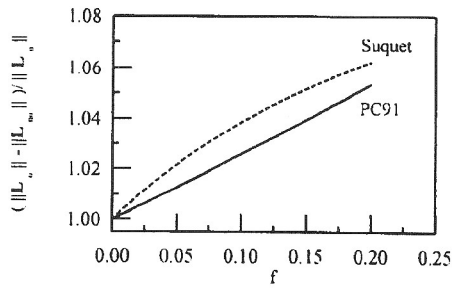


Figure 2
Normalized deviation from the orthotrop properties for the PC'91 and the Suquet criterion

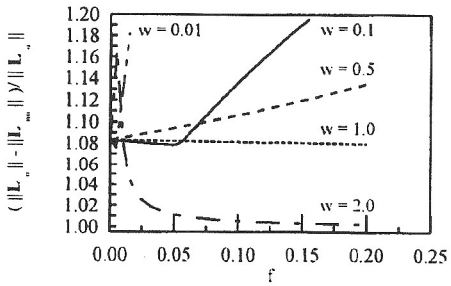


Figure 3
Normalized deviation from the orthotrop properties for the PC'94 criterion, for different aspect ratios

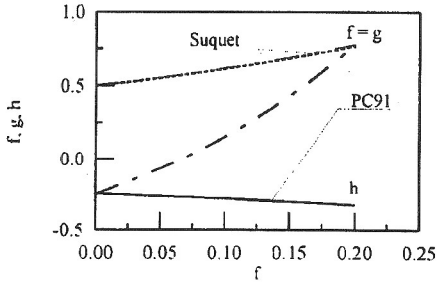


Figure 4
Value of orthotrop constants for the PC'91 and the Suquest criteria

We can conclude, than in the case of ellipcical voids a more fundamental research is required, using a sophisticated approximation. This can be done by optimization the symmetric deviation tenzor with respect of an angle in the plane of the sheet, as it have been proposed by BOEHLER [14].

Finally, in the **figure 4**, some values of orthotropic constants, expressed in the system of principal stress axes, are given. The study of the evolution of these constants in function of porosity, and the effect of the porosity on the sheet metal formability will be presented in the next part.

3. APPLICATIONS OF THE ORTHOTROP APPROXIMATION

The objective of this part is to give some few example for application of the orthotrop approximation for damaged materials. In this part the following suppositions will be used: the material is anisotrop, but the deviation from the orthotrop properties can be neglected. The void volume fraction is sufficiently small ($f \leq 0.3$) to be in the domain of the validity of Ponte Castañeda's variational principles.

3.1 Hill's parameters and Lankford number

As first application, the Lankford coefficient of materials will be calculated. In order to use a FEM modell to evaluate the formability of damaged sheets, the following constants should be also calculated.

The constants of anisotropy for different orientation respecting the axes of orthotropy (using the notation of (5) and [17]):

$$r_0 = \frac{h}{g};$$
$$r_{45} = \frac{1}{2}\frac{2n - f - g}{f + g}; \tag{9}$$
$$r_{90} = \frac{h}{f}.$$

Using the equation above, the Lankford coefficient can be defined by:

$$\bar{r} = \frac{1}{4}(r_0 + r_{90} + 2r_{45}) \tag{10}$$

In the **figure 5** the variation of r values is presented for two void geometry. The numerical calculations in the next part will be based on these constants. In the **figure 6** the same variation for elliptical voids is presented for different void shapes.

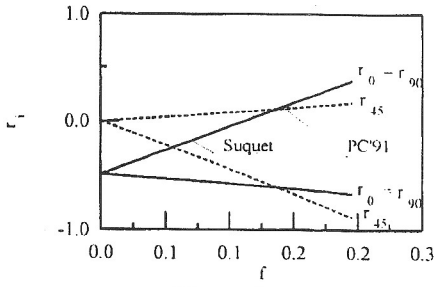


Figure 5

Variation of the coefficients of anisotropy on the sheet plane for PC'91 and Suquet materials

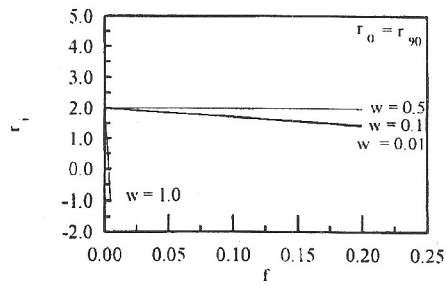


Figure 6

Variation of the coefficients of anisotropy on the sheet plane for PC'94 materials

The following question is the variation of the Lankford coefficient. This variation is the same for the different void shapes. The increse of the void volume fraction does not effect the value of the Lankford coefficient.

3.2 FEM study of porous sheet formability

The most important application of the orthotropic approximation made for the general yield law is its introduction to the finite element codes. This makes possible the evaluation of the formability of complex parts. The following calculation is based on (9), and we suppose, that the void volume fraction is constant during the calculation. For the calculus, we have used the Pam-Stamp™ FEM system.

In the **figure 7a and b** the effect of the void shape on the sheet thickness changes is presented. It is clearly seen, that the damage mode - witch influence the void shape - has a significant effect on the formability.

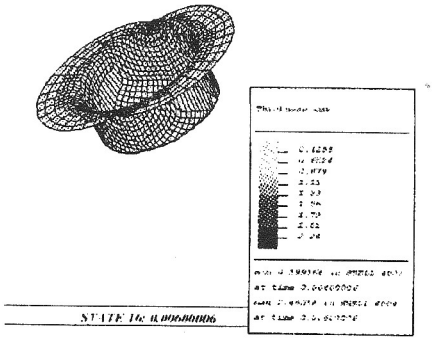


Figure 7a
Thickness distribution in a formed cup – PC'91 material

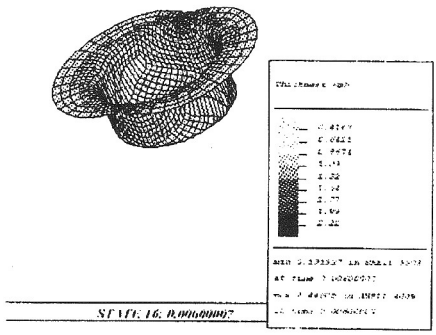


Figure 7b
Thickness distribution in a formed cup – Suquet material

4. APPLICATION OF THE GENERAL YIELD SURFACE - FLDs

The concept of the general yield surface is usefull for some numerical calculations. Instead of using a class of different yield criteria, we must introduce only one function, and calculate its constants for the special cases. In this part an example to this method of solution will be presented in order to determine the FLD for damaged materials.

4.1 Method of calculus

As it was mentioned in the Introduction, our work on FLDs is based on the Neale-Chater [7] analysis. The general form for quadratic yield surfaces is given by (1). From the flow theory a constitutive law can be derived. To incorporate the strain (n) and strain rate (m) dependence of the matrix, the following yield law will be assumed:

$$\sigma_e = k\varepsilon_e^n \dot{\varepsilon}_e^m$$

where **k** is a material constant.

Following the supposition of Marciniak - Kuzynski , initially a non-uniformity is assumed to exist in the form of a neck perpendicular to the major principal strain. Let this initial geometric non-uniformity be defined by . It can be connected to the presence of the surface rugosity [12] or to the initial contraction. Considering a sheet subjected to the proportional straining (which gives a lower FLD, than the assumption of the proportional stressing) and using the yield law, the following constant can be defined:

$$\rho = \varepsilon_2 / \varepsilon_1$$

where $_2$ and $_1$ are the strains measured in the homogeneous regions, outside the necking. The gouverning equation can be easily obtained for the yield law considered.

4.1 Results

The FLDs, using the governing equation has been calculated using the MapleV system [15].

In this section we analyze the effect of the porosity and the void shape on the FLDs.

The power-law hardening exponent have been taken to be n=0.1 and the value of strain rate sensitivity was supposed to be m=0.01 [6].

Analysing the constants of (1) yield law, we can show, that in case of zero porosity - f 0 - the material model leads to the original matrix properties. Increasing the porosity this constants will be increased. This means a more easy deformation, as it is shown in **figure 1**. Here also the dependence on the hydrostatic stress can be seen.

Concerning the effect of the void shape, it can be easily demonstrated, that the cylindrical voids are much more dangerous (higher yield constants), than the spherical ones. The importance of shape ratio can be seen for the elliptical form [16]. For more elongated voids - higher w - the dependence of the yield law on the porosity is more representative.

This yield function can be used to determine the FLD. The **Figures 8** and **9** gives some few examples of the effect of porosity and the void shape on the FLD curves.

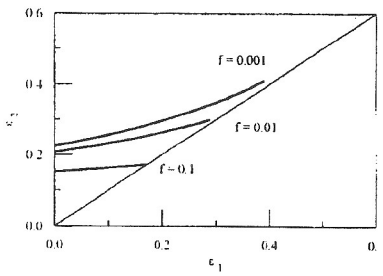


Figure 8
Effect of the porosity on the FLD for spherical case

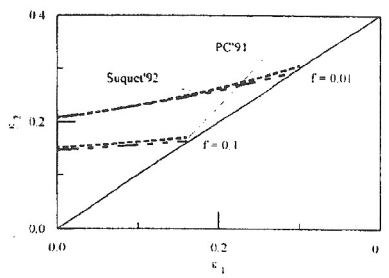


Figure 9
Effect of the void shape on the FLD – spherical (PC'91) and cylindrical (Suquet'92) case

Following the **Figure 8**, we can conclude, that the changes of the limit strains with increased porosity are adequate to the precedent results. The presence of higher porosity give a lower formability.

Similar results can be obtained using the Figure 9. The formability of a material containing cylindrical voids is smaller as compared to the material with spherical cavities. This can be explained by the values of the yield constants.

5. CONCLUSION

In the work above the concept and application of a "generalised" second order yield surface has been presented. Different applications have been elaborated to evaluate the sheet metal formability. We have obtained the following results:

1. The new yield surface can be directly used to evaluate the FLDs of composites. In this work the forming limit diagrams' have been elaborated for a class of materials, containing voids with different shape.
2. The orthotropic approximation of this general yield surface made possible their direct introduction to a FEM code, without any modification of the solver.
3. Concerning the microstructure of the composites, it can be seen that the formability of sheets is heavily influenced by the presence of the cavities. If the void volume fraction increases, the formability will decrease. This can be shown by the FLDs and by the FEM results.
4. The simple orthotropic approximation (with axes of the orthotropy parallel with the axes of the principal stresses) can be applied for materials containing spherical and cylindrical voids. For the elliptical shapes, a more sophisticated study should be used.

Finally a remark can be made concerning the basic assumption, that the void volume fraction is constant during the deformation. This assumption is not valid at high temperature, and it is also an approximation in cold forming. However, to take into account the changes of the microstructure, a program modification sholud be made, to incorporate the evolution of the yield surfaces into the FEM codes. This modification is the subject of a following part of our research work.

6. ACKNOWDLEDGEMENT

This work was partially supported of the Hungarian National Fundation for Scientific Research, under the contract No. F 019002, which is gratefully aknowledged.

7. REFERENCES

[1] LEMAITRE - CHABOCHE, *Méchanique des matériax solides*, pp. 343-444, Bordas, Paris, 1989

[2] HASHIN, *J.Appl.Mech.*, V50, pp.481-505, 1983

[3] GURSON, *J.Engng, Mater. Tech. Trans.* ASME, V90, pp.2., 1977

[4] PONTE CASTAÑEDA P., *J. Mech. Phys. Solids*, V40 No.8, pp.1757-1788, 1992
[5] BUDIANSKY, *J. Appl. Mech.*, 26, 259-264, 1959
[6] YEONG-PAN, *Int. J. of Solids and Structures*. V32 pp.3669-3693 , 1995
[7] NEALE-CHATER, *Int.J.Mech.Sci*. V22. pp.563-574, 1980
[8] PONTE CASTAÑEDA - ZAIDMAN, *J. Mech. Phys. Solids*, V42, No.9, pp.1459-1497, 1994
[9] PONTE CASTAÑEDA - ZAIDMAN, *Int. J. of Solids and Structures*. V33 pp.1271-1286 , 1996
[10] SUQUET, *J. Mech. Phys. Solids*, V41, No.6, pp.981-1002, 1993
[11] PONTE CASTAÑEDA , in CISM Cours and Lectures, Springer Verlag, Wien, 1996
[12] DARRIEULAT - MONTHEILLET, *Int. J. Mech. Sci.*, V38, No.12, pp. 1273-1284, 1996
[13] ZAVALIAGNOS-ANAND, *J. Mech. Phys. Solids*, V41, No.6, pp.1087-1118, 1993
[14] BOEHLER, in CISM Cours and Lectures 292, Springer Verlag, Wien, 1987
[15] http://irix.met.uni-miskolc.hu/~fulop/
[16] FULOP-TISZA, ICIT'97, Szlovenia, 1997
[17] CAILLET, in *Séminaire de Plasticité*, organized by J-L Chenot, Sophia Antipolis, Ch.3, pp29-33, 1994

8. APPENDIX

In this study, yield criteria based on the PONTE CASTAÑEDA's variational principles have been used. They are based on a micro-mechanical approach. In this method the first step is the calculation of the properties of an elementary cell containing an isolated microvoid, submitted to a loading compatible with the global forces. After the determination of the plastic properties of this elementary cell, the global properties of the material can be calculated [4]. In case of periodic distribution of heterogeneity, the effective properties of the nonlinear composite can be easily obtained. PONTE CASTAÑEDA has shown, that the damaged material behavior can be expressed in terms of the effective yield function, given by:

$$F(s) \geq \frac{Q[s, f, \ldots, \sigma_y]}{\sigma_y} - \sigma_y, \qquad (A1)$$

where $_y$ is the yield stress of the isotropic von Mises matrix.

In this work, the following expressions have been used for Q^2:

Spherical case - PC [4], - **fig. A1a**:

$$Q^2 = \sigma_e^2 + \frac{f}{1-f}\left(\frac{2}{3}\sigma_e^2 + \frac{9}{4}\sigma_m^2\right). \qquad (A2)$$

Cylindrical case - SUQUET [10] - **fig. A1b**:

$$Q^2 = \sigma_e^2 + \frac{f}{1-f}\left[4\sigma_p^2 + \sigma_n^2 + 6\left(\tau_p^2 + \tau_n^2\right) - 2\sigma_p\sigma_n\right] \qquad (A3)$$

Elliptical case - P-C - ZAIDMAN [8] - **fig. A1c**:

$$Q^2 = q_1\sigma_p^2 + \frac{1}{2}q_2\sigma_n^2 + q_3\tau_p^2 + q_1\tau_n^2 + 2q_5\sigma_p\sigma_n, , \qquad (A4)$$

where q_i are geometrical constants given in detail in [9].

In these equations the following notations have been used:

$$\sigma_p = \frac{1}{2}(\sigma_1 + \sigma_2), \ \tau_n = \sqrt{\sigma_{13}^2 + \sigma_{23}^2},$$

$$\sigma_n = \sigma_3, \ \tau_p = \sqrt{\sigma_{12}^2 + \frac{1}{2}(\sigma_1 - \sigma_2)^2}.$$

The equivalent and the hydrostatic stresses satisfies the relations:

$$\sigma_e^2 = (\sigma_p - \sigma_n)^2 + 3\tau_n^2, \text{ and } \sigma_m = (\sigma_n + 2\sigma_p)/3$$

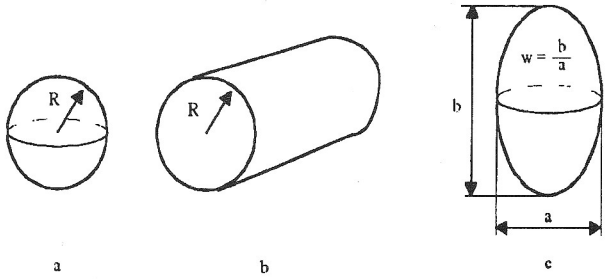


Figure A1
The void geometries used

PLASTIČNE KARAKTERISTIKE OŠTEĆENOG LIMA

Tibor Fülöp - Miklós Tisza
Univerzitet u Miškolcu, Odsek mašinstvo, Miškolc, Mađarska
H3515 Miskolc - Egyetemváros

REZIME

Određivanje karakteristika kompozitnih materijala je predmet intezivnih istraživanja već duži niz godina. U cilju analize uticaja stepena oštećenja na obradivost heterogenog lima može se koristiti Kačanova metoda koja elaborira globalne kriterijume, kao i homogenizovane metode (varijacioni principi Hašina i Štrinmana i dr.). U radu je prikazana primena funkcije naprezanja, određene na bazi Ponte Castanedas-avog varijacionog principa. Uveden je pojam generalizovane ravni naprezanja drugog reda. Na bazi toga određena je obradivost lima u raznim aplikacijama. Novouvedena ravan može se direktno koristiti u određivanju FLD kompozita. Ortotropska aproksimacija ove generalizovane ravni omogućava direktno implementaciju konačnih elemenata bez ikakvih modifikacija.

Zaključeno je da je obradivost lima u direktnoj zavisnosti od prisustva šupljina u materijalu. Povećanjem učešća šupljina obradivost opada. To je pokazano u FLD dijagramu i preko metode konačnih elemenata. Metoda prikazana u radu omogućava analizu materijala sa sferičnim i cilindričnim šupljinama. Za eliptične oblike šupljine potrebo je razviti dodatnu sofisticiranu metodu.

Journal for Technology of Plasticity, Vol.22 (1997), Number 1-2

LUBRICATION AND THE CHOICE OF LUBRICANTS FOR DEEP-DRAWING

M. Stefanović, S. Aleksandrović, M. Samardžić
Faculty of Mechanical Engineering, Kragujevac, Yugoslavia

ABSTRACT

The role and the importance of lubricants and lubrication in the process of metal forming are complex, and have been the object of many researches. In deep-drawing of thin sheets, the tribological conditions influence the forming process in a very complex manner and on equal terms with other elements of the forming system (machine, tool, material). The comments on the significance of the optimal choice of lubricant for deep-drawing, the methods and procedures for the evaluation of the technical quality of the lubricant are given in this paper. For two basic procedures of research, so called "complex " tribological models-stretching and pure deep-drawing-and many investigated lubricants, the results are given from different categories: limit relations in forming and presentation in forming limit diagram. The compared results for stainless and low-carbon steel sheets, in drawing of axis-symmetrical and square-section parts, are given.

1. INTRODUCTION

The right choice of lubricants in metal forming, especially in deep-drawing, includes implicitly that the role and importance of lubrication should be ragarded as equal as others elements of forming system. In selecting lubricant and a lubrication zone, the following demands must be fulfilled [1], [2]:

- the existance of the desired friction resistance in all part zones (control of metal-flowing);
- the decrease of metal to metal contact in critical zones, leading away of heat and the decrease of tool wear;
- obtainment of the desired quality of the part surface.

This should be completed by the characteristics of lubricants regarding the manner of application and the easiness of removing, coordination with the following forming process , protection from corrosion in parts storing, Fig 1.

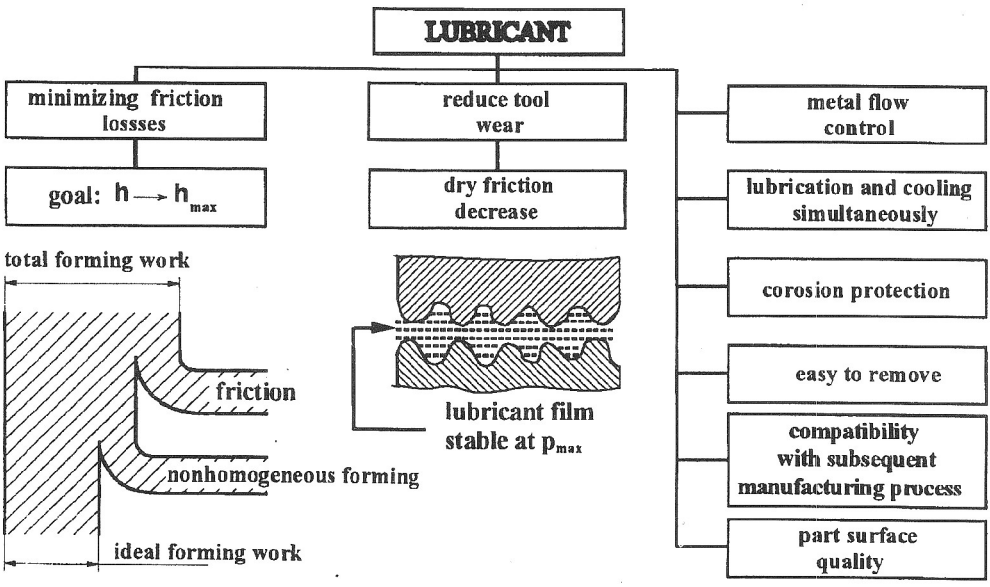


Fig.1. Schematic summary of the functions of a lubricant

It has long been recognized that, concerning the elements of complex geometry, in different zones, very different schemes of forming could exist: pure deep-drawing, stretching, bending with tension and so on. In tribological researches, these areas are described by special models [3].

The results of tribological researches, which are also partly related to the evaluation of the technological characteristics of lubricants for deep-drawing, can be basically divided into three groups. The first group includes physical indicators - friction force and coefficient, roughness parameters, etc, the second one includes macro indicators in forming - force and the depth of drawing, etc-and the third one includes the parameters of realized stress-strain fields - strain distribution, presentation in forming limit diagrams (FLD). The third group parameters are the most complete, but most difficult to be determined [4].

2. THE ELEMENTS IMPORTANT FOR THE CHOICE OF LUBRICANT

The specific tribological problems are also caused by different part dimensions, materials, sheet thickness and its surface characteristics. However, the basic form and type of forming have the greatest influence. It is particularly important to pay attention to the

interpretation of the effects of some forming types influence in cases when they occur at same time. The most important tribological influential factors are: the contact pressure in blank holder zone, the relative sliding speed, heating of parts, the intensity of heat transfer onto the tool, the quantity of lubricant etc.

The speed of sheet sliding in the contact zone of die and holder in deep-drawing is the same as the speed of press-slide, but it is considerably smaller in the case of stretching. The heat primarily develops in those part zones in which large deformations, increased speeds and high local pressures are achieved (for example, the zones which slide across the draw bead, etc). In this conditions of lubricative film interruption, well-known "galing" phenomenon and sheet and tool surface damage may occur.

The control of friction conditions in deep-drawing is most successfully achieved by using the lubricant which has the correct combination of shear strength and film thickness, wherefore the qualities of a lubricant in conditions of boundary lubrication are of particular significance. In such conditions, the lubricant must have the considerable film strength in order to prevent interruption and enable metal to metal contact. However, the certain sheare resistance in the lubricant layer is also necessary, in order to reduce the friction forces.

For example, in operations of deep drawing, the value of the total strain and strain distribution depends primarily on viscosity and lubricant stickness, and less on separately composed additions. At the high viscosity, the application of a lubricant can be problematic, and therefore the dry lubricative films can be problematic, and therefore the dry lubricative films can be used. The choice of lubricant in particular case depends on a part type-for example, parts with slight change of profile, or parts with strong change of form.

In ordinary deep-drawing, the difficulties occur when high pressures upon the blank holder are necessary, or when very precise outlines are being drawn. In such a case we must use the lubricant with special additions for high pressures or dry films with carefully controlled thickness.

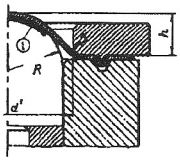
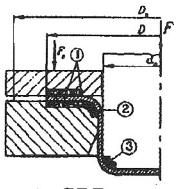
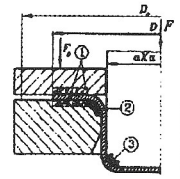
The particular problems appear in case of multi-operational deep drawing, long lasting storage, differential lubrication etc.

According to the Fig.1, it is practically impossible to give a simple universal rule for the selection of a lubricant because of many tribological factors and some other kinds of problems. The adequate literature offers some generally defined references to the lubricant selection, defined on the basis of the type of material being drawn, part geometry, manner of application, storage, cleaning etc [5].

3. EXPERIMENTAL DETAILS

In previous papers the thorough analysis of tribological models in deep-drawing has been performed, and systematic selection of important parameters has been conducted, according to the structure of outputs from some tribological researches. According to the degree of complexity, the defined tribological models are: basic - sliding of the thin sheet between the flat surface of die and holder, sliding by bending with tension across the die edge, sliding across the draw bead, and complex-two-sided stretching and pure deep-drawing [3]. Each of these models can be successfully used in the evaluation of lubricants, in correspondence with characteristics and aim of research.

Table 1

Models	Experimental Procedure				Indicators		
	mater.	lubricant	speed	geometry	force	depth	distribution
Stretching  STR	Č4580 Č0147	Lub.1 Lub.2 Polyeth. + oil Dry	20 mm/min	R=25 mm D_0=120 mm d_0=50 mm	$F_{FR.}$	$h_{FR.}$	$\varphi_1=f(loc.)$ $\varphi_1=f(\varphi_2)$ FLD
Pure deep-drawing  PDD	Č4580			D_0=100 mm p_H=4,27 MPa F_H=2,5 kN d_0=50 mm	F $F_{FR.}$	h $h_{FR.}$	$\varphi_3=f(loc.)$ $\varphi_1=f(\varphi_2)$ FLD
	Č0147			D_0=100 mm p_H=2,05 MPa F_H=1,2 kN d_0=50 mm			
Deep-drawing  DD	Č4580			D_0=90 mm p_H=6,9 MPa F_H=3 kN a=40 mm			
	Č0147			D_0=95 mm p_H=2,36 MPa F_H=1,2 kN a=40 mm			

For the evaluation of the influence of tribological conditions in deep drawing, the parameters of the third group are the most complete; they represent the " internal "indicators of the forming process, and in the course of determination of them, it is necessary to know the critical deformation zone. The parameters of this group are grapho-metrically determined, along with the knowledge of all elements of complex deformation analysis: strain distribution in critical section, the distribution in forming limit diagram (FLD), defining of elements of the deformation history, strain path etc.

The paper also includes some results of lubricants evaluation by complex tribological models: stretching, pure deep-drawing of axis-symmetrical piece and deep-drawing of the square section piece, according to the Table 1.

The lubricants selection has been performed by using two different groups of steel-sheets intended for the forming by deep-drawing: Č0147 (AKDQ)-low-carbon steel-sheet and Č4580 (AISI 304)- stainless steel-sheet. The characteristics of these materials are given in the Table 2.

Table 2

Material	R_P [Mpa]	R_M [MPa]	R_P/R_M -	A_{80} %	n -	r -
Č0147	220,9	321,8	0,69	37	0,22	1,407
Č4580	309,2	655,8	0,47	33,6	0,351	1,017

Many lubricants for deep-drawing from different manufacturers have been investigated; here results are given for two best samples (Lub.1 and Lub.2). The cases of completely clean surfaces (dry) and the usage of polyethylene foil with lubricant (Polyeth.+oil). have been taken as special cases. In course of investigation by stretching, only the zone under the punch is being lubricated, whereas in deep-drawing the annular surface in both holder and die zone is being lubricated.

The basic and oldest criterion of formability in stretching-the biggest fracture depth, can also be used in quantitative evaluation of lubricant which is being used. In course of that, there are often no important differences in the fracture forces. However, deformation analysis provides a considerably better approach in the interpretation of the results. Strain distribution in main sections with ordinary presentation in the system of main line strain represents the basic of such analysis. Quantification in the evaluation of the distribution forms is enabled by the characteristic indicators of strain distribution at the limiting or common forming depth, such as distribution gradient in critical zone, coefficient of distribution favourableness, the reserve of plasticity [6], the pick locality and the width of necking zone etc [7].

4. RESULTS AND DISCUSSION

In Fig.2 and Fig.3, the depths in the course of fracture and adequate main strain distributions for different experimental conditions, are given. in order to achieve better lubrication, the deformation should be homogeneous, with the rupture place near the piece pole.

The connection between achieved deformations and those ones which are possible to the utmost, with many strain paths, is shown by the distribution in forming limit diagram. In the course of that, the other main tangential deformation is being taken into consideration, and it highly influences the value of the major deformation, Fig. 4 and Fig. 5.

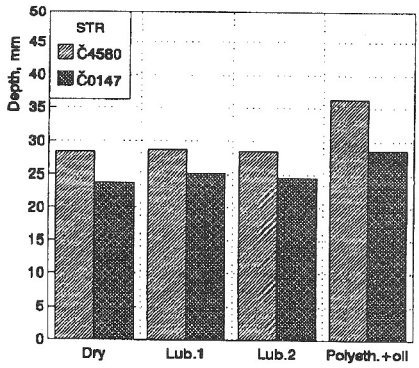


Fig.2. Drawing depth in stretching

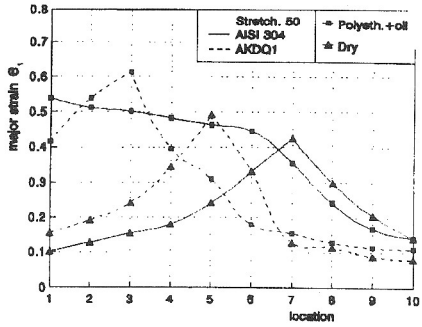


Fig.3. Strain distribution in different contact conditions

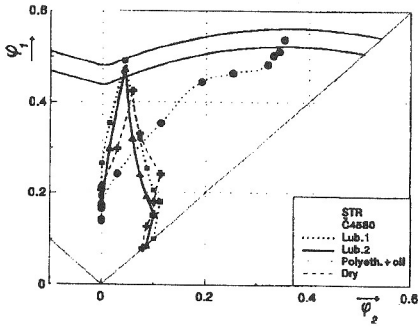


Fig.4. Strain distribution in FLD for Č4580

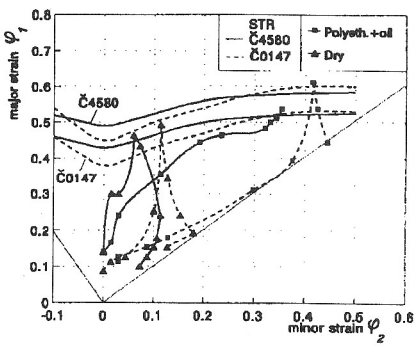


Fig.5. Strain distribution in FLD

The deformation force and the achieved depth with high values of limiting drawing ratio are the classic indicators of the influence of friction in pure deep-drawing. The achieved drawing forces in different contact conditions, according to the experimental conditions in Table 1, are given in Figure 6. Comparative distributions for different materials, contact conditions and tribological models are given in Fig.7 and Fig.8. Big differences in quality of examined materials influence the obvious differences in the influence of tribological conditions on the piece flange. Material C.0147 does not grow harder intensively as stainless does, and therefore the localization zone becomes narrower and restricted to the fields nearest to rupture place. High deformation gradients and high degrees of major deformations are thus achieved, but the realized fracture depth is smaller.

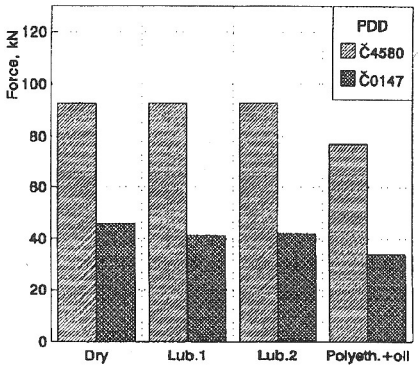


Fig.6. The biggest forces in drawing of ∅50

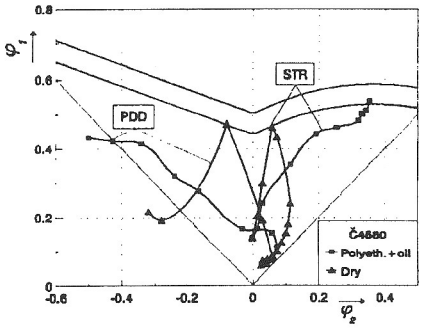


Fig.7. Strain distribution in FLD for Č4580

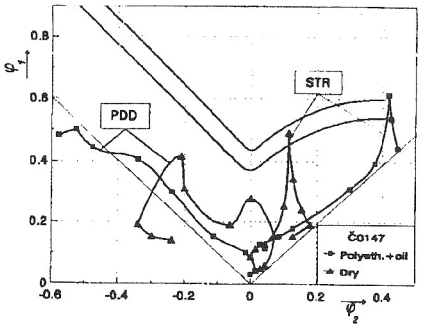


Fig.8. Strain distribution in FLD for Č0147

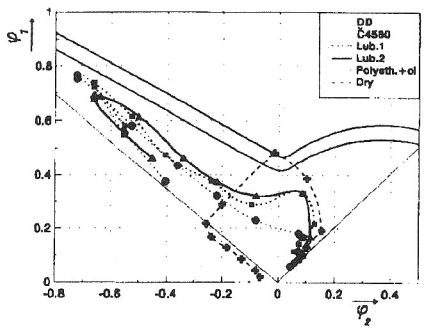


Fig.9. Strain distribution in FLD for Č4580

Distribution in deep-drawing square pieces 40x40 are given in Figures 9 and 10, and distribution in drawing axis-symmetrical piece ∅50 with flat punch are given in Fig.11. In such drawing conditions, localization occurs on the place of rounding of punch, in conditions when $\varphi_2=0$.

According to Fig.9, fracture appears in case of unlubricated contact surfaces. However, when using both lubricants, high degrees of deformation are achieved, in course of which unstable deformation may occur. At the same time, this is the zone of intensive thinning.

According to Fig.11, with regard to high values of holder pressure (p_H=4,27 MPa) , the drawing is possible only in conditions of lubrication by foil.

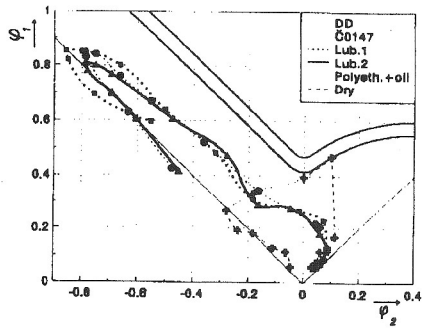


Fig.10. Strain distribution in FLD for Č0147

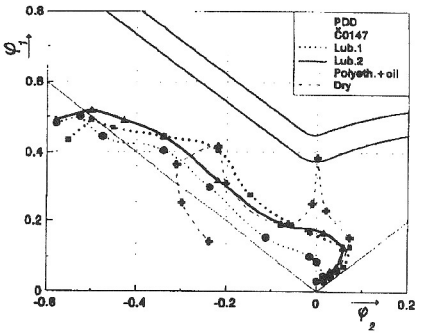


Fig.11. Strain distribution in FLD for Č0147

5.CONCLUSION

Complex tribological models of deformation and deep-drawing, can be successfully used in the evaluation of technological qualities of lubricants for deep-drawing, and they are the most complete indicators of deformation analysis. The applied methodology is efficient even in the conditions of more difficult lubrication which exists in forming of stainless steel-sheets.

Besides the usual indicators for this kind of research, the elements of deformation analysis with presentation in forming limit diagram are given too. The extreme importance of conditions for lubrication in realization of so called " complex " tribological models for different kinds of steel-sheets for deep-drawing, is pointed out.

There is no significant difference between the examined lubricants, while the Lub.1 lubricant is of much higher viscosity and its application is more difficult. Investigations in production conditions, the results of which are not given here, besides the analogous deformation analysis also include the tests of storing, stability at increased speeds and temperatures, the possibility of easy cleaning, etc.

6. REFERENCES

[1] FUNKE. P.: *Criteria Governing the Selection of Lubricantes for Sheet Metal Forming, Blech Rohre Profile, 27, 1980, 394-398.*

[2] DABROVSKI J. R., ADAMUS J., GIERZINSKA-DOLNA M.: *The Investigation of Lubricants for Sheet Metal Working, 10th Int. Coloq., TA Esslingen, 1996., 2439-2445.*

[3] STEFANOVIĆ M., ALEKSANDROVIĆ S.: *Complex approach to tribo-modelling in deep drawing of thin sheets, Balkantrib 96, Thessaloniki, 1996., Proceedings, 214-221.*

[4] STEFANOVIĆ M., ALEKSANDROVIĆ S.: *Importance of Strain Analysis in Tribo-Modelling in Deep Drawing, 1st World Tribology Congress, London, 1997, Abstract of papers, pp. 626.*

[5] SHEET METAL INDUSTRIES YEAR BOOK, 1975/76, pp. 129-134.

[6] STEFANOVIĆ M.: *Tribology of Deep Drawing, Yugoslav Tribology Association, Kragujevac, 1994, (in Serbian).*

[7] SCHEDIN E., MELANDER A.: *On the Strain Distribution During the Stretch-Forming of Low and High-Strength Steels, Journal of Mechanical Working Technology, 15 (1987) 181-202.*

PODMAZIVANJE I IZBOR MAZIVA ZA DUBOKO IZVLAČENJE

Stefanović M., Aleksandrović S., Samardžić M.
Mašinski fakultet u Kragujevcu, Jugoslavija

REZIME

Uloga i značaj maziva i podmazivanja u procesima plastičnog deformisanja metala su složeni i predstavljaju predmet brojnih istraživanja. Pri dubokom izvlačenju tankih limova, triboloski uslovi na izuzetno kompleksan način utiču na proces deformisanja, ravnopravno sa uticajem ostalih elemenata obradnog sistema (mašina , alat, materijal). U radu se komentariše značaj optimalnog izbora maziva za duboko izvlačenje, pokazuju metode i postupci za ocenu tehnoloških kvaliteta maziva. Za dva osnovna postupka ispitivanja (tzv. "složeni" tribo-modeli)-razvlačenje i čisto duboko izvlačenje i više ispitivanih maziva, navode se rezultati iz različitih kategorija: granični odnosi pri oblikovanju i prikazi u dijagramu granične deformabilnosti. Posebno se daju uporedni rezultati za nerđajuće i niskougljenične čelične limove, pri izvlačenju osnosimetričnih i komada kvadratnog preseka.

Journal for Technology of Plasticity, Vol.22 (1997), Number 1-2

THE ANALYTICAL METHOD OF DEFINING THE INFLUENCE OF MACHINING THE SURFACE OF THE WIRE UPON THE MINIMUM THICKNESS OF THE COATING OF THE WIRE AT DRAWING

Ogarkov N.N., Nalimova M.V., Mining and Metallurgical Academy, Magnitogorsk, Russia

ABSTRACT

The analytical method of defining the influence of machining the surface of the wire upon the minimum thickness of the coating of the wire at drawing is presented in this paper. Dependences of coating thickness on form of machining, roughness of the surface coefficient of friction were noticed. The formula for determination of coating metal consumption of minimal thickness was made. The analytical dependences allow to estimate the quaranteed minimal coating on the stage of making design for technological process of drawing.

1. INTRODUCTION

When one draws the wire with coating the problem is to ensure good coating at the minimum of it's waste. The influence of such factors as the degree of deformation, the time of the yield of the core and the coating, the coefficient of friction and the angle of the die, upon the thickness of the coating was studied in the articles [1,2,3,4,5].

2. CONTENTS

In this research we tried to work out the analytical method of defining the critical thickness of the coating and took into consideration the condition on the surface of the drawn

wire.The basis of the analysis was supposed to be the assumption that the quality of the contact of the core and coating is determined by the surface roughness.We know that the determination of the thickness of the covering during the contact of rough bodies under weak load may be taken from the following dependence [6]:

$$\Delta_{cr} = \left[\left(2NR^{\nu}{}_{\max} / \bar{\sigma} A_a b \right)^{1/\nu} r(1-2\mu) \right]^{1/2}, \tag{1}$$

where N — the ultimate load carried by the surface;
R_{max} — the height of the highest microunevenness;
$\bar{\sigma}$ — the average real contact stress;
A_a — the nominal area of the contact microunevennesses;
b, ν — the coefficient and index of the degree of the supporting surface curve;
r — the average radius of microunevennesses;
μ — the coefficient of friction.

To work out the formula (1) only the beginning of the supporting curve, described by the dependence $t_p = b\varepsilon^{\nu}$ was used. Consequently,the application of the formula to great loads typical for drawing leads to numerous errors.

The formula (1) was acquired with the use of correlation between load N and the area of real contact A_r as $N = \bar{\sigma} A_r$. Using the dependence between the real and nominal areas of the contact as $A_r = A_a t_p$, it may be rearranged to the form:

$$\Delta_{cr} = \left[\left(\frac{2R_{\max} t_p}{b} \right)^{1/\nu} r(1-2\mu) \right]^{1/2}. \tag{2}$$

In accordance with the results of the work [7] it is advisable to determine the parametre t_p

within the range $0 < \varepsilon \le (1/b)^{1/(\nu-1)}$ $t_{p1} = b\varepsilon^{\nu}$; (3)

within the range $(1/b)^{1/(\nu-1)} < \varepsilon \le 1$ $t_{p2} = 1 - \dfrac{(1-\varepsilon)^{\nu}}{\left[1 - (1/b)^{1/(\nu-1)} \right]^{\nu-1}}$, (4)

where ε is the relative approach of surfaces.

Taking into consideration that we deal with close and free contacts at drawing, it is easier to make the calculations using the average integral values of t_{pm} :

for $b \le 1$ $t_{pm} = \dfrac{b}{\nu+1}$; (5)

for $b > 1$ $t_{pm} = \dfrac{1}{\nu+1}\left(\dfrac{1}{b}\right)^{2/(\nu-1)} + 1 - \left(\dfrac{1}{b}\right)^{1/(\nu-1)} - \dfrac{1}{\nu+1}\left[1 - \left(\dfrac{1}{b}\right)^{2/(\nu-1)} \right]^{2}$. (6)

3. EXAMPLES

The values of t_{pm} for different forms of machining the surfaces, which were found with the help of formulae (5) and (6) are given in the Table.1:

Table.1

Form of machining the surfaces	R_{max}, mkm	b	ν	t_{pm}
Grinding	9,37	0,6	2,0	0,2
	4,72	0,9	1,95	0,305
	2,40	1,3	1,90	0,424
	1,20	2,0	1,50	0,55
Turning	37,5	1,0	2,1	0,322
	18,75	1,4	1,9	0,442
	9,37	1,8	1,8	0,506
	4,72	2,0	1,6	0,545
Polishing	4,72	2,0	1,7	0,533
	2,4	2,5	1,6	0,566

The consumption of coating metal for different forms of machining the surfaces can be calculated with the help of cross-section area of the wire and including the microrelief of the surface.

The section area of the coating is found with the help of the following dependence (Fig.1):

$$S_{all} = \frac{\pi}{4}\left(D^2_{wire} - d^2_{in}\right) + \frac{\pi\left(2d_{in} + R_{max}\right)^2}{16} R_{max}(1 - t_{pm}) \qquad (7)$$

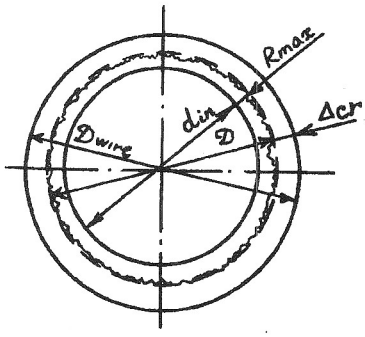


Fig. 1

The formula (7) indicates that the cross-section area of the wire is influenced by the quantity of roughness (R_{max}), the form of machining the surface (t_p) and the technological parametres of drawing as well.

Applying this problem to the drawing of bimetallic Steel-Cu wire with the diameter of 1,29 mm and the diameter of the core equal to 1,224 mm for the surfaces with different forms of preliminary preparation of the core, we get the following values (Table 2).

Form of machining the surfaces	R_{max}, mkm	μ=0				μ=0,4			
		Δ_{cr}, mkm	$S_{\Delta cr}$, mm^2	$S_{hollows}$, mm^2	S_{all}, mm^2	Δ_{cr}, mkm	$S_{\Delta cr}$, mm^2	$S_{hollows}$, mm^2	S_{all}, mm^2
Grinding	9,37	7,82	0,0303	0,0089	0,0392	3,50	0,0135	0,0089	0,0224
	4,72	6,81	0,0263	0,0039	0,0302	3,04	0,0117	0,0039	0,0156
	2,40	6,19	0,0239	0,0016	0,0255	2,77	0,0107	0,0016	0,0123
	1,20	4,83	0,0186	0,0006	0,0192	2,15	0,0083	0,0006	0,0089
Turning	37,5	21,37	0,0836	0,0308	0,1144	9,56	0,0370	0,0308	0,0678
	18,75	17,18	0,0670	0,0125	0,0795	7,68	0,0297	0,0125	0,0422
	9,37	15,12	0,0588	0,0055	0,0643	6,71	0,0259	0,0055	0,0314
	4,72	13,33	0,0518	0,0025	0,0543	5,91	0,0228	0,0025	0,0253
Polishing	4,72	27,41	0,1077	0,0026	0,1103	12,26	0,0476	0,0026	0,0502
	2,40	25,66	0,1007	0,0012	0,1019	11,47	0,0445	0,0012	0,0457
	1,20	19,32	0,0754	0,0001	0,0755	8,64	0,0334	0,0001	0,0335

4. CONCLUSION

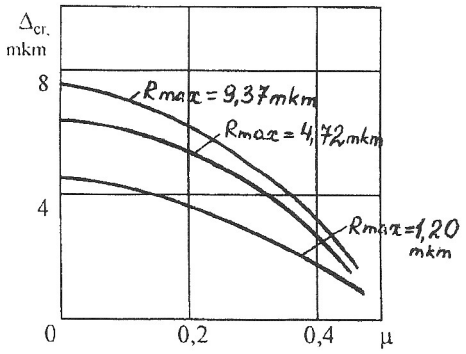
1) These results confirm the fact that the rougher the surface is treated, the more is the consumption of coating metal on filling of hollows formed by the value R_{max} between the peaks.

2) When we have equally rough surface (for example with R_{max}=4,72 mkm) after different forms of machining, the area of the hollows and the consumption of the coating metal used for filling them will be the greatest after grinding (0,0039 mm) and not after polishing (0,0026 mm) and turning (0,0025 mm).

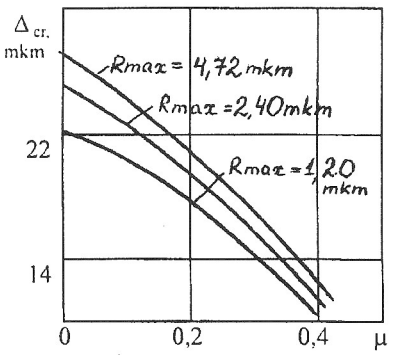
3) If we have the same coefficient of friction (for example with μ=0,1) and the same roughness of the surfase (for example with R_{max}=4,72 mkm) the quaranteed critical coating will be greater after polishing (24,51 mkm) then after turning (11,92 mkm) and grinding (6,09 mkm).

4) After the same cycles of drawing but different preparation of the surface of the wire the quaranteed critical coating and the consumption of metal change 5-6 times. With the increase of the coefficient of friction from "0" to "0,4", the quaranteed critical coating and the consumption of metal will increase 2,24 times after different forms of the preparation of the surface (Fig. 2,3).

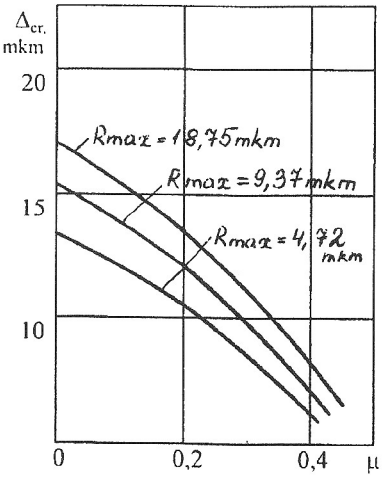
Dependence of the critical coating thickness upon the coefficient of friction



a)



b)



c)

Fig. 2

a) for grinding; b) for polishing; c) for turning

Dependence of the critical coating thickness upon R_{max}

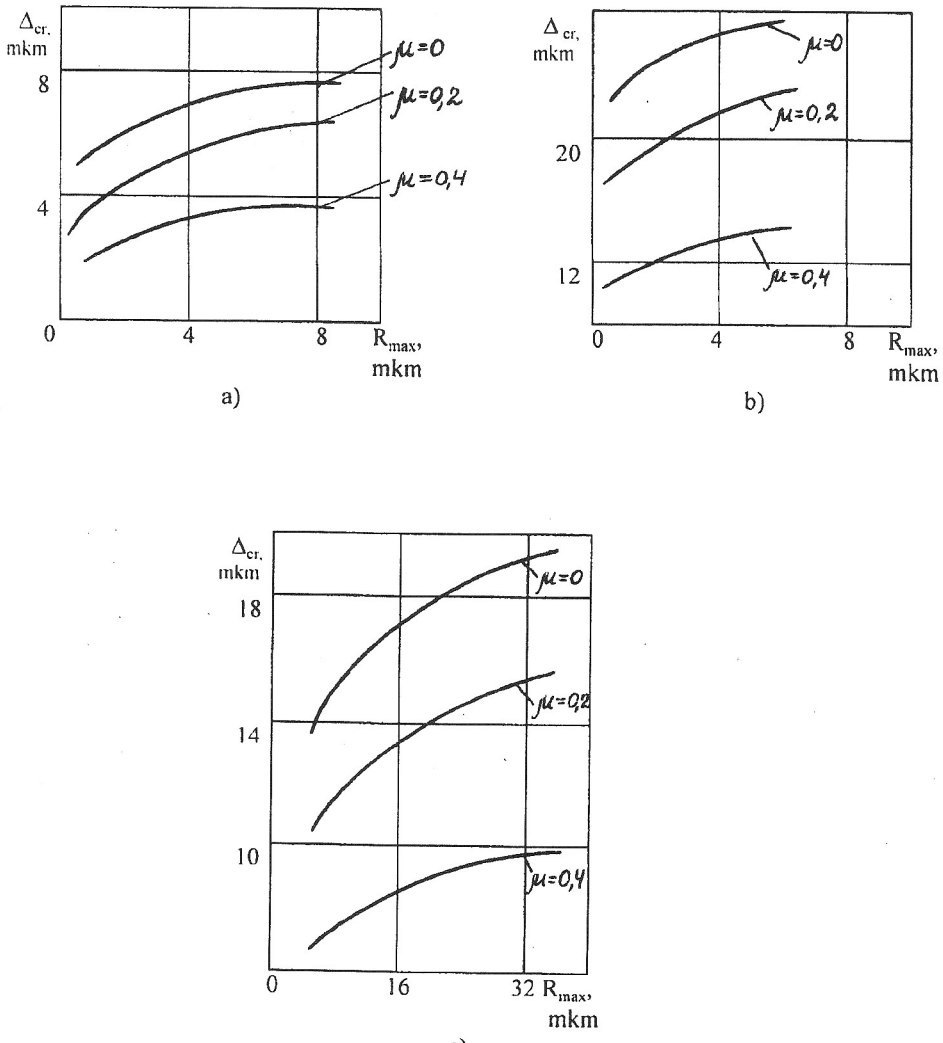


Fig. 3

a) for grinding; b) for polishing; c) for turning

5. REFERENCES

1) Alekseev Y.G., Kuvaldin N.A., Fetisov V.P. "The influence of drawing conditions on the formation of the brass coating on the wire for metal cord // "Steel", 1986. N3. - P.73-76.

2) Stepanenko A.V.,Sytcov E.G.,Belsky A.T." About the thickness of the formed layer on wire // Gomelsky filial of Belorus.politehn.inst.Gomel,1980.- 8 p.,ill..

3) Entsthchung von Oberflachenerhcbungen an der Stahl-ZinkschichtGrenze wahrend des Zichens feuerverzinkter Stahdrahte. Szota Jerzy, Domagala Roman. "Arch.Eisenhuttenw.", 1983, 54, N11, 437-438.

4) Grubość i structura ognowych poufok cynkowych na drutach staiowych. Szota Jerzy, Domagala Roman. "Wiad.hutn", 1983, 39, N1,9-11.

5) Calcul de l'épaisseur passante d'un revêtement métallique au cours d'un formage multipasse.Montmitonnet P.,Delamare F. "Met.et étud.sci. Rev.Mét.", 1986, 83,N7-8, 347-354.

6) Alekseev N.M. "The steel coating of sliding bases. - M.: Nauka, 1973. - 76 p.

7)"The calculation of the degree of printing of the roughness of the roll surface on the rolled strip" / Ogarkov N.N., Mining and Mettallurgical Academy.- Magnitogorsk,1995. - 10 p. Dep. VINITI 10.01.95, N 2 - B.95.

8)"Reference book on tribotechnique"/ Under the general editiong of M.Hebda,A.V.Chichinadze. In 3 t.T.1.Theoretical basis - M.: Mechanical engineering,1989. - 400 p.:il..

ANALIZA METODA DEFINISANJA UTICAJA OBRADE SPOLJNE POVRŠINE ŽICE REZANJEM NA MINIMALNU KRITIČNU DEBLJINU POVRŠINSKOG SLOJA (PRESVLAKE) KOD VUČENJA ŽICE

Ogarkov N.N., Nalimova M.V.,
Rudarsko-Metaluška akademija, Magnitogorsk, Rusija

REZIME

Kod vučenja žice na njenu spoljnu površinu najčešće se nanosi poseban sloj - nosač mazivnog sredstva. Problem debljine tog sloja u zavisnosti od polazne spoljen površine žice kao i od uslova obrade analiziran je u ovom radu. Data je zavisnost koja omogućava izračunavanje potrošnje površinskog sloja. Analitička metoda koja je razvijena i prikazana u ovom radu omogućava određivanje minimalne potrebne (kritične) debljine sloja u zavisnosti od gore navedenih parametara.

U slučaju da spoljna površina žice ima veću hrapavost veća je potrošnja materijala površinskog sloja (zbog ispunjenja šupljina formiranih između vrhova sa R_{max}). Utvrđeno je da su te šupljine najveće kog glodanja, a znatno manje kod struganja.

U radu su takođe analizirane veličine kritične debljine površinski nanesenog sloja u zavisnosti od koeficijenta trenja kao i od maksimalne hrapavosti spoljne površine R_{max}.

Journal for Technology of Plasticity, Vol.22 (1997), Number 1-2

HOT FORGING PROCESS ANALYSIS OF BRASS NUTS

Stoiljković V., Randjelović S., Faculty of Mechanical Engineering, Niš, Yugoslavia
Mijailović, V., Copper Smelters and Refineries, Bor, Yugoslavia

ABSTRACT

Light metals suitability for forming by plastic deformation methods was used for obtaining very complex forms. Required force, depending on dimension work piece at same volume, is analyzed on a forging example of two types the brass nuts in open tool. Dependence of deformation force and path of upper tool part was recorded by measuring tapes, connected into Weatstone's bridge by the measurement methods of mechanical values by electronically means. Introduction part of this work gives general attitudes about the forming of the light metals, but the second part gives conditions and measuring methods of forging process parameters. Third part of the paper gives results of required deformation force obtained by use of known formulas from literature. The conclusion gives a comparison of obtained experimental data with literature data.

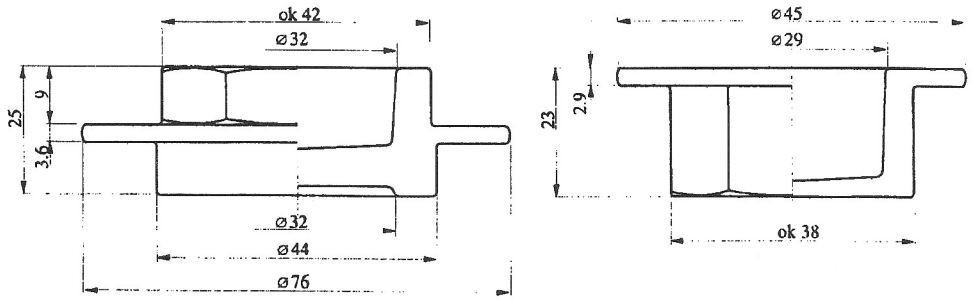
1. INTRODUCTION

Light metals forming on higher temperatures presents a method of volume forming which is often used. From one side, there are considerable smaller deformation forces in the forming process, what causes considerable smaller production capacities (smaller nominal press forces, sizes and tool shape, accompanied operations), but on the other side, these materials are suitable for special purposes (parts of water fittings, gas fittings, parts of high pressure, and so on). Hot forming of light metals gives a possibility of obtaining the very complex geometrical forms. Besides required geometry, higher material deformability, the higher material uniformity of internal forged piece structure, the decrease of grain in structure, etc. are obtained by these methods. The obtained part quality depends, first of all, on input material quality, structure, surface condition, heating temperature regime, deformation degree and rate, and similar.

2. MEASURING OF FORGING PROCESS PARAMETERS

Process of volume brass forming was analyzed on a forging example of two types nuts with approximate same geometrical shapes (fig.1). The two nuts, different in size, have been taken from each nuts group. Work pieces have cylindrical shape with different sizes of diameter and height with constant volume for each type of nut (total 160 samples). They were obtained by

turning methods from bar material. Surface layer of brass bar was removed by this processing, and the same surface structure and geometry of all samples was obtained. As it is hot forming, each group of work piece was heated into furnace before forging on the press. Heating temperature in furnace is about 750°C, and a work piece temperature on a tool is about 650°C. The decrease of work piece temperature is consequence of two reasons. The method of work piece transport from furnace to tool on a press causes decrease of work piece temperature, as well as due to a lower tool temperature. Upon positioning the suitable tool and before the start of forging the certain group of nuts, the tool is heated to work temperature (Ta ≈ 70-100°C) to reduce this difference. The real work piece temperature placed in a tool, before shot of upper tool part, was in a range 500-600°C.



"B" and "C" type of forged piece "A" and "D" type of forged piece

Figure 1. Forms of forged pieces of brass nuts

By forging method, complex geometrical form is obtained on cranked press from cylindrical work piece with various sizes, where outer form of forged piece obtains characteristic from of hexagonal prism, key hole (fig.1). Forging process is carried out in one stroke of press. From these reasons, in any phase, this process could be adopted as free compression, from the reason that the speed of upper tool part i.c. deformation rate, is not high (fig. 2).

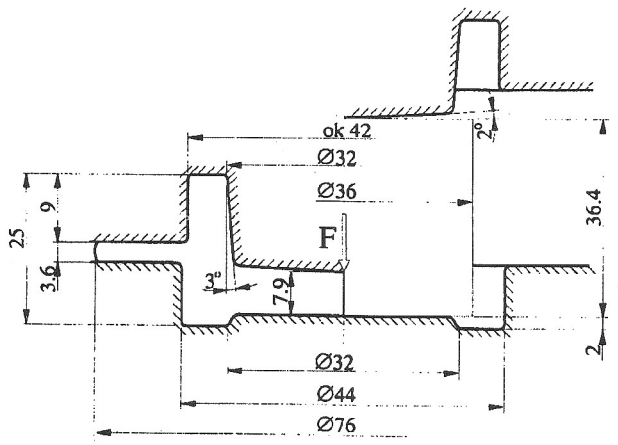


Figure 2. Work piece in a tool at the beginning and end of forging process

The cranked press is used for forging, with nominal force of 800 kN and deformation rate of 0.12 m/s. Measuring tapes, connected into Weatstone's half bridge, are used for elastic deformations measurements in upper tool part, in order to measure the deformation force. Two of four tapes are measuring (active), until the other two are used for the compensation of the ambient temperature influence. The factor of used measuring tape is k=2.03, according to the HMB producer data. Factor of formed bridge is B = 2.6 due to half-bridge [3]. Place of

measuring tapes positioning is in upper tool part, on tool position over which a deformation force is transformed. Expression for deformation force has now the following form:

$$F = \sigma \cdot A = E \cdot \varepsilon \cdot \frac{d^2 \cdot \pi}{4} = E \cdot \frac{2C \cdot \varepsilon_{in}}{B \cdot \alpha \cdot k} \cdot \frac{d^2 \cdot \pi}{4} \quad [kN] \qquad (1)$$

where is: $E = 2.1 \cdot 10^5$ kN/cm^2 - material elasticity modules of upper tool part, d - diameter of upper tool part, C = 1 correction factor when resistance of measuring tape is different from nominal one for certain device, $\alpha = 1$ - correction factor due to a conductor length.

Unless measuring of deformation force, a passed path of upper tool part was measured simultaneous on second channel (fig.3). This gives a total insight into force change during relatively movement of upper tool part toward a work piece. Induction path pickup W200, producer HMB, is used for path measuring. Diagram of deformation force and path dependence during process time (fig.3) clearly shows maximum force realization during the lowest tool position, i.e. in a final part of forging when a work piece gravitates toward total filling of mold cavity. Moment of appearance the maximum force its sizes depends of geometry and forged work piece size. There are no other changes in the rest part of measuring range, because the forging process is very short.

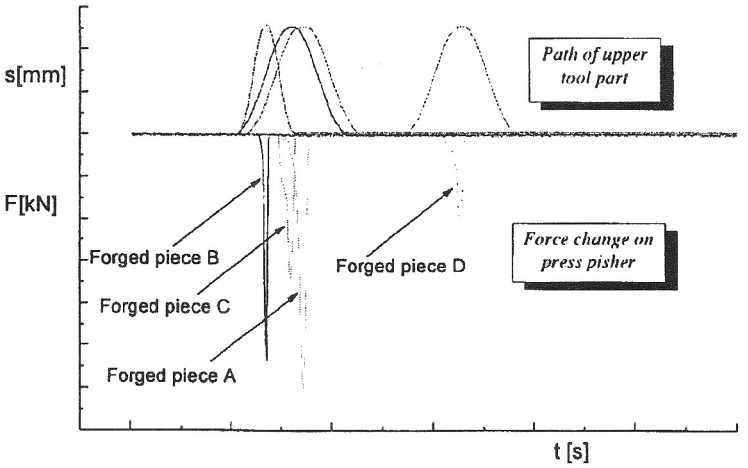


Figure 3. Change of deformation force and tool path in a given measuring range

Dependence of deformation force of tool passed path gives more information on process (fig.4). The moment when the force raise depends directly on work piece height, until a further force increase is a function of more factors. With different work piece diameters, lines of material flowing are different, and also resistance to plastic deformation, what causes the different dependence of force and stroke. Also, the tool is in contact with material by its surface at this phase, so there is the higher heat transfer from forged work, what increases deformation resistance depending on work piece sizes. At the end of process, an evident increase of deformation force is obvious, which suddenly increase. At all measurements, at the end of forging process, an rapid increase of force is obvious with very small change of path. This part of diagram is responding to so-called "ironing" of forged piece, when a material complete fills the mold cavity. Measuring shows that the force increase with an increase of material flowing resistance on a rim, i.e. with an decrease of passing bridge height.

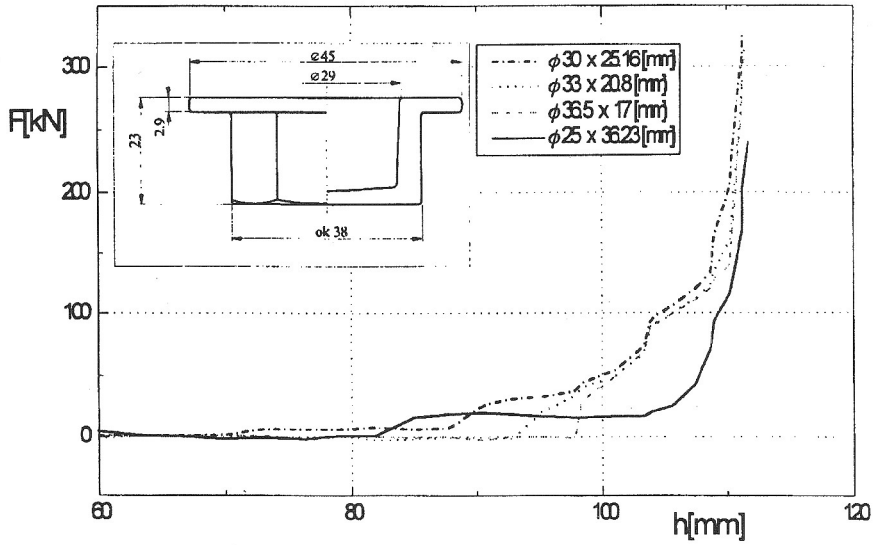


Figure 4. Dependence of deformation force from tool passed path of same type forged piece, type "D", for different sizes of work piece

3. PARAMETERS CALCULATION FOR FORGING PROCESS

There are many authors in literature who dealed with estimation of deformation force at free forging [1,2,6,7]. Many authors at the analysis is of forces separated adopt process of material deformation in mold cavity - F_k, from its deformation on forged piece rim, passing bridge - F_v.

$$F = F_k + F_v \tag{2}$$

Storozev:
$$F_k = \frac{\pi \cdot d^2}{4} K \left[2\frac{\mu \cdot s}{h_v} - 0{,}375 + 1{,}25\left(\ln\frac{d}{h_v} + 2\frac{h_v}{d} \right) \right]$$

$$F_v = K \cdot \pi(d+s) \cdot s \cdot \left[1{,}5 + \frac{\mu \cdot s}{h_v} \cdot \frac{d + 0{,}66 \cdot s}{d+a} \right] \tag{3}$$

where is: h_v, s - height and width of passing bridge; d - maximum diameter forged piece in plane sunder; μ - coefficient of friction (for warm forging process with grease μ=0.35), K - specific resistance deformation at higher temperatures.

Semenov:
$$F = \sigma_s \cdot \left(\left(2 + \frac{s}{2h_v} \right) \cdot A_v' + \left(2{,}5 + \frac{s_v}{h_v} + 0{,}185\left(\frac{D}{h_v} - 2 \right) \right) \cdot A_k' \right) \tag{4}$$

where is: A_v, A_k - reduced surface of rim and mold.

The work deformation balance:

$$F = \sigma_s \cdot \pi \cdot R_v^2 \cdot \left(1 + 0{,}17 \frac{2 \cdot r_v}{h_v} - 0{,}13 \cdot \left(\frac{2 \cdot r_v}{h_v} \right)^{1.5} \cdot \left(\frac{r_k}{r_v} \right)^{1.5} \right) \qquad (5)$$

where is: r_k r_v - radius of mold cavity and radius of rim.

Very complex processes of material plastic deformation should appear during filling of mold cavity, which are so complex to be described by the precise mathematical methods. On the rim of forged piece can be considered, that this the case of the plane deformation state, i.e. deformation by length is neglected, so in general case we have compression of endless belt [2].

It is seen from tool geometry and forged piece (fig.2) that there is no formed material surplus and passing bridge for flowing. From these reasons, a calculation of deformation force on the rim of forged piece should be adopted with a reserve.

Exact and precise mathematical description of mentioned process is difficult due to a fact of plastic deformation at higher temperatures. These conditions cause a change of mechanical characteristics of starting material, i.e. a decreased specific deformation resistance K[N/mm^2] appears. These change are considered by expression [4]:

$$K = K_n \cdot C_T \cdot C_\varphi \cdot C_\varepsilon = \text{const} \qquad (6)$$

where is: K_n - constant for specific deformation resistance at deformation rate 1s^{-1}, at melting temperature; C_T - temperature coefficient; C_φ - rate coefficient; C_ε - deformation coefficient. For above mentioned conditions, regard to higher temperature, value of specific deformation resistance in calculation was K = 35[N/mm^2].

4. CONCLUSION

The investigation has showed the expected results which depend on mentioned factors. It is reasonable that a heating temperature of work piece is the most important, where small decrease of part temperature results in considerable increase of force. The obtained results, upon calculation, have more correct values for "A" and "D" types of forged pieces. The reasons should be possible due to a fact of less complex forged pieces geometry, which causes simpler lines of material flowing. Part geometry has direct influence on deformation force increase, from contact moment. The dependence of deformation force at the end of process from starting form of piece is nearly absent, because there are insignificant difference without influence at this regime (temperature, deformation rate, part geometry). The subject of detailed analyzing assumes more measuring points (measuring of radial forces in tool) and also better and more precise process control of work piece heating.

REFERENCES

[1] K. Lange, Lehrbuch der Umformtechnik, Band 2 Massivumformung, Springer - Verlag, Berlin-Heidelberg-New York, 1974

[2] V. Stoiljković, Teorija obrade deformisanjem, Mašinski fakultet Univerziteta u Nišu 1984.

[3] V. Stoiljković, Merenje mehaničkih veličina električnim putem, Mašinski fakultet Univerziteta u Nišu, 1980.

[4] B. Musafija, Obrada metala plastičnom deformacijom, Sarajevo 1988.

[5] B. Musafija, Primjenjena teorija plastičnosti I i II, Sarajevo 1973.

[6] Engineering plasticity, theory and application to metal forming processes, R.A.C. Slater, London 1977.

[7] Plastomechanik der Umformung metallischer Werkstoffe, H. Lippmann, O. Mahrenholtz, Springer-Verlag, Berlin/Heidelberg/NewYork 1967.

[8] Određivanje napona u procesima hladnog istiskivanja metodom vizioplastičnosti, Jugoslovenski časopis za obradu materijala deformisanjem, M. Plančak, Novi Sad 1985.

[9] Kinematika tečenja materijala u procesima hladnog istiskivanja čelika, Jugoslo-venski časopis za obradu materijala deformisanjem, M. Plančak, Novi Sad 1986.

[10] K. Lange, Lehrbuch der Umformtechnik, Band 1 Grundlagen, Springer - Verlag, Berlin-Heidelberg-New York, 1972

[11] Die beanspruchung von werkzeugen beim vorwärts - fliesspressen unrunder querschnitte, Technische Universität Brno, Tschechische Republik, Novi Sad 1995

[12] Lj.Bogdanov, Lj. Đorđević, M.Dragan, Kovanje otkovaka od mesinga sa ubadanjem, 26. Savetovanje proizvodnog mašinstva Jugoslavije, Budva 1996.

[13] V. Domazetović, M. Vukčević, M. Janjić, Upoređenje teorijskih i eksperimentalnih pritisaka pri zapreminskom oblikovanju osnosimetričnih elemenata u otvorenim kalupima, 26. Savetovanje proizvodnog mašinstva Jugoslavije, Budva 1996.

[14] D.Vilotić, M. Plančak, V.Vujović, I. Trbojević, M. Milutinović, P. Skakum, Analiza procesa sabijanja valjaka pomoću sferičnih alata, 26. Savetovanje proizvodnog mašinstva Jugoslavije, Budva 1996.

ANALIZA PROCESA TOPLOG KOVANJA MESINGANIH NAVRTKI

V. Stoiljković, S.Ranđelović, Mašinski fakultet u Nišu,
V. Mijailović, TIR-Bor, Yugoslavia

Rezime

Pogodnosti lakih metala za oblikovanje postupcima plastične deformacije iskorišćene su kod dobijanja vrlo složenih geometrijskih oblika. Na primeru kovanja dva tipa mesingane navrtke, sa po dve navrtke različitih dimenzija, u otvorenom alatu, analizira se potrebna sila u zavisnosti od dimenzija pripremka pri istoj zapremini. Veličina završne sile kovanja je gotovo ista za sve otkovke, dok se tok porasta sile razlikuje za različite pripremke u zavisnosti od trenutka kada gornji deo alata dolazi u kontak sa pripremkom i načina ispunjavanja kalupne šupljine. Zavisnost sile deformisanja i puta gornjeg dela alata snimljena je pomoću mernih traka vezanih u Winstonov most, tačnije u polu most, postupkom merenja mehaničkih veličina električnim putem. Merenje sile dformisanja vrši se preko merenja elastičnih deformacija u gornjem delu alata, odnosno tela pritiskivača koje se registruju promenom otpora provodnika merene trake. Uvodni deo rada daje opšte stavove oblikovanja lakih metala, dok u drugom delu daju se uslovi i načini pod kojima je vršeno merenje parametara procesa kovanja. Treći deo rada daje rezultate potrebne sile deformisanja dobijene primenom poznatih obrazaca iz literature. Zaključna razmatranja daju poređenje dobijenih eksperimentalnih rezultata sa rezultatima iz literature. Dobijeni rezultati prema navedenim obrascima pokazuju dobro poklapanje sa rezultatima merenje kod otkovaka jednostavnije geometrije, tip "A" i "D". Složeniji oblik otkovka i tečenje materijala prilikom njegovog oblikovanja uslovljava veće odstupanje stvarnih rezultata. Najpribližniji rezultati dobijaju se po obrascima Storoževa dok druga dva pristupa daju veće odstupanje istih. Činjenica da se radi o kovanju na visokim temperaturama, i opis ponašanja materijala pripremka u tim uslovima, preko krivih očvršćavanja za obradu na toplo, takođe ima uticaja na odstupanje konačnih rezultata.

Journal for Technology of Plasticity, Vol 22 (1997), Number 1-2

AXISYMMETRICAL ELEMENT CONTOUR MODELLING AT DIE FORGING

Janjić M., Vukčević M., Domazetović V., University of Montenegro, Yugoslavia

ABSTRACT

This paper describes application of finite-element method, based on elastic-plastic formulation, in die forging analyses. An axisymmetrical contour of the elements within a wide deformation range has been modellied. By using an advanced software there have been obtained the results experimentally proved and graphically presented.

1. INTRODUCTION

Bulk metal forming is for its complexity of a special importance within the field of metal working, this, above all, being conditioned by a fact that by such metal working, two criteria appear difficult to reconcile: solution correctness and simplicity. Though great efforts have been made on the part of many research workers, it may be said that there is neither a definitely adopted method nor a definite solution, not even of the most simple procedures in bulk metal working. The underlined properties are specially emphasized at die forging as a most commonly used procedure.

This makes the field of investigating geometrical and mechanical parameters at die forging very actual and insufficiently researched one. The very complexity of the problems has made it necessary for the following interrelated approaches to be used: theoretical, experimental and numerical ones. Of a special interest is the application made on the class of axial and symmetrical forging pieces, being used very frequently.

An axisymmetrical element contour modelling at die forging by using a method of finite elements has been done. Experiments have been carried out verify the results.

2. FINITE ELEMENT FORMULATION

In the finite-element method, the deformation process is modelled by examining only a finite number of points or nodes of the workpiece. By interpolating the field variables between these nodes, the physical principles of deformation allow a set of stiffness equations to be constructed relating nodal force to nodal displacement.

The geometry of the workpiece, the boundary conditions and the material properties may all change during the process, and so the relationship between nodal force and nodal displacement is highly non-linear. The process must therefore be examined in small but finite increments of deformation [1,2,3].

The finite-element program used here is based on that for three-dimensional analysis. Mises yield criterion (1) and Prandtl-Reuss equations (2) relating stress to strain increment are used:

$$\frac{3}{2}\sigma'_{ij}\sigma'_{ij} = Y^2 \tag{1}$$

$$d\varepsilon'_{ij} = \frac{1}{2G} d\sigma'_{ij} d\lambda; d\varepsilon_{ii} = \frac{1-2\nu}{E} d\sigma_{ii} \tag{2}$$

in which: Y is yield stress; σ'_{ij} are deviatoric components of stress; ε'_{ij} are deviatoric components of strain; G is shear modulus of elasticity; $d\lambda$ is factor proportionality; σ_{ij} are normal component of stress; ε_{ij} are normal components of strain; E is Young's modulus elasticity.

The approach used here is the updated Lagrangian approach which considers displacement of a point of an element in terms of the reference coordinates of the element in the start of the increment. Hence for each increment a new set of reference coordinates apply to each element. Without going into detail, this leads to possibility the present method adopts a finite deformation, where the incremental equations are derived from the elastic-plastic constitutive relationship.

Let Δf_{Ii} be the i-th Cartesian component of the change in force at the I-th node of a given element during an increment of the analysis, and let Δd_{Ii} be the i-th Cartesian component of the corresponding change in displacement of that node from its reference position. The element stiffness equations may be written as [1]:

$$\Delta f_{Im} = \left(K^{(\varepsilon)}_{ImJn} + K^{(\sigma)}_{ImJn} + K^{(\phi)}_{ImJn}\right)\Delta d_{Jn} \tag{3}$$

where the implied summation is carried out over all the nodes of the element for a repeated upper-case subscript, and over the three Cartesian components for a repeated lower-case subscript. The three terms inside the parentheses are called, respectively, the deformation-stiffness matrix, the stress-increment correction matrix and the constant-dilatation correction matrix.

The volume integrals in the incremental stiffness matrices for all the elements are evaluated by Gaussian quadrature and the assembled global matrix solved Gaussian elimination and back-substitution. In order to improve the accuracy of the solution, a second-order Runge-Kutta technique is adopted in which the FE equations are based upon the values of the state variables half-way through the increment. These mid-increment values are first estimated by a preliminary solution of the FE equations based upon the state of the workpiece at the start of the increment.

The frictional boundary conditions for the solution of the FE equations are imposed by means of the beta-stiffness technique using friction elements at the die surfaces.

3. EXPERIMENTAL PROCEDURES

3.1 Defining the experiment

Both geometrical and technological parameters were defined at the beginning of experimental procedures. A family of the degree axisymmetrical elements of two height degrees on one side and one height degree of the other side of a graded plane was adopted (Fig.1) [6]. Lead was used as an experimental material. The very experiment was carried out at 10 [mm/min].

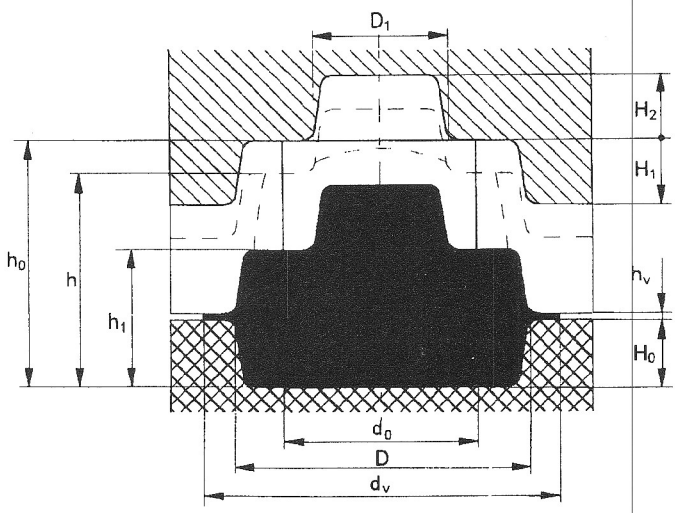


Fig. 1 Working piece seized with die in the course of deformation

A reduced degree of deformation ε* expressed as a ratio of an instantaneous tool stroke and total tool stroke is defined as a deformation measure, given by the formula:

$$\varepsilon^* = \frac{h_0 - h}{h_0 - h_1}, \tag{4}$$

where,

h - immediate height reached by the upper die points getting into contact with the billet at the beginning of die forging (Fig.1). At the initial phase $h=h_0$.

h_1 - final height reached by the upper die points getting into contact with the billet at the beginning of die forging (Fig.1).

3.2 Information measuring system

Measuring at the above mentioned the experimental procedures were done by a precise analog-digital measuring equipment connected with an information measuring system [6,10], consisting of sensor unit, measuring bridge, transitional unit, A/D card and computer, illustrated by a block diagram in Fig.2.

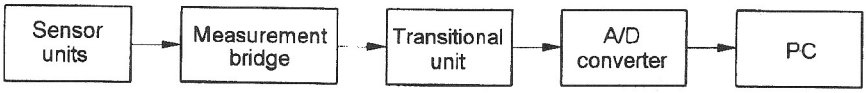


Fig.2. Information measurement system block diagram

Two inductance sensors placed on an universal grinding machine utilizing the possibility of a precise moving of the working table were used to make record of the workingpiece contours (Fig.3).

On the movable grinding machine table (1) tightening head is mounted (3) with the grading device (2) within whose mouths a workingpiece is tightened (8), its axis being horizontal to the direction of the table moving.

A stroke inductance sensor (5) of HBM make, type W40K and measuring range ±40 [mm] is placed in workingpiece axial direction and makes measurements of the working table shifting and the value of y workingpiece contour coordinate.

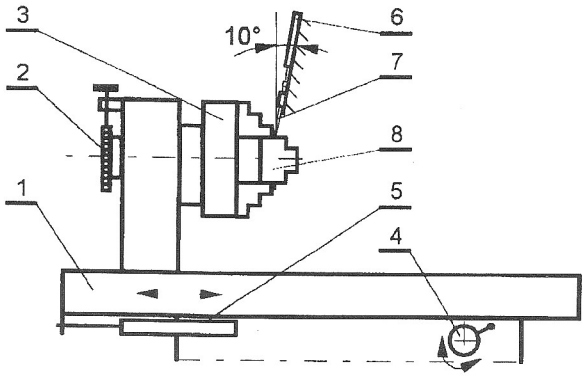


Fig.3. Device for registering recording workingpiece contours;
1 - movable grinding machine table; 2 - grading device; 3 - tightening head;
4 - handle for shifting the table; 5 - stroke inductance sensor in axial direction;
7 - measuring needle; 8- workingpiece

Another stroke inductance sensor (6) is of HBM make, type W20K and measurement range of ±20 [mm] and is placed at the angle of $\beta=10°$ in relation to the workingpiece radial direction. The sensor's body is fixed to a non-movable part of the grinding machine, whereas the movable armature is attached to a measurement needle specially made for that purpose (7) (Fig.4).

Measuring needle (1) is made of a fine road machined out of the fast-cut steel and it slides by an action of its own weight within a tolerant container (2). By moving the movable part of the grinding machine table (1) it slides over an surface of the workingpiece (Fig.4) and makes the measuring inductance sensor armature move (5), this representing x coordinate of the workingpiece armature in the acute triangle system. A signal from the sensor was amplified in the digital six-channel HBM measuring bridge, type KWS.637.D4. An output analog signal from the bridge was converted by AD/DA card of DT 2801-A type into a digital one and stored in the PC/AT/486 computer with the installed system for data activating GLOBAL-LAB.

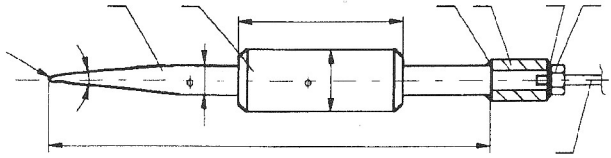


Fig.4. Measuring needle;
1 - needle; 2 - needle container; 3 - bushing; 4 - nut;
5 - movable inductance sensor armature; 6 – solder

3.3 Experimental contour registering

The contours were registered on a sample defined in point 3.1 by the information measuring system described in point 3.2. The process was discreted, this making it possible for the deformed sample contours for different values of the reduced deformation degree ε^* to be obtained (Fig.5).

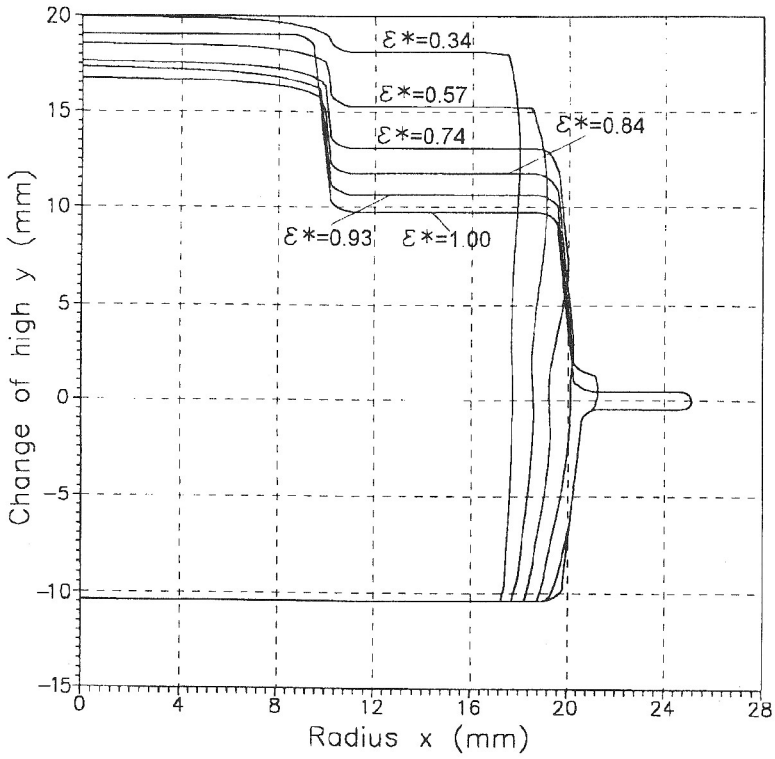


Fig.5 Sample contours recorded in deformation

4. CONTOUR MODELLING

Based on the theory presented in point 2, a program package for elastic-plastic analysis by a method of finite elements (EPFEP3 - Elastic-Plastic Finite-Element Program for 3 Dimensions) was made. The pachage was supported by a powerful graphical result presentation. Out of the many results obtained, those referring to the sample contour modelling are presented..

A net of finite elements consisting of 380 elements and 852 knots was made after the sample's cross-section. The look of the deformed net is given in Fig.6.

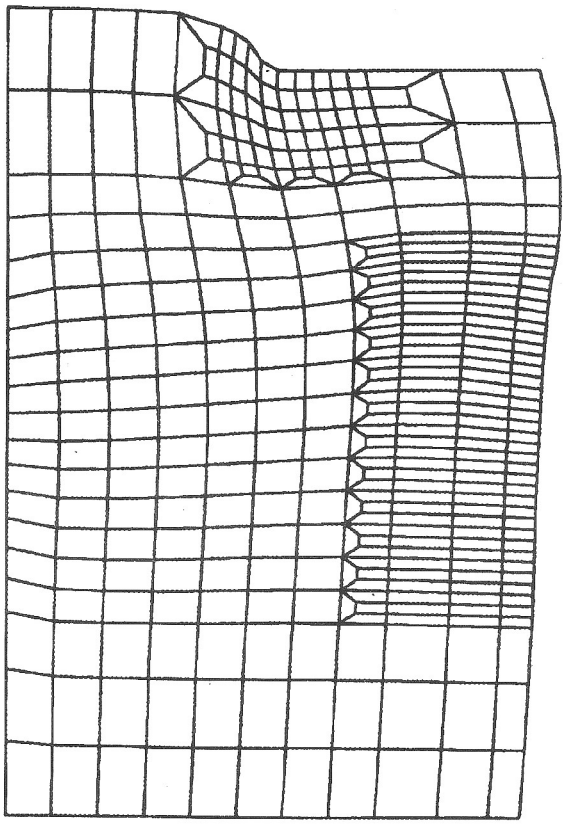


Fig.6 The look of the deformation net of finite elements

Bath model and experimental deformed sample contours for different values of the reduced deformation degree ε^* are presented in Fig.7 up to Fig.9.

The geometry of the samples is defined by the following values: $\phi d_0 \times h_0 = \phi 33.4 \times 32.27$ [mm], $H_0 = 9.2$ [mm], $H_1 = 9.2$ [mm], $D_1 = 20$ [mm] and $h_v = 1$ [mm].

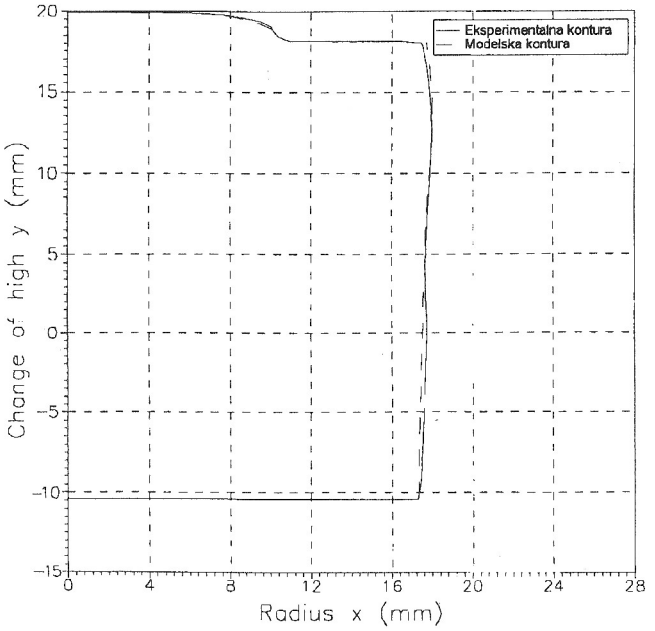


Fig.7 A deformed sample contour modeling for ε=0.34*

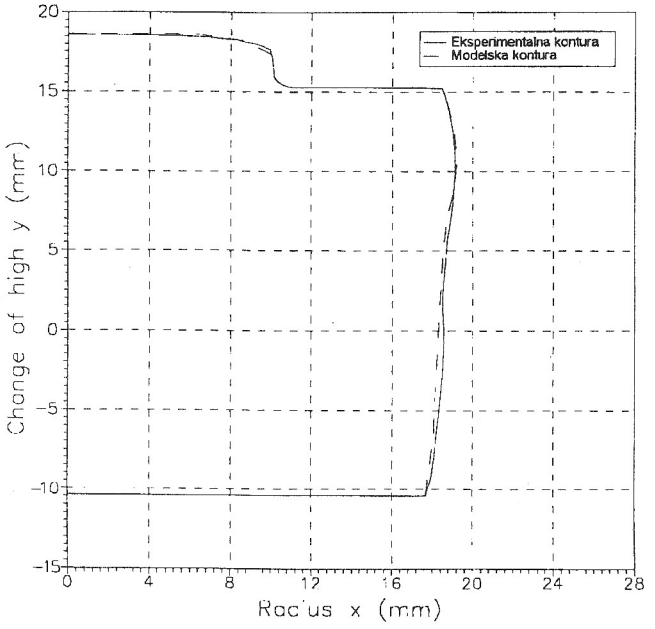


Fig.8 A deformed sample contour modeling for ε=0.57*

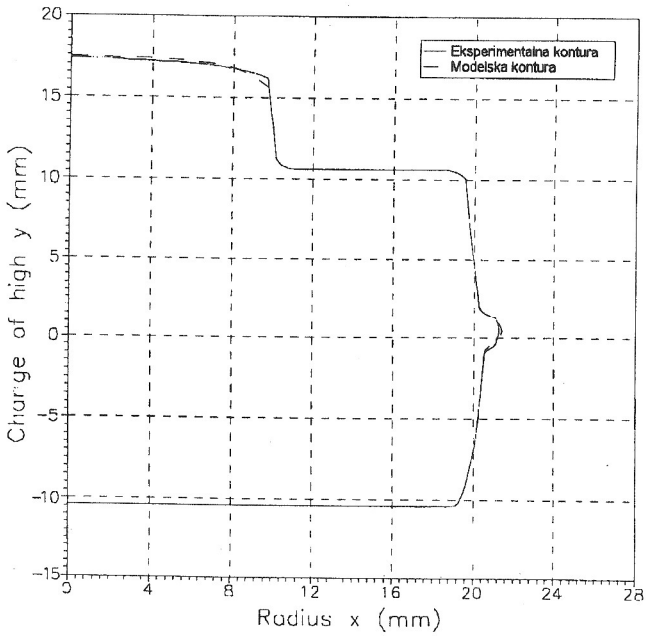


Fig.9 A deformed sample contour modelling for $\varepsilon^*=0.93$

4. CONCLUSION

Elastic-plastic formulation of finite-element method may be successfully used for modelling of die forging processes which are followed with large deformations. A very aplicative software is developed based on this theory.

The contour modelling results obtained for the axisymetrical two-degree elements are experimentally proved. A high agreement between model and experimental results within a wide deformation range is confirmed.

Evidently, program can be used for simulation of other forging processes. In this cases it is necessary to include the particularities of considered problems. Because of that we have to know physics of the problem and the finite-element technique.

REFERENCES

[1] Hartley P., Pillinger I., Sturgess C. (Eds.): Numerical Modelling of Material Deformation Processes, Springer-Verlag , London, 1992.

[2] Pillinger I., Hartley P., Sturgess C.E.N., Rowe G.W.: Thermo-Mechanical Modelling of Metalforming Using the Finite-Element Method, Comput.Plast.Models Software and Appl: Pros.Int.Conf., p.p. 1073-1085, Barcelona, 1987.

[3] Rowe G,W., Sturgess C.E.N., Hartley P., Pillinger I.: Finite-element plasticity and metalforming analysis, Cambridge University Press, Cambridge, 1991.

[4] Vukčević M.: Finite Element Modelling of Forging Processes, Report, University of Birmingham, Birmingham, 1992.

[5] Vukčević M.: A Finite Element Method at Mechanical Working. Monograph on occasion of the jubilee of 25 years of the studies of Mechanical Engineering in Montenegro, Podgorica, 1996.

[6] Janjić M.: A Contribution to Metal Yield Flow at Volume Axysymmetric Elements Treatment. Mr. thesis, Mechanical Faculty, Podgorica, 1997.

[7] Domazetović V., Vukčević M., Janjić M.: Modeling of the die forging procesess, Internacional Conference on Industrial Tools, Maribor, Slovenia, 1997.

[8] Domazetović V., Vukčević M., Janjić M.: Research of the working pressure and change of geometry in the forging deformation, Nove trendy v strojarstve na prahu trejteho tisicročija, Košice, Slovenska Republica, 1997.

[9] Korn G., Korn T.: Mathematical handbook, Mc Graw-Hill Book Company, New-York, 1968.

[10] Stanić J.: Method of Engineering Measurements. Faculty of Mechanical Engineering, Belgrade, 1990.

[11] Stanić J., Kalajdžić M., Kovačević R.: Measuring Technique and Technology at Metal Working by Cutting. Faculty of Mechanical Engineering, Belgrade, 1983.

MODELIRANJE KONTURE OSNOSIMETRIČNIH ELEMENATA PRI KOVANJU U OTVORENIM KALUPIMA

Janjić M., Vukčević M., Domazetović V.
Mašinski fakultet u Podgorici

REZIME

Područje ispitivanja geometrijskih i mehaničkih parametara pri kovanju u otvorenim kalupima je aktuelno i nedovoljno istraženo. Složenost problematike je uslovila neophodnost korišćenja međusobno povezanih pristupa: teorijskog, eksperimentalnog i numeričkog. Posebno je aktuelna primjena na klasu osnosimetričnih elemenata koji se veoma često koriste.

U ovom radu je modelirana kontura stepenastih osnosimetričnih elemenata u širokom rasponu deformisanja. Modeliranje je izvršeno primjenom programskog paketa koji se bazira na elasto-plastičnoj teoriji metode konačnih elemenata (EPFEP3 - Elastic-Plastic Finite-Element Program for 3 Dimensions).

Radi verifikacije modelskih rezultata izvršena su eksperimentalna istraživanja. Korišćena je analogno-digitalna mjerna oprema povezana u informacioni mjerni sistem. Konture su snimane za različite vrijednosti stepena deformacije.

Modelski i eksperimentalni rezultati su grafički prezentirani. Pokazana je visoka tačnost modelskih rezultata u širokom rasponu deformisanja.

Journal for Technology of Plasticity, Vol.22 (1997), Number 1-2

MATHEMATICAL MODELLING OF CALIBRATION PROCESS OF BARS FROM FREE CUTTING STEEL

P.I.Denisov, D.B.Zuev, A.I.Beliaev, R.V.Nekit
Mining and Metallurgical Academy of Magnitogorsk, Russia.

ABSTRACT

This paper is dedicated to solve the actual problem of getting products from free cutting steel with decreasing declination to crack formation without disrupting the machinability index.

1. INTRODUCTION

Producing a product of automatic steel without crack is a hard task and long-standing problem, but it remains actual till now, because output of useful products in metallurgical and machinebuilding plants while producing hexahedronical and round hot-rolled and kalibrated free cutting steel is 50..70%. Main defect-crack in every production occurs due to contradicting demands for characteristics of free cutting steel and its productions. On one hand they should be plastical and should deform without crackformation, and on the other hand they should be brittle and should work properly in transfer machines /1/.

2. CONTENTS

Crack formation and splitting the front end bars arises as effect of local character. Mechanical properties of free cutting steel by the force of lot of factors, effecting on metal in the process of transformation from ore to hexahedron change in the section /2,3/. Mechanical characteristics like ultimate strength, conditional yield point, relative extraction and contraction, plasticity also change from one part of section to another. Here we may assume that there are some elements of material whose plastical resource is not too much and its destruction occurs very fast.

Mathematical modelling, whose conditional yield point $\sigma_{0,2}$ and plasticity λ_p are constant for given material, can not explain why crack formation and destruction mostly occurs in the central part of cylindrical billet in the process of its fettling and calibration.

Consequently, it is very necessary to note the change of conditional yield point $\sigma_{0,2}$ in the section of hot-rolled bars.

3. EXPERIMENTAL RESULTS

There are 3 diferent kind of free cutting steel were used for the research hot-rolled bars from. These free cutting steels which were used as experimental research and those, which are used in industrial productions. Chemical compositions of experimented marks of steel are given below.

N	Steel	C,%	Si,%	Mn,%	S,%	P,%	Ca,%	Ba,%
1.	**A11**	**0,145**	**0,085**	**1,09**	**0,23**	**0,089**		
2.	**A12 with Barium**	**0,13**	**0,13**	**1,09**	**0,135**	**0,1**	**0,002**	**0,001**
3.	**A12**	**0,135**	**0,145**	**1,1**	**0,135**	**0,09**		

Relations of variation of conditional yield point of experimented free cutting steel in the section of hotrolled bars were determined. It have shown, that contents of alloyed and micro-alloyed elements in steel effect on conditional yield point $\sigma_{0,2}$. In this context increase of contents of sulphur canses the decrease of yield point on the other hand availability of calcium and barium increases it (see Fig.1).

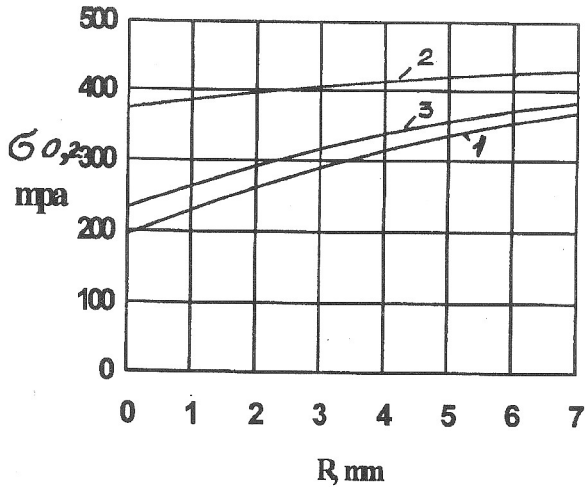


Fig.1 Distribution of conditional yield point of free cutting steel in the section of hot-rolled bars: 1-A11; 2-A12(Ba); 3-A12

It is established, that value of conditional yield point effects on plasticity of bars. Steel, containing less yield point $\sigma_{0,2}$ have less plasticity. On Fig.2..4 diagram is shown of plasticity of experimented steels with different conditional yield point $\sigma_{0,2}$.

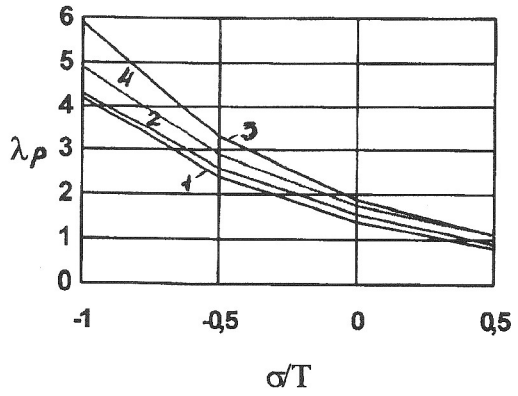


Fig.2 Diagram of plasticity of steel A11: 1-R=0; 2-R=2,5mm; 3-R=5mm; 4-R=6,5mm

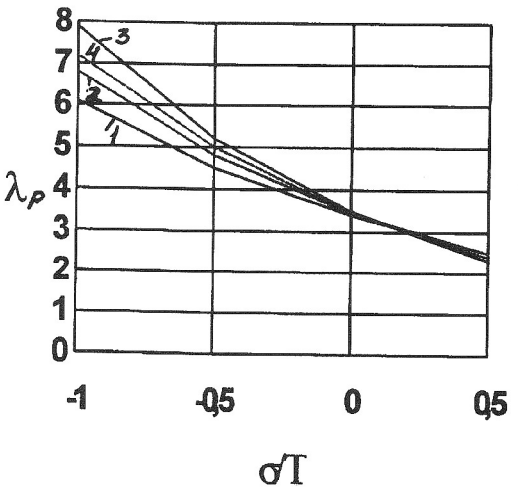


Fig.3 Diagram of plasticity of steel A12(Ba) : 1-R=0; 2-R=2,5mm; 3-R=5mm; 4-R=6,5mm

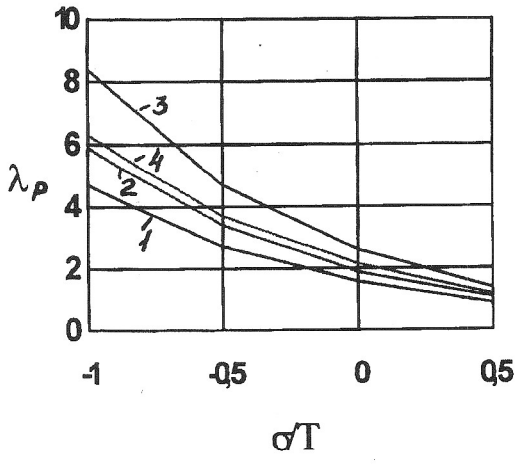


Fig.4 Diagram of plasticity of steel A12: 1-R=0; 2-R=2,5mm; 3-R=5mm; 4-R=6,5mm

Value of damage ω of all experimented steels were determined. In this context it was established that if micro alloyed with calcium or barium steel characterises less magnitude of ω which is different from sulphurous steels A11 and A12 withaut microalloyed addition.

Equation of change of damage ω in this section of calibrated bars from 3 marks of steels (Fig.5).

For steel A11

$$\omega = 0{,}34 - 0{,}018\ R + 0{,}0013\ R^2 \qquad (1)$$

For steel A12 with barium

$$\omega = 0{,}219 - 0{,}014\ R + 0{,}0014\ R^2 \qquad (2)$$

For steel A12 without micro-alloyed addition

$$\omega = 0{,}3 - 0{,}044\ R + 0{,}0047\ R^2 \qquad (3)$$

It have shown, that damage increases in great extent towards symmetrical axis of billet and in less extent towards its edge.

Distribution of damage ω of steels microalloyed with barium or calcium are more uniformly than of sulphurons A11 or A12 without microalloyed addition, which positively effects on the workability of cutting of all these steels.

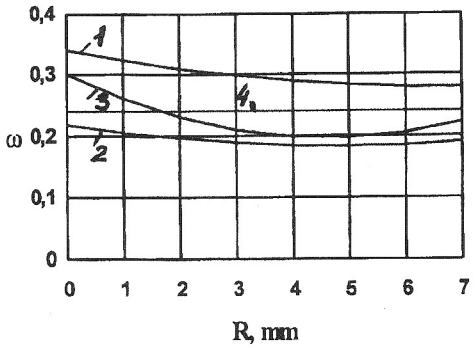


Fig.5 Distribution of damages in the section of calibrated bars of exeperimented steels: 1-A11; 2-A12(Ba); 3-A12; 4-criteria of microdamage ω^*

4. CONCLUSION

Said above things found reflection in the worked methodics of evaluation of declination to crack formation of calibrated bars from free cutting steels. To take into account the changes of mechanical characteristics in the section of billet is one of the different characteristics of method from famous plan of Ural Politechnic Institute (Ekaterinburg).

Practical use of acceptance of this method results in the increase of quality of rolled products due to sorted steel with decreasing plastical property.

This type of approach to the value of quality of rolled products allows not only to determine the role of different technological factors of its production,but upto the process of metalworking to choose the rational regime of calibration (angle of entrance cone of die, calibrated belt, reduction) and lubricated things characterising koefficient of friction.

Planned method became useful as base of algorithm of applied programm used for approximation of curve hardening diagram of plasticity indicator,conditional yield point, also for account of damage.

Proposed method is recommended for doing first control of material for example rolled output for production of different products of machine building (bolt, connection of pipe, bott). Factory or plant which produces bars, basing upon these type of methods are capable of assigning

one or the other bars for different products of machine building depending upon the demand of its exploitation character.

On the base of planned method value of declination of free cutting steel towards crack-formation in calibration bars, further things are recommended:

1) Calibration of hexahedron 17mm, from steel A11 with increasing contents of sulphur should be done in the die with the angle of first cone $2\alpha = 16^{\circ}$, with reduction of 1 mm. In this context choice of lubrication must be done very carefully, pay attention to the fact that koefficient of friction lies in the limit of 0,1..0,12.

2) During calibration of hexahedron 38 mm, it is necessary to decrease reduction by the method of changing the size of billet from 40 mm to 39 mm.

In the Magnitogorsk metallurgical plant a big party of hexahedrons 39 mm were rolled from steel A12 and were sent to Gorki automobile plant for calibration of hexahedron 38 mm. During the use of billet hexahedron 39 mm outcome of usefulness is 100%, which is twice more than during the use of billet of hexahedron 40 mm.

5. REFERENCES

1. Denisov P.I., Zuev D.B. Increasing deformation of free cutting steel for production of products by operation of cutting / Institute "Chermetinformatsia". Moscow. 1990 (Reference inform. Metalwire production. Prod.1. p.21.

2. Use of method Monte-Carlo for valuation of declination of free cutting steel for crack-formation / B.A.Nikiforov, P.I.Denisov, D.B.Zuev and others of MMMA: Magnitogorsk. 1991. p.8. Dep. of "Chermetinformasia". 1991. N 5967.

3. Modelling of crack formation of free cutting steels in the process of cold droffing / B.A.Nikiforov, P.I.Denisov, D.B.Zuev and others of MMMA. Magnitogorsk. 1991. p.8. Dep. in "Chermetinformatsia". 1991. N 5966.

MATEMATIČKO MODELIRANJE KALIBRACIJE ŠIPKI OD ČELIKA ZA AUTOMATE

Denisov P.I., Zuev D.B., Beliaev A.I., Nekit R.V.
Rudarsko-Metaluška Akademija, Magnitogorsk, Rusija

REZIME

Pojava pukotine kod šipki od čelika za automate je veoma aktuelan problem. Pred ove čelike postavljaju se dva kontradiktorna zahteva: da poseduju izvestan nivo plastičnosti, a sa druge da budu krti i da se dobro obrađuju na transfer mašinama.

U ovom radu dat je prikaz eksperimentalnih istraživanja ove problematike. Korišćena su tri različita materijala u obliku toplo valjanih šipki. Analiziran je $\sigma_{0.2}$ i λ_p kao i uticaj pojedinih faktora na te velične. Autori zaključuju da nivo $\sigma_{0.2}$ stoji u direktnoj proprcionalnosti sa plastičnošću; većem $\sigma_{0.2}$ odgovara i veća sposobnost deformabilnosti i obrnuto. Analiza je sprovedena preko dijagrama λ_p-σ/T (dijagram obradivosti).

Metodologija data u ovom radu preporučuje se kao prva kontrola materijala (šipki), pre proizvodnje raznih elemenata u daljem procesu deformisanja. Ova metodologija primenjena je u Magnitogorovskom metalurškom kombinatu.

Journal for Technology of Plasticity, Vol.22 (1997), Number 1-2

COMPUTER SIMULATION SYSTEM OF HEAT PRODUCTION DURING EXTRUSION OF ALUMINIUM ALLOYS

Petzov G., Markov V., Arsenov R.., Technical University, Varna, Bulgaria

ABSTRACT

This work get acquainted with the possibility of predicting and ruling the temperature variations in nonlubricated extrusion of aluminium sections by means of elaborated computer simulation system. The system is based on mathematical models of the metal flow through two-orifice flat die and the heat production due to plastic deformation and friction.

The computer system encloses Data base program with the thermal/physical constants, the reological behaviours of most widely used aluminium alloys and geometrical and energy characteristics of the extrusion tooling and equipment, as well as application software for computational operations. The system occurs to get solutions in dialogue mode.

1. INTRODUCTION

Manufacturing and applying of aluminium extruded production has trend to grow in last years. However, the crisis of energy and the scarcity of raw material resources has led to more economical using of these resorts. By grown use of aluminium sections in the structural engineering the necessity of technology for extruded sections obtained at minimum metal and energy loss is arising.

It is known that heat-treatable aluminium alloys have been processed to quenching at the press. This manner the hot-worked structure under extrusion can be retained and thereby a higher strengthening and efficiency of the quality can be achieved. According to the advanced scientific and production experience the advantages by quenching at the press are mainly greater productivity due to the shorting technological cycle, more uniform grain structure after suspended recrystallization and as result elevated service behaviours and lower manufacturing consumption in comparison to the conventional heat treatment.

The higher requirements to the quenching conditions require specifying and more effective control of the heat production, which takes foremost place in nonlubricated extrusion. This act depends mainly from the extrusion speed and ratio, as well as from the chemical composition of the aluminium alloys. By that, the temperature tends to become uniform throughout the extruded length.

For predicting temperature variations in the emerging product it is useful to apply computer simulation. Some existing program system built on finite element method (FEM) [1] are quite expensive to use in terms of required facilities. A partial solution for the heat generation in nonlubricated extrusion of round shape based on streamlined metal flow and experimental data for the temperature alteration during processing has been shown in our previous work [2]. For introducing such numerical simulation in industrial practice it is necessary to elaborate computer system disposing with a lot of databases for the variety of shapes produced from various aluminium alloys and for the extrusion equipment. Using in simulation formal approach, the solution should be improved to less formal approach by means of interactive conversation between designer and computer in dialogue mode. Dialogue systems posses essential advantages ensuring a permanent control of the computational process [3].

2. MODELS OF METAL FLOW AND TEMPERATURE VARIATIONS IN NONLUBRICATED EXTRUSION THROUGH TWO-ORIFICE DIE

Some general assumptions have been used in these models.

•In nonlubricated extrusion through flat die the appearing dead zones $\Omega^*_{1,2}$ form an flow angle $\alpha_k < 180°$ (**Fig.1**).

•The current extrusion ratio at various shapes and number of die orifice is determined by the cross-sectional surface relations

$$\lambda_i = \frac{\pi R_0^2}{qS_i}, \tag{1}$$

where i = 1,2,...,K is number of cross section with current surface S_i along the deformation area, q is number of the orifices.

•There exist under streamlined metal flow two velocity fields in the container [4]. The speed in the fields Ω_1 and Ω_2 nearly closed to the dead zone is lower than this in the central zone. So we have the relations:

$$v_{\rho i} = v_0 \lambda_i \cos\theta_j / \cos(\alpha_1 - \theta_j) \tag{2}$$

$$v^*_{\rho i} = b v_0 \lambda_i \cos\theta_j / \cos(\alpha_k - \theta_j) \tag{3}$$

$$b = \cos(\alpha_k - \theta_j)/\cos(\alpha_1 - \theta_j) \tag{4}$$

where v_0 is ram speed, $v_{\rho i}$ and $v^*_{\rho i}$ are flow velocities in the central and nearly the dead zone.

The angle of the central zone α_1 can be defined from the expression:

$$tan\alpha_1 + \left(\lambda_k^{1/2} - \lambda_k^{-1/2}\right) tan(\alpha_1 / 2) = 2l_P / \left[2a(\lambda_k^{1/2} - 1\right] \qquad (5)$$

where λ_K is the final extrusion ratio at the die exit, l_P - length of the isochrone beginning at point A; l_P requires experimental determination.

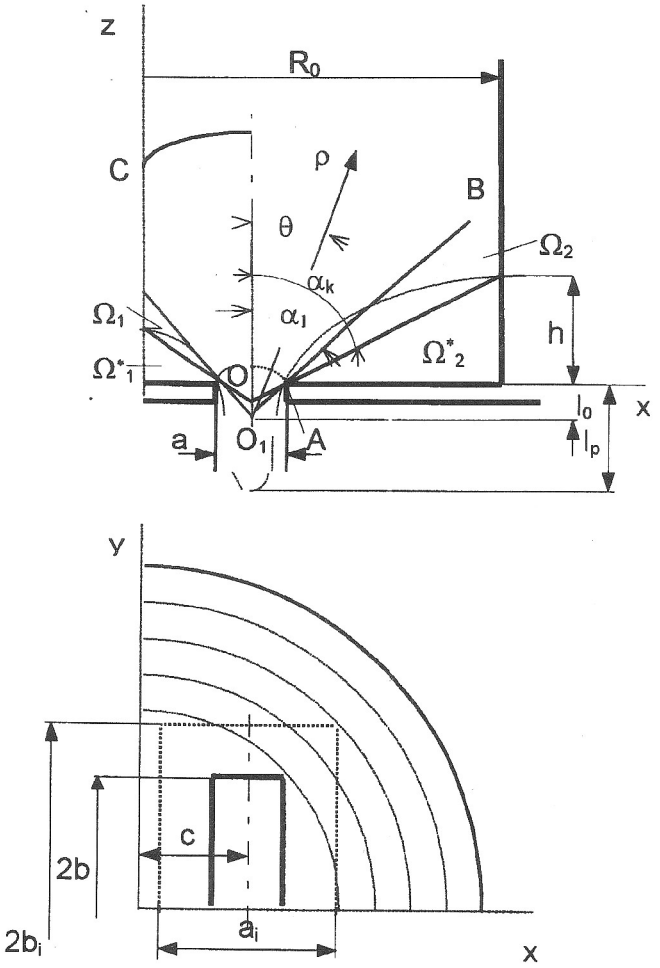


Fig. 1. Model of the deformation zone (right half) in extrusion through two-orifice die.

•The variable strain-rate and strain resistance in the deformation area are determined by

$$\dot{\bar{\varepsilon}}_j = 2v_0 \cos\theta_j \frac{\lambda_i}{\rho_i}\sqrt{1+1/12\tan^2\theta_j}, \tag{6}$$

$$\sigma_{wi} = \left\{\sigma_0 \dot{\bar{\varepsilon}}^{n_0} + D\exp\left(-\frac{\varepsilon_i}{\varepsilon_{x1}\dot{\bar{\varepsilon}}^{n_1}}\right) - \left(\sigma_0 \dot{\bar{\varepsilon}}^{n_0} - \sigma_E \dot{\bar{\varepsilon}}^{nE}\right)\left[1-\exp\left(-\frac{\varepsilon_i}{\varepsilon_{x2}\dot{\bar{\varepsilon}}^{n_2}}\right)\right]^{\frac{T}{T_b}}\right\} \exp\left[n_T\left(1-\frac{T}{T_b}\right)\right], \tag{7}$$

where $\varepsilon_i = \ln\lambda_i$, σ_0 , σ_E , D, ε_{x1} , ε_{x2} are characteristics of the strain resistance, $\dot{\bar{\varepsilon}}^{n_{0,1,2,E}}$ are strain-rate factors, n_T - temperature factor, T and T_b are current and basic temperatures of the extruded metal in the Shvartsbart relation [5].

•The temperature at the exit is influenced by heat generation due to plastic deformation, friction between the deforming material and heat transfer to the dead zones. The heat transfer within the billet and throughout the tooling are negligible in case of preheated container to the billet temperature.

The temperature rise along a flow line is expressed by

$$\Delta T_j = \sum_{i=1}^{K}\left\{\left[A\frac{\sigma_{wij}\dot{\bar{\varepsilon}}_{ij}\Delta\rho_i}{\rho_m c_m\sqrt{3}v_{ij}} + A_1\frac{\tau_{kij}\Delta v_{ij}F_C\Delta\rho_i}{\rho_m c_m V_C v_{ij}}\right] - H^*\left[T(\omega_{1,2}) - T(\omega^*_{1,2})\right]\right\} \tag{8}$$

where $\Delta\rho = \rho_i - \rho_{i-1}$ is the calculation step along the deformation area, ρ_m , c_m are thermophysical constants of the formed metal, A and A_1 are characteristics of the heat production in extrusion. By F_C/V_C is denoted the relative friction surface and by Δv_{ij} - the relative friction speed. The frictional shear stress τ_k is given by

$$\tau_{ki} = m(\sigma_{0i})/\sqrt{3} \tag{9}$$

where (σ_{0i}) is the average over the used strain-rate range flow stress and m is the friction factor - $m = 0{,}7 \div 1$ [6].

H* is relative coefficient of heat transfer to the dead zone with temperature $T(\Omega^*_{1,2}) \cong T_0$. where T_0 is the billet temperature.

The average in cross section temperature at the die exit can be calculated from

$$\langle T_A \rangle = T_0 + \sum_{J=1}^{N}\Delta T_{K,J}/N, \tag{10}$$

where $\Delta T_{K,j}$ is the total temperature rise of each flow line according (8) in the range $1 \le j \le N$.

•The temperature variations of the extruded product to a steady-stay may be described by the approximate expression:

$$T_E = \langle T_A \rangle + (T_S - \langle T_A \rangle)(t/t_S)^m , \tag{11}$$

where T_S is temperature and t_S - time for attaining the steady-state process. The value of these variables and the exponent m is experimentally definable, as will be shown later.

•The variable temperature at the initial stage of extrusion ought to be limited to within the temperature interval

$$T_{Wmin} \leq T_E \leq T_{Qmax} \tag{12}$$

where T_W, T_Q are temperature limits of hot workability and tempering (in case of quenching at the press) respectively.

At commonly used temperature-speed parameters of extrusion the temperature difference between tempering and forming for middle-strength aluminium alloys is about 50 °C [6] and may be shortened by intensified heat production.

3. DEVELOPMENT OF COMPUTER SIMULATION SYSTEM

In coincidence with the functional requirements to numerical simulation of technological processes the system consists three general modules (**Fig.2**):

•*Relational data base*

•*Data scheduler*

•*Computational module*.

On this stage of development it is possible without an optimization module.

The *Relational data base* encloses all relevant thermal/physical constants and reological properties as strain resistance, temperature limits of maximum plasticity and quenching, upper extrusion temperature and limitations of extrusion speed for the most widely used heat-treatable aluminium alloys AlMgSi and $AlCu_4Mg$. They are devised in several groups in coincidence with the variations of chemical composition and strengthening level. Here are involved geometry of the shapes under extrusion and dimensions of the tooling for 12.5, 16 and 25 MN hydraulic press, as well as relevant technological parameters - extrusion ratio, temperatures and speeds. As processing media the *dBase III* software has been used.

A part of the data base information is submitted to processing by application programs. The program *Dimension* deals with the cross-section reducing of the billet in relation with the extrusion ratio, *Speed* takes care of the speed limitations. The program *Sigma* computes strain resistance and its characteristics according the approximation (7). The primary data for three base temperatures and strain-rates are taken from Ref.[7].

The *Data scheduler* realises setup of the system into conditions of the simulation experiment. The call of data can be executed in two operating modes. The automated call takes place after verification of the operated base data for the current experiment. Some decisions may be taken in dialogue mode.

The program generated polar mesh is a ground for projecting the results of the computed temperatures in the *Computational* module and thereby creates the extrusion temperature files. The algorithm of these calculations including a coupled mechanical-thermal solution is given in Ref.[4]. The application programs are built in *Pascal*.

The calculations obtained in the *Computational* module are middling. The results may be taken as suitable after their comparing with the temperature limitations according (11), (12)

and the upper extrusion temperature for the alloy under consideration. Then follows graphical representation of the temperature field by isometric lines, using *Matlab for Windows*, and safety of these files in *Library*.

In case of discrepancy the simulation experiment ought to be repeated with some corrections of the input data.

The system built allows to be enhanced with new data for aluminium alloys and section shapes.

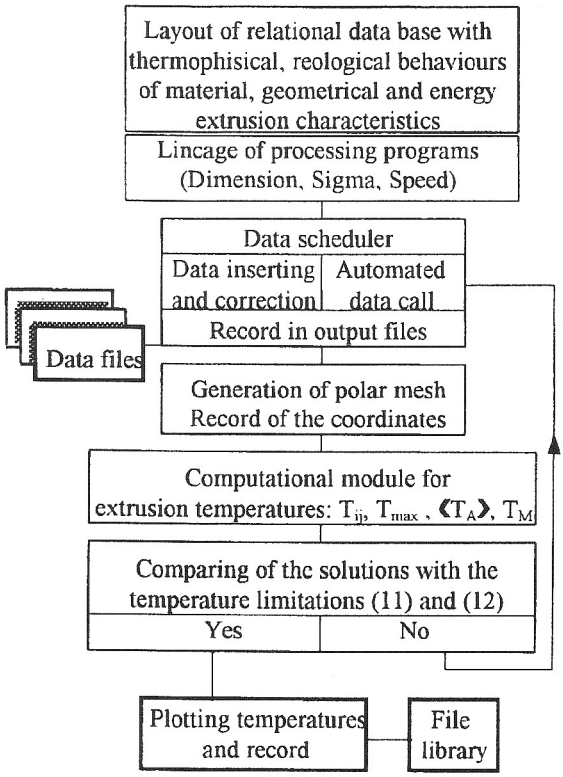


Fig.2. Block diagram of the computer simulation system

4. NUMERICAL SIMULATION AND EXPERIMENTAL RESULTS

For preliminary test of the simulation system the extrusion of $AlMgSi_{0,5}$ - alloy was investigated. The operating conditions were set to those used on 12,5 MN hydraulic press of "Alumina" Shoumen.

The container employed had diameter 0,15 m and the dimensions of the two-hole die were a = 0,045 m, 2b = 0,05 m and c = 0,025 m according to Fig.1. The single logarithmic extrusion ratio was $\ln\lambda = 3{,}6$. After experiments was found that $l_P \cong 3a$. The ram speed taken at

middle level was v_0 = 0,26 m/min. As variable technological parameter the initial temperature of the billet over the range 420 - 460 °C was used. The container was pre-heated to the same temperature.

For computations the following thermal/physical data are taken: ρ_m = 2770 kg/m^3, c_m = 940 J/(kg.grad), λ_m = 210 J/(s.m grad), (σ_{0i}) = 37,1 MPa and 24,2 MPa relatively to the temperatures 420 and 460 °C, A = 1, A_1 = 0,5, m = 0,8.

The mesh with 11 x 25 = 275 elements was generated properly to the model of metal flow. The steep number taken down the deformation area occurs an easy fit of the heat generation.

Calculated by the computer simulation system temperatures in extrusion through isometric lines are shown in **Fig. 3**. The maximum temperature effect $\Delta T = T_A - T_0$ about 70 °C was obtained at initial temperature 420 °C because of the higher strain resistance leading to intensified heat production. In extrusion at 460 °C the temperature rise is lower - about 50 °C and $\langle T_A \rangle$ attains nearly the required tempering temperature.

Further augmentation of the temperature is appearing to the steady-state of extrusion. The temperature computed according to (11) is represented and compared to experimental data in **Fig.4**. By using these experimental results the values of the exponent were determined over the range m = 0,2 - 0,25 responding to temperatures 460 °C and 420 °C. At the present extrusion conditions the initial temperatures 460 °C reaches to about 525 °C and thereby occurs the requirement in (12).

The theoretical curves approximate well the experimental results, from which follows that the steady-state at lower billet temperature appears later than at 460 °C. As result it may be expected an increasing of the properties uniformity of the extruded section.

A further improving of the extrusion schedule respecting the heat production can be realised by means of the elaborated computer system by varying with the extrusion speeds.

5. CONCLUSION

As a mater of record it was established that the thermal activation during extrusion can be prescribed and controlled by numerical simulation.

In order to provide temperature of the extruded AlMgSi-alloy nearly closed to the tempering temperature it is desirable to keep relatively low work hardening, i.e., the billet temperature must not be lower than 460 °C. The combination with logarithmic extrusion ratio not less than 3,5 and exit speed over the range 5 - 15 m/min leads to considerable rise in temperature about 65 °C.

Further limiting the uniformity of the mechanical properties of the extruded product is achievable by shortening the unsteady stage of extrusion. There exist some solutions like this by using steeply decreasing ram speed in the beginning of extrusion (K. Laue, 1960).

The present computer system permits predicting of the temperature variation to the steady-state of extrusion and its controlling in the limits required for several aluminium alloys.

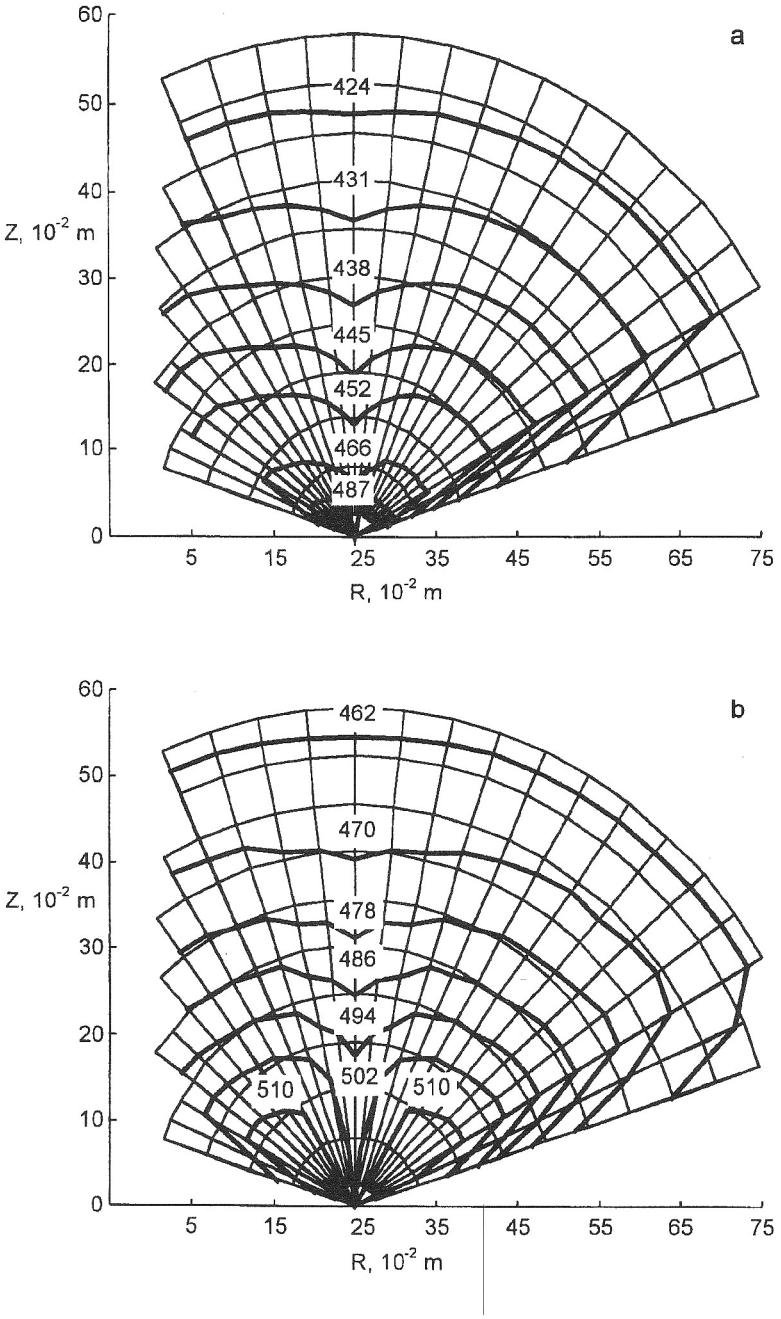


Fig. 3. Temperature fields in extrusion area after initial temperatures, °C: 420 (a), 460 (b).

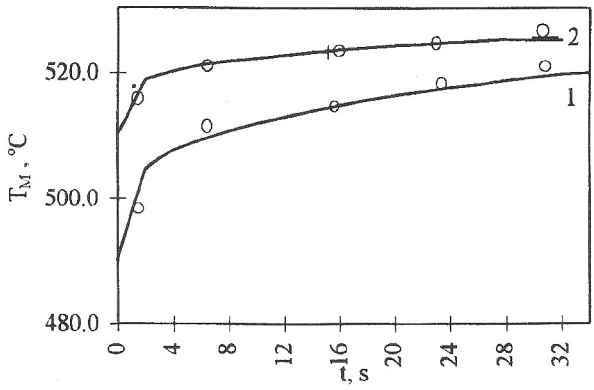


Fig. 4. Computed temperature alterations of $AlMgSi_{0,5}$ at the die exit after initial extrusion temperatures, °C: 420 (1) and 460 (2); o - experimental results.

REFERENCES

[1] Oh S.-I.: Finite Element Analysis of Metal Forming Processes with Arbitrarily-Shaped Dies, Int. J. Mech. Sci., 24 (1982), 479.

[2] Petzov G.: Specifying and optimizing of the thermomechanical conditions during the extrusion of reinforced $AlCu_4Mg_1$ bars, J. Mat. Proc. Technology, Elsevier, 53 (1995), 827-836.

[3] Guhn G., A. Averchenko: Elaboration and realisation of computer dialogue desing method in metal forming (in Russian), Theory and technology of metal- and energy-cconomical metal forming processes, Metallurgia (Moscow) (1986), 21-32.

[4] Petzov G., L. Kovachev: Simulation model of the thermoplastic process in flat-die extrusion (in Bulgarian), Actual Problems of Metal Forming, (Varna) (1995), 35-38.

[5] Zuev, L., G. Nikitin: (in Russian), Izv. AN USSR, Metally (1984), 1, 138-144.

[6] Altan, T. et al.: Metal Forming, ASM, Metals Park (1986), 85.

[7] Polukhin P. et al.: Strain resistance of metals and alloys (in Russian), Handbook, Metallurgia (Moscow) (1983), 251-265.

SISTEM KOMPJUTERSKE SIMULACIJE RAZVOJA TOPLOTE ZA VREME ISTISKIVANJA ALUMINIJUMOVIH LEGURA

Petzov G., Markov V., Arsenov R.
Tehnički Univerzitet u Varni, Bugarska

REZIME

U radu je opisana mogućnost određivanja i upravljanja temperaturom i njenim promenama za vreme istiskivanja aluminijumovih legura. To određivanje i kontrola se vrši pomoću u radu prezentiranog kompjuterskog simulacionog sistema. Sistem sadrži datoteku sa fizičko/termičkim konstantama, reološke parametre, kao i geometrijske i energetske karakeristike alata i opreme. Pored toga u okviru sistema je i aplikacioni software. Ovaj deo programa sadrži algoritam proračuna uključujući mehaničko termička rešenja. Program je kreiran u Pascalu. Omogućena je dogradnja (obogaćivanje) programa novim podacima. Sistem funkcioniše u dijalogu.

Analizirano je istiskivanje AlMg6 legure sa stepenom istiskivanja 3.5 i brzinom 5 do 15 m/min. Ovakvi režimi obrade dovode do rasta temperature za 65°C.

Prikazani sistem onogućava analizu stacionarnih procesa istiskivanja i upravljanja njihovim termičkim karakteristikama za nekoliko vrsta aluminijumovih legura.

Journal for Technology of Plasticity, Vol 22 (1997), Number 1-2

CONTACT STRESSES AND DEFORMATION LOAD IN UPSETTING OF CYLINDER BETWEEN SPHERICAL AND FLAT DIES

Vilotić D., Plančak M., Vujović V., Milutinović M., Skakun P.
Faculty of Technical Sciences - University of Novi Sad, Yugoslavia

ABSTRACT

As it is known, in the processes of bulk cold metal forming, tool and billet geometry has a great influence on stress-strain state and material deformability. For that reason, in this paper, stress state and process parameters in upsetting of cylinder by spherical and flat dies have been analyzed. Stress components were determined by using the method of solving approximate equilibrium equation, whereas forming load was obtained by integration of normal contact stresses.

1.0 INTRODUCTION

Processes of upsetting describe the basic operations which investigation play a great role in designing of technology of bulk metal forming.

In the Laboratory of Technology of Plasticity - University of Novi Sad, for a long time, theoretical and experimental investigation of stress-strain states, process parameters and material deformability has been conducted where special attention was paid to processes of upsetting. The influence of tool and billet geometry on relevant process parameters and material behavior from the deformability potential point of view has been investigated as well.

In this paper theoretical analysis of contact stresses and forming load in the case of upsetting by combination of spherical (top die) and flat (bottom die) dies, has been carried out. In the table which shows scheme of processes of upsetting by different combinations of top and bottom dies, upper quoted die is defined as model 3.3 [1]. Contact stresses were determined by using the method of solving approximate equilibrium equation (SLAB metod), where real yield stress over the radius of plane was involved. Concrete estimate was made for plane from steel C1431(DIN: Ck35).

2.0 CONTACT STRESSES AND FORMING LOAD

The scheme of upsetting of cylinder with stress components is shown on Fig. 1. Analysis of stress-strain state has been accomplished by using some assumptions and simplifications as it had been done at the process of upsetting by spherical die [1].

- All plane sections parallel to the axis of cylinder remain plane during the upsetting.
- The height of plane out from the zone of contact between workpiece and die, is constant (H=const., Fig. 1)
- Tangential contact stress τ_k is proportional to normal stress σ_n and friction coefficient μ:

$$\tau_k = \mu \cdot \sigma_n \tag{1}$$

- Radial stress σ_r is equal to tangential stress σ_t

$$\sigma_r = \sigma_t \tag{2}$$

- For the assumed stress scheme presented on Fig. 1, yield criteria is:

$$\sigma_n - \sigma_r = K \tag{3}$$

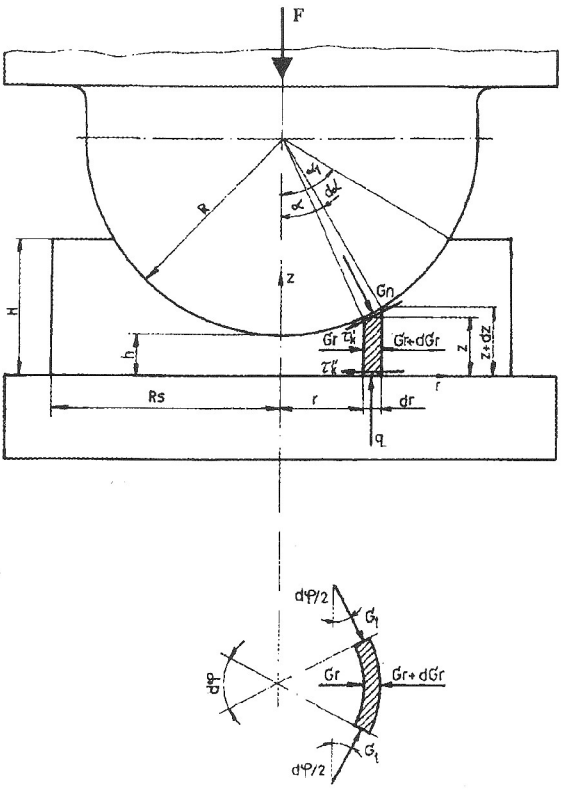


Fig. 1 – Stress scheme in upsetting of cylinder between spherical and flat dies

In accordance with the stress scheme presented on Fig. 1, the basic equilibrium equation of all load components in the radial direction is:

$$\sigma_r \cdot r \cdot d\varphi \cdot z - (\sigma_r + d\sigma_r) \cdot (r + dr) \cdot (z + dz) \cdot d\varphi + \sigma_n \cdot r \cdot d\varphi \cdot \frac{dr}{\cos\alpha} \cdot \sin\alpha - \\ - \mu \cdot \sigma_n \cdot r \cdot \frac{dr}{\cos\alpha} dr \cdot \cos\alpha - \mu \cdot q \cdot r \cdot d\varphi \cdot dr + 2 \cdot \sigma_t \cdot \frac{z + (z + dz)}{2} dr \cdot \sin\frac{d\varphi}{2} = 0 \tag{4}$$

After transformations of equation (4) by using latter presumption and simplifications, the following expression has been obtained:

$$d\sigma_r \cdot z + \sigma_r \cdot dz - \sigma_n \cdot (tg\alpha - \mu) \cdot dr + \mu \cdot q \cdot dr = 0 \tag{5}$$

The connection between stresses σ_n and q, can be achieved by setting equilibrium equation in radial direction, and it gives:

$$q = \sigma_n \cdot (1 + \mu \cdot tg\alpha) \tag{6}$$

If we accept:

$$\sigma_n = q \tag{7}$$

to the first order of small quantities, the equation (5) is reduced to:

$$d\sigma_r \cdot z + \sigma_r \cdot dz - \sigma_n \cdot tg\alpha \cdot dr = 0 \tag{8}$$

Elimination of radial contact stress σ_r from upper equation, was made by using the yield criteria (3), where K≠const. It means that the first derive of yield criteria is:

$$d\sigma_n = d\sigma_r + dK \tag{9}$$

so, expression (8) becomes:

$$\frac{(d\sigma_n - dK)}{dr} \cdot z + (\sigma_n - K) \cdot \frac{dz}{dr} - \sigma_n \cdot tg\alpha \cdot dr = 0 \tag{10}$$

Moreover, yield stress **K** has been assumed on the next analytical form:

$$K = K_0 + A \cdot \varphi_e^b \tag{11}$$

where are:

K_0, A, b – constants for the given material

$\varphi_e = Ln\frac{H}{z}$ – effective strain

Substituting (11) in (10), and using next geometrical relation obtained from the scheme (fig. 1):

$$\begin{aligned} z &= R\cdot(a-\cos\alpha) & dz &= R\cdot\sin\alpha\, d\alpha \\ r &= R\sin\alpha & dr &= R\cos\alpha\, d\alpha \\ a &= \frac{h}{R}+1 & \frac{dz}{dr} &= tg\alpha \end{aligned} \tag{12}$$

the final differential equilibrium equation can be written in the form:

$$\frac{d\sigma_n}{d\alpha}+2\cdot\mu\cdot\sigma_n\frac{\cos\alpha}{a-\cos\alpha}= \left(K_0+A\cdot\left[Ln\frac{H}{R\cdot(a-\cos\alpha)}\right]^b-A\cdot b\cdot\left[Ln\frac{H}{R\cdot(a-\cos\alpha)}\right]^{b-1}\right)\cdot\frac{\sin\alpha}{a-\cos\alpha} \tag{13}$$

The numerical solution of equation (13) for σ_n, has been obtained by using following boundary condition:

$$for\quad r=R_1\quad\Rightarrow\sigma_{r1}=1.1\cdot Ln\frac{R_s}{R_1} \tag{14}$$

Yield stress K_1 has been determined on the base of effective strain φ_{e1}, which represents the possible change of billet's dimension for the observed die stroke:

$$\varphi_{e1}=\frac{2}{\sqrt{3}}\cdot Ln\frac{R_s}{R_1} \tag{15}$$

The forming load **F** is obtained by integration of contact stresses:

$$F=2\pi\cdot R^2\cdot\int_0^{\alpha_1}\sigma_n\cdot(\sin\alpha\cdot\cos\alpha+\mu\cdot\sin^2\alpha)\,d\alpha \tag{16}$$

The illustrations of theoretical solution of contact stress (fig. 2, fig. 3, fig. 4) as well as forming load (fig. 5) are given for the billets with initial geometry: ϕ 30x10mm, ϕ 30x15mm and ϕ 30x20mm, made from C1431 (DIN: Ck35). The flow curve for the given material has been obtained by Rastegaev test, and following expression was determined:

$$K=312.2+720.29\cdot\varphi_e^{0.344928}[MPa] \tag{16}$$

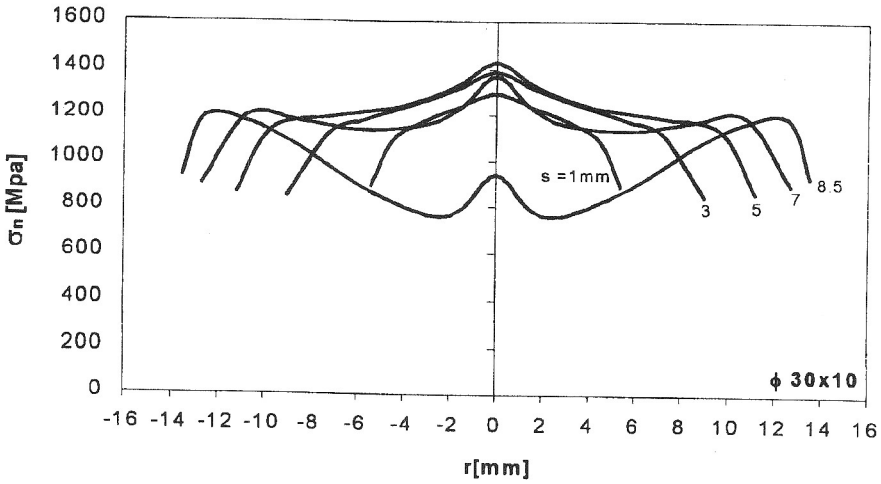


Fig. 2 – Distribution of normal contact stress for specimen ϕ30x10

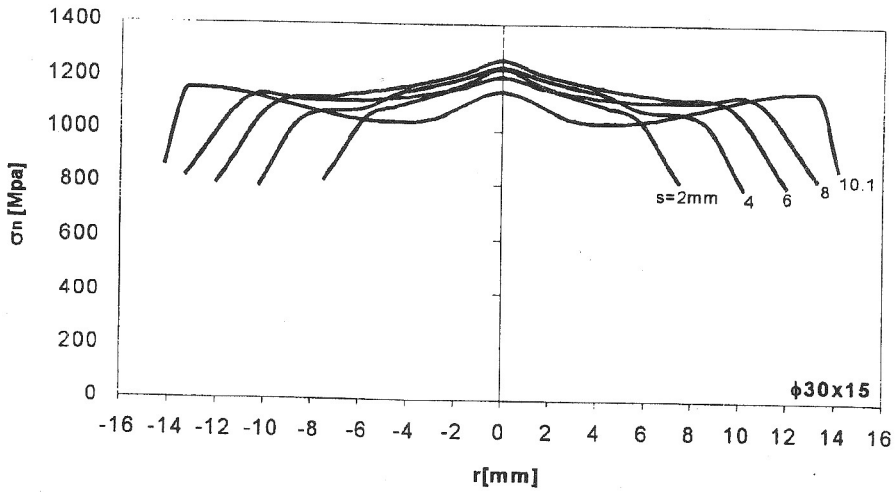


Fig. 3 – Distribution of normal contact stress for specimen ϕ30x15

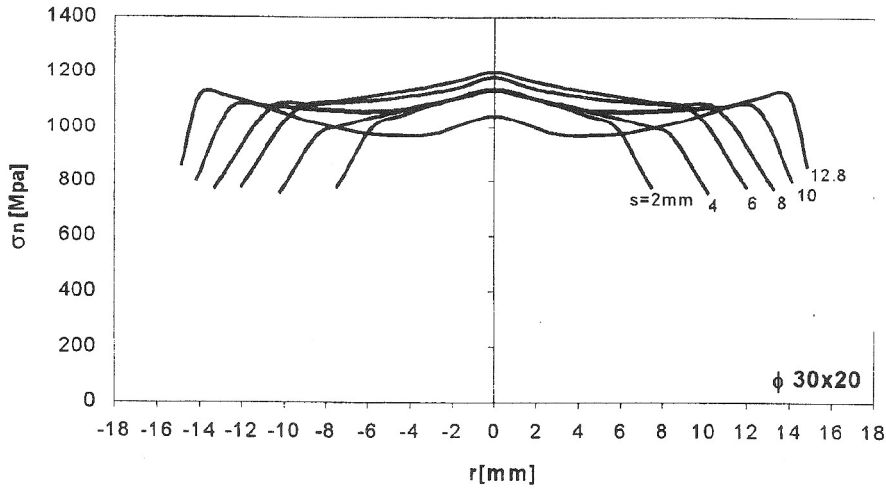


Fig. 4 – Distribution of normal contact stress for specimen ϕ30x20

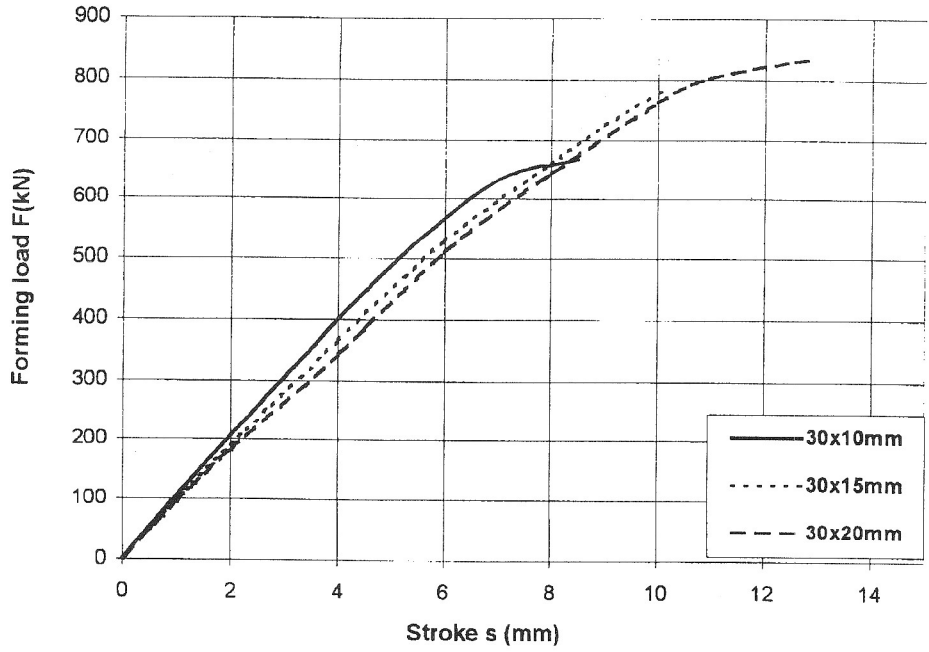


Fig. 5 – Forming load-die stroke diagram

3.0 CONCLUSION

Theoretical solution for contact stresses in upsetting of cylinder by spherical and flat dies, presented in this paper, is one of some possible, that was received by using simple method of solving approximate equilibrium equation. As it can be seen, the diagrams of normal stresses of analyzed specimen (fig. 2, fig. 3, fig. 4) completely correspond by the form to the diagrams of normal stresses in the case of upsetting by two identical spherical dies [1]. However, the values of normal stresses in the case of upsetting by the combination of spherical and flat dies are something higher than in the case when both dies are spherical. This gives higher values of forming load too.

LITERATURE

1. Vilotic, D., Plancak, M., Vujovic, V., Milutinovic, M., Gelei, S.:
Theoretical Solution of Contact Stresses and Forming Load in Upsetting of Cylinder by Spherical Dies. Journal for Technology of Plasticity, Vol. 21, No. 1-2, pp. 1-9, Faculty of Technical Sciences, Novi Sad, 1993.

2. Johnson, W.:
Plasticity for Mechanical Engineers. Van Nostrand Reinholds Company, London, 1962.

3. Musafija, B.:
Theory of Plasticity (in Serbian). University of Sarajevo.

4. Storozev, M.V., Popov, E.V.:
Theory of Plasticity (in Russian). Masinostroenie, Moscow, 1971.

5. Vilotic, D.:
Steel Material Behavior in Different Working Systems of Bulk Cold Deformation Processes (in Serbian). University of Novi Sad, 1987.

6. Vilotic, D., Vujovic, V., Plancak, M., Trbojevic, I., Francuski, P.:
General Solution of Contact Stress and Forming Load in Upsetting of Cylinder by Conical Dies. Journal for Technology of Plasticity, Vol. 18, No. 1-2, pp. 59-65, Faculty of Technical Sciences, Novi Sad, 1993.

7. Vilotic, D., Plancak, M., Vujovic, V., Trbojevic, I., Milutinovic, M.:
Analysis of Upsetting of Cylinder by Spherical Dies (in Serbian). Proceedings of the Conference of Plasticity, Budva, Yugoslavia, 1996.

KONTAKTNI NAPONI I DEFORMACIONA SILA PRI SABIJANJU VALJKA POMOĆU SFERIČNE I RAVNE PLOČE

Vilotić D., Plančak M., Vujović V., Milutinović M., Skakun P.
Fakultet tehničkih nauka, Novi Sad, Yugoslavia

REZIME

Kao što je poznato, sabijanje valjka može se vršiti alatima (pločama) čije radne površine mogu biti ravne, konusne, sferične ili konbinovane. U ovom radu razmatran je problem sabijanja valjka pomoću alata kod kojeg je gornji element sferičnog oblika, a donji ravna ploča. Ovakav postupak sabijanja ima određeni značaj za operacije slodobnog kovanja, utiskivanja, i istiskivanja. U ovom radu prikazano je teorijsko rešenje za kontaktne napone i deformacionu silu.

Kontaktni naponi određeni su metodom rešavanja približne jednačine ravnoteže na osnovu šeme napona prema sl.1. Deformaciona sila određena je numeričkom integracijom kontaktnog napona.

Vrednosti izračunatih napona i sila za uzorke od Č. 1431 su nešto više u odnosu na iste veličine dobijene kod sabijanja valjka sa dva identična sferična alata.

Journal for Technology of Plasticity, Vol.22 (1997), Number 1-2

APPLICATION OF WORKABILITY DIAGRAM AND DISCONTINUOUS VELOCITY FIELDS TO FRACTURE ANALYSIS DURING METAL FORMING PROCESS

Alexandrov S., Institute for Problems in Mechanics, Russian Academy of Science, Moscow, Russia*

ABSTRACT

An approximate method for analysis of fracture during metal forming operations is proposed. The method is based on discontinuous velocity fields and a workability diagram and is applicable for rigid/plastic, hardening materials with the plastic work as a hardening parameter. For such materials, the approximate relationship across velocity discontinuity surfaces can be obtained by applying the divergence theorem. This relationship may be used to account for a contribution of velocity discontinuity surfaces in the fracture process. Predictions of fracture initiation are based on the workability diagram which is written in terms of the triaxiality ratio and the plastic work. Using the plastic work instead of the equivalent plastic strain allows one to account for a contribution of velocity discontinuity surfaces in the fracture process in simple manner. As an example of the application of the method, extrusion (drawing) of round rods is considered.

1. INTRODUCTION

A few approaches are used to predict fracture during metal forming operations. Avitzur [1], Avitzur and Choi [2], and Turczyn [3] have applied the classical upper bound theorem to predict the appearance of defects of infinitesimal size during extrusion and rolling. No fracture criterion has been adopted in these studies. The classical upper bound theorem has been modified by Alexandrov and Goldstein [4] to include the appearance of cracks of finite size. This variational principle has been based on the maximum tensile stress fracture criterion. The application of this approach to rolling of three-layer sheets has been given by Alexandrov and Chicanova [5]. Also, this approach

*Currently with GKSS Research Center, Institute of Materials Research, Geesthacht, Germany

Journal for Technology of Plasticity, Vol.22 (1997), Number 1-2

APPLICATION OF WORKABILITY DIAGRAM AND DISCONTINUOUS VELOCITY FIELDS TO FRACTURE ANALYSIS DURING METAL FORMING PROCESS

Alexandrov S., Institute for Problems in Mechanics, Russian Academy of Science, Moscow, Russia*

ABSTRACT

An approximate method for analysis of fracture during metal forming operations is proposed. The method is based on discontinuous velocity fields and a workability diagram and is applicable for rigid/plastic, hardening materials with the plastic work as a hardening parameter. For such materials, the approximate relationship across velocity discontinuity surfaces can be obtained by applying the divergence theorem. This relationship may be used to account for a contribution of velocity discontinuity surfaces in the fracture process. Predictions of fracture initiation are based on the workability diagram which is written in terms of the triaxiality ratio and the plastic work. Using the plastic work instead of the equivalent plastic strain allows one to account for a contribution of velocity discontinuity surfaces in the fracture process in simple manner. As an example of the application of the method, extrusion (drawing) of round rods is considered.

1. INTRODUCTION

A few approaches are used to predict fracture during metal forming operations. Avitzur [1], Avitzur and Choi [2], and Turczyn [3] have applied the classical upper bound theorem to predict the appearance of defects of infinitesimal size during extrusion and rolling. No fracture criterion has been adopted in these studies. The classical upper bound theorem has been modified by Alexandrov and Goldstein [4] to include the appearance of cracks of finite size. This variational principle has been based on the maximum tensile stress fracture criterion. The application of this approach to rolling of three-layer sheets has been given by Alexandrov and Chicanova [5]. Also, this approach

*Currently with GKSS Research Center, Institute of Materials Research, Geesthacht, Germany

in Fig.1. β is the triaxiality ratio

$$\beta = 3\sigma/\sigma_{eq} \tag{1}$$

where σ is the hydrostatic stress and σ_{eq} is the equivalent stress defined by

$$\sigma_{eq} = \sqrt{(3/2)s_{ij}s_{ij}} \tag{2}$$

where s_{ij} are the components of the deviatoric stress tensor. ε_{eq} is the equivalent strain defined by the following equation

$$\dot{\varepsilon}_{eq} = \sqrt{(2/3)\xi_{ij}\xi_{ij}} \tag{3}$$

where ξ_{ij} are the components of the strain rate tensor and the superposed dot denotes the material time derivative. The von Mises yield criterion is given by

$$\sigma_{eq} = \sigma_Y \tag{4}$$

where σ_Y is the yield stress in tension. Usually, it is assumed that σ_Y is a function of ε_{eq}. However, it is easy to show that ε_{eq} can be replaced by the plastic work, W_p, which is defined by the following equation

$$\dot{W}_p = \sigma_{ij}\xi_{ij} \tag{5}$$

where σ_{ij} are the components of the stress tensor. Due to the incompressibility equation, (5) can be rewritten in the form

$$\dot{W}_p = s_{ij}\xi_{ij} \tag{6}$$

The flow rule associated with the yield criterion (4) is given by

$$\xi_{ij} = \frac{3}{2}\frac{\dot{\varepsilon}_{eq}}{\sigma_Y}s_{ij} \tag{7}$$

Combining (6) and (7), with the use of (2) and (4), we arrive at

$$\dot{W}_p = \sigma_Y\dot{\varepsilon}_{eq} \tag{8}$$

If σ_Y is a prescribed function of ε_{eq} then (8) can be integrated to give W_p as a function of ε_{eq}. After this, σ_Y can be determined as a function of W_p. In the following we assume that σ_Y is a prescribed function of W_p.

As an example, we consider the workability diagram for the C1431 steel (Serbian standard) of the following chemical composition: 0.32-0.39% *C*, 0.15-0.35% *Si*, and 0.5-0.8% *Mn*. The stress strain curve of this material may be approximated by [17]

$$\sigma_Y = 720.29\left(0.435 + \varepsilon_{eq}^{0.345}\right) \quad \text{[MPa]} \tag{9}$$

with sufficient accuracy. Vilotic [17] has conducted tests to determine the shape of the workability

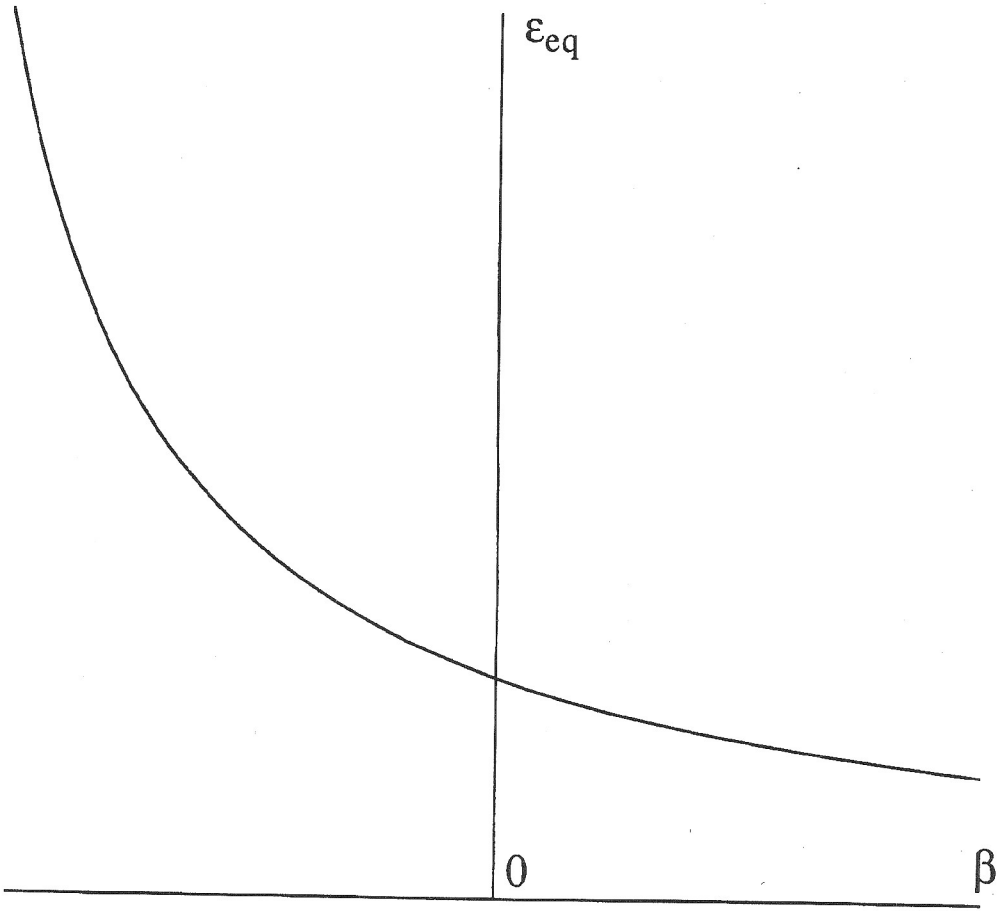


Fig.1. Schematic representation of the workability diagram proposed by Vujovic and Shabaik [12].

diagram proposed in [12]. He has found the critical values of the equivalent strain to fracture as follows: $\varepsilon_{eq} = 0.133$ at $\beta = 1$ (uniaxial tension), $\varepsilon_{eq} = 0.663$ at $\beta = 0$ (pure torsion), and $\varepsilon_{eq} = 1.291$ at $\beta = -0.96$ (near uniaxial compression). This workability diagram is shown in Fig.2[a]. Additional tests, compression with cylindrical dies, have been conducted by Vilotic [17] and investigated theoretically by Alexandrov et. al [18]. These results have confirmed the shape of the workability diagram shown in Fig.2[a]. Combining (8) and (9) we obtain

$$\dot{W}_p = 720.29\left(0.435 + \varepsilon_{eq}^{0.345}\right)\dot{\varepsilon}_{eq} \tag{10}$$

At the beginning of plastic deformation $W_p = 0$ and $\varepsilon_{eq} = 0$. Using this condition, equation (10) can be integrated to give

$$W_p = 720.29\varepsilon_{eq}\left(0.435 + \varepsilon_{eq}^{0.345}/1.345\right) \tag{11}$$

Equations (9) and (11) determine σ_Y as a function of W_p in implicit form. Using the experimental results given above we may find the critical values of W_p to fracture from (11) as

$W_p/W_p(1) = 0.091$ at $\beta = 1$, $W_p/W_p(1) = 0.608$ at $\beta = 0$ and $W_p/W_p(1) = 1.366$ at $\beta = -0.96$

where $W_p(1) = 848.86$ MPa is the value of W_p at $\varepsilon_{eq} = 1$. The workability diagram based on these data is shown in Fig.2[b].

3. RELATIONSHIP ON VELOCITY DISCONTINUITY SURFACES

If the velocity components, v_i, are given by differentiable functions then equation (5) can be rewritten in the following form

$$\partial W_p/\partial t + \left(W_p v_i\right)_{,i} = \left(\sigma_{ij} v_i\right)_{,j} \tag{12}$$

where we have taken the equilibrium equations, $\sigma_{ij,j} = 0$, and the incompressibility equation, $v_{i,i} = 0$, into account. Equation (12) is written in divergent form, therefore, the divergence theorem can be applied to determine the jump conditions across velocity discontinuity surfaces. Using the standard procedure (see, for example [16]) we obtain

$$v_n\left[W_p\right] = \left[\sigma_Y v_\tau\right]/\sqrt{3} \tag{13}$$

with the usual square brackets notation for the amount of jump. v_τ is the velocity tangent to the velocity discontinuity surface. The normal velocity, v_n, must be continuous. In exact formulation, σ_Y must also be continuous [16]. However, in our approximate analysis we assume that σ_Y may be discontinuous. This means that it is not always possible to satisfy the equilibrium equations across velocity discontinuity surfaces. Note that many approximate methods violate the

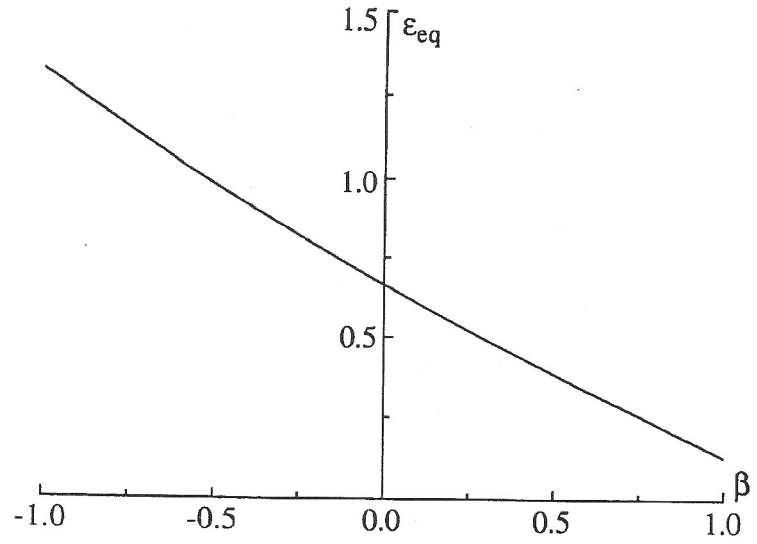


Fig.2[a]. Workability diargam proposed in [12] for the C1431 steel.

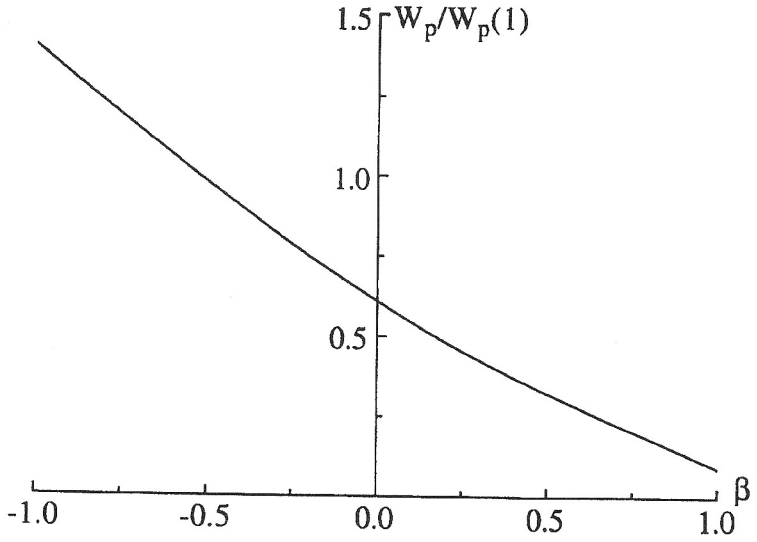


Fig.2[b]. Modified workability diagram for the C1431 steel.

equilibrium equations, for example the upper bound method. Since σ_Y is a prescribed function of W_p, equation (13) gives the relationship between $[W_p]$ and $[v_\tau]$ across velocity discontinuity surfaces. This relationship may be used to evaluate a contribution of such surfaces in fracture initiation.

Note that another method to deal with discontinuous velocity fields in rigid/plastic, hardening materials has been proposed by Korobkhin and Chudakov [19]. However, using the equations in divergent form provides a more direct approach.

4. EXTRUSION (DRAWING) OF ROUND RODS

Radial velocity fields are commonly used to describe the material flow during extrusion (drawing) [20, 21]. Usually, such fields involve velocity discontinuity surfaces. In order to illustrate the approach proposed, we consider the simplest field by assuming that the velocity discontinuity surfaces (l_1 and l_2 in Fig.3) coincide with coordinate surfaces ($r = R_0$ and $r = R_1$) of the spherical coordinate system $r\theta\varphi$ shown in Fig.3. R_0 and R_1 are also shown in Fig.3. In this case the velocity field in the deforming zone 2 (Fig.3) is given by

$$v_r = -v_0\left(R_0/r\right)^2 \cos\theta, \qquad v_\theta = 0, \qquad v_\varphi = 0 \tag{14}$$

where v_r, v_θ, and v_φ are the velocity components in the spherical coordinate system and v_0 is the velocity of the rigid zone 3. Using the incompressibility equation we may find the velocity of the rigid zone 1 in the form

$$v_1 = v_0\left(R_0/R_1\right)^2 \tag{15}$$

It follows from (14) that

$$\left[v_\tau\right] = v_0 \sin\theta \tag{16}$$

across the surface l_1 and from (14) and (15) that

$$\left[v_\tau\right] = v_0\left(R_0/R_1\right)^2 \sin\theta \tag{17}$$

across the surface l_2. Substituting (14), (16), and (17) into (13) gives

$$W_p^{(pl1)} = \tan\theta\,\sigma_Y^{(0)}/\sqrt{3} \tag{18}$$

on the surface l_1 and

$$W_p^{(r)} = \tan\theta\,\sigma_Y^{(r)}/\sqrt{3} + W_p^{(pl2)} \tag{19}$$

on the surface l_2. Here $W_p^{(pl1)}$ is the plastic work on the plastic side of the rigid/plastic boundary

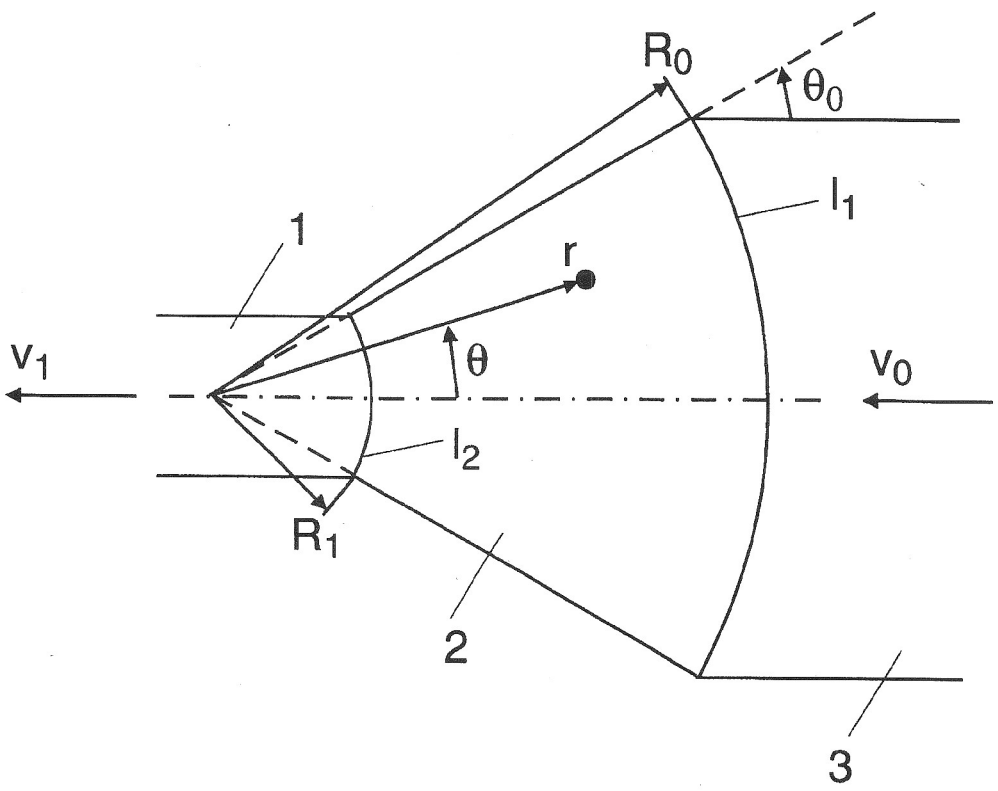


Fig.3. Schematic representation of extrusion (drawing).

l_1, $W_p^{(pl2)}$ is the plastic work on the plastic side of the rigid/plastic boundary l_2, $W_p^{(r)}$ is the plastic work on the rigid side of the rigid/plastic boundary l_2, $\sigma_Y^{(0)}$ is the initial yield stress in tension, and $\sigma_Y^{(r)}$ is the yield stress in tension on the rigid side of the rigid/plastic boundary l_2. $\sigma_Y^{(r)}$ is a given function of $W_p^{(r)}$ (for example, by means of (9) and (11) for the C1431 steel). Therefore, once $W_p^{(pl2)}$ has been determined, $W_p^{(r)}$ can be found from equation (19). Substituting (14) into (3) gives

$$\dot{\varepsilon}_{eq} = \frac{v_0 R_0^2}{\sqrt{3}\, r^3}\sqrt{11\cos^2\theta + 1} \tag{20}$$

within the plastic zone. Taking into account that $\partial\varepsilon_{eq}/\partial t = 0$, equation (20) may be transformed, with the use of (14), to

$$\frac{\partial\varepsilon_{eq}}{\partial r} = -\frac{\sqrt{11\cos^2\theta + 1}}{\sqrt{3}\, r\cos\theta}$$

This equation can be immediately integrated to give

$$\varepsilon_{eq} = -\frac{\sqrt{11\cos^2\theta + 1}}{\sqrt{3}\,\cos\theta}\ln(r/R_0) + \varepsilon_0(\theta) \tag{21}$$

where $\varepsilon_0(\theta)$ is an arbitrary function of θ and $\varepsilon_{eq} = \varepsilon_0(\theta)$ at $r = R_0$. For the C1431 steel, it follows from (11) and (21) that

$$W_p^{(pl1)} = 720.29\,\varepsilon_0\left(0.435 + \varepsilon_0^{0.345}/1.345\right) \tag{22}$$

The value of $\sigma_Y^{(0)}$ can be determined from (9) at $\varepsilon_{eq} = 0$, $\sigma_Y^{(0)}$ = 313.2 MPa. Then, combining (18) and (22) we obtain the following equation in $\varepsilon_0(\theta)$

$$\varepsilon_0\left(0.435 + \varepsilon_0^{0.345}/1.345\right) = 0.25\tan\theta \tag{23}$$

Substituting (23) into (21), one can find the distribution of ε_{eq} at $r = R_1$, on the plastic side of the rigid/plastic boundary l_2. This distribution when combined with (11) determines $W_p^{(pl2)}$ which is needed to find $W_p^{(r)}$ from (19). These calculations have been performed numerically at $\theta_0 = \pi/6$ and $R_0/R_1 = 2$. The variation of the dimensionless plastic work, $\omega = W_p^{(r)}/W(1)$, with the dimensionless distance from the axis of symmetry, $\rho = (R_1/R_0)\sin\theta$, in the final product is given in Fig.4.

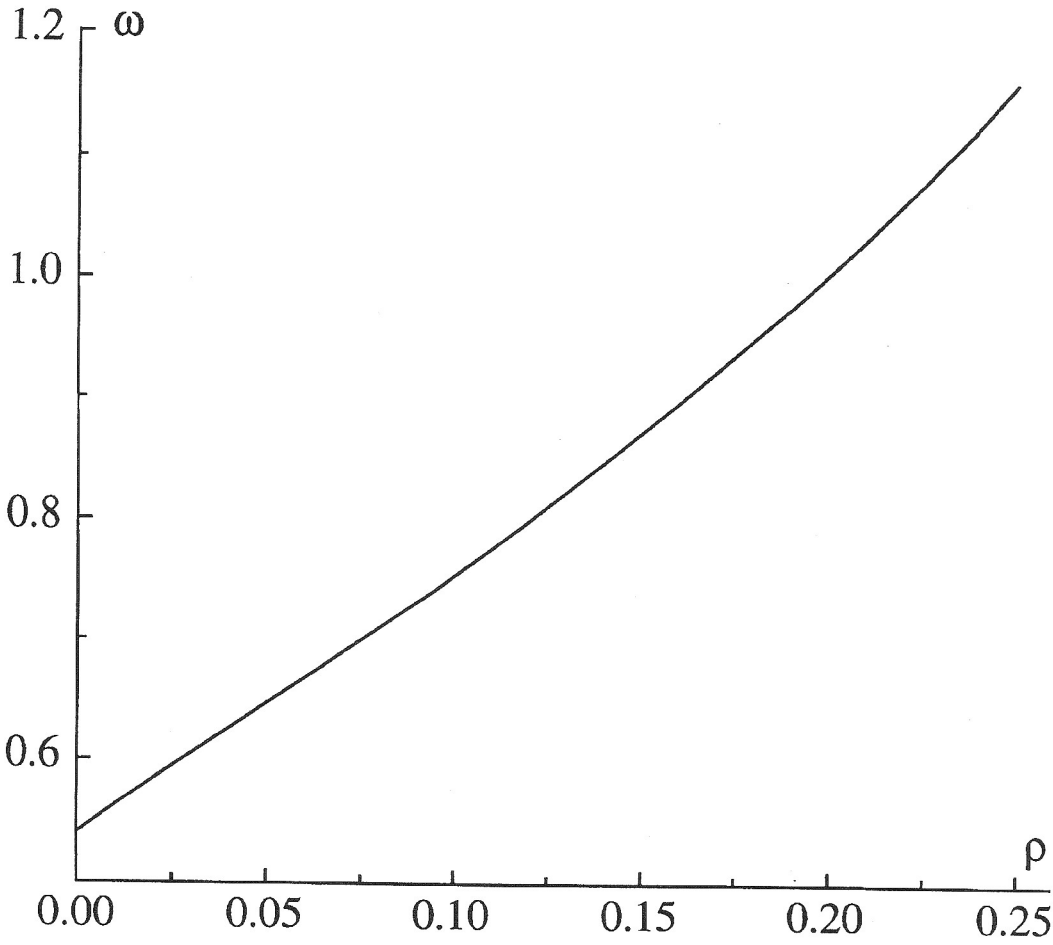


Fig.4. Variation of the dimensionless plastic work , ω,
with the dimensionless distance from the axis of symmetry, ρ.

In order to determine the distribution of the hydrostatic stress, σ, which is needed to apply the workability diagram proposed in the Section 2, the Hill's method [22] is used. Because the kinematically admissible velocity field chosen involves no arbitrary functions, the structure of orthogonalizing motion depends on assumptions made concerning the distribution of σ. It is clear that σ must be an even function of θ. Therefore, the simplest assumption is

$$\sigma/\sigma_Y^{(0)} = \sigma_0(r)\cos\theta \tag{24}$$

where $\sigma_0(r)$ is an arbitrary function of r. In this case, the orthogonalizing motion may be chosen in the form

$$u_r = u(r), \quad u_\theta = 0 \quad \text{and} \quad u_\varphi = 0 \tag{25}$$

where u(r) is an arbitrary function of r. In addition, a friction law should be adopted on the die surface. It is very often that the following friction law is used

$$f_s = mk \tag{26}$$

where f_s is the friction stress, k is the shear yield stress, and m is the friction factor. Usually, $m = 0.05 \div 0.15$ in cold forming of steels, using conventional lubricants [23, p.32]. Also, for materials which obey von Mises yield criterion $k = \sigma_Y/\sqrt{3}$. By assuming that the shear stress $\tau_{r\theta}$ does not influence yielding we obtain from (2) and (4) that

$$\sqrt{(3/2)\left(s_r^2 + s_\theta^2 + s_\varphi^2\right)} = \sigma_Y \tag{27}$$

It follows from equation $\xi_\theta = \xi_\varphi$ that $s_\theta = s_\varphi$. Then, using equation $s_r + s_\theta + s_\varphi = 0$ we may find from (27) that

$$s_r = (2/3)\sigma_Y \quad \text{and} \quad s_\varphi = s_\theta = -(1/3)\sigma_Y \tag{28}$$

Combining the procedure proposed by Hill [22] with the assumptions (24) and (25) and equations (28) we arrive at the single equilibrium equation in the form

$$\frac{(1-\cos 2\theta_0)}{4}\frac{d\sigma_0}{dx} + \frac{2}{3}\frac{\partial}{\partial x}\left(\int_0^{\theta_0}\sigma_Y \sin\theta d\theta\right) + 2\int_0^{\theta_0}\sigma_Y \sin\theta d\theta + f_s \sin\theta_0 = 0 \tag{29}$$

with $x = \ln(r/R_0)$. Since ε_{eq} has been determined (see equation (21)), σ_Y is the known function of the coordinates due to (9). In particular, the friction stress is given by (26) if σ_Y is calculated at $\theta = \theta_0$. The boundary condition to equation (29) is

$$\sigma_Y^{(0)}\sigma_0\int_0^{\theta_0}\cos^2\theta d\theta = -\int_0^{\theta_0} s_r \cos\theta d\theta \quad \text{at} \quad x = \ln(R_1/R_0) \tag{30}$$

if extrusion is considered and

$$\sigma_Y^{(0)}\sigma_0 \int_0^{\theta_0} \cos^2\theta d\theta = -\int_0^{\theta_0} s_r \cos\theta d\theta \quad \text{at} \quad x = 0 \tag{31}$$

if drawing is considered. Using (28), s_r in (30) and (31) can be replaced by $(2/3)\sigma_Y$ which is known from the velocity field and equation (9). Equation (29) with the boundary condition (30) (and (31)) has been solved numerically at m = 0.1. The variation of σ_0, which is the dimensionless hydrostatic stress at the axis of symmetry, with x is shown in Fig.5. Fracture may occur at a point on the surface $x = x_0 = \ln(0.5)$. The variation of β with θ at $x = x_0$ may be found from (1), (9), (21), and (24). This variation is shown in Fig.6. It follows from Fig.6[b] that β is larger than 1.8 everywhere on the surface $x = x_0$. On the other hand, one can see from Fig.4 that ω is larger than 0.55 (approximately) on this surface. Therefore, it follows from the workability diagram shown in Fig.2[b] that drawing without fracture is impossible under the conditions considered. In contrast, one can conclude from Figs 2[b], 4, and 6[a] that no fracture occurs in the extrusion process.

5. CONCLUSION

The workability diagram based on the triaxiality ratio and the plastic work has been proposed. Using the plastic work as a parameter in the workability diagram allows one to account for a contribution of velocity discontinuity surfaces in fracture process in simple manner. A procedure for obtaining the workability diagram proposed from any conventional workability diagram based on the equivalent strain has been given. An approach which accounts for a contribution of velocity discontinuity surfaces in fracture process has been proposed. As an example of the application of this approach and the workability diagram, extrusion (drawing) of round rods has been considered.

ACKNOWLEDGEMENT

The author acknowledges the support of the Russian Foundation for Fundamental Research (Grant 96-01-05017).

6. REFERENCES

1. Avitzur B.: Analysis of Central Bursting Defects in Extrusion and Wire Drawing, *Trans. ASME, J. Engng Ind.*, **90**, 79 (1968).

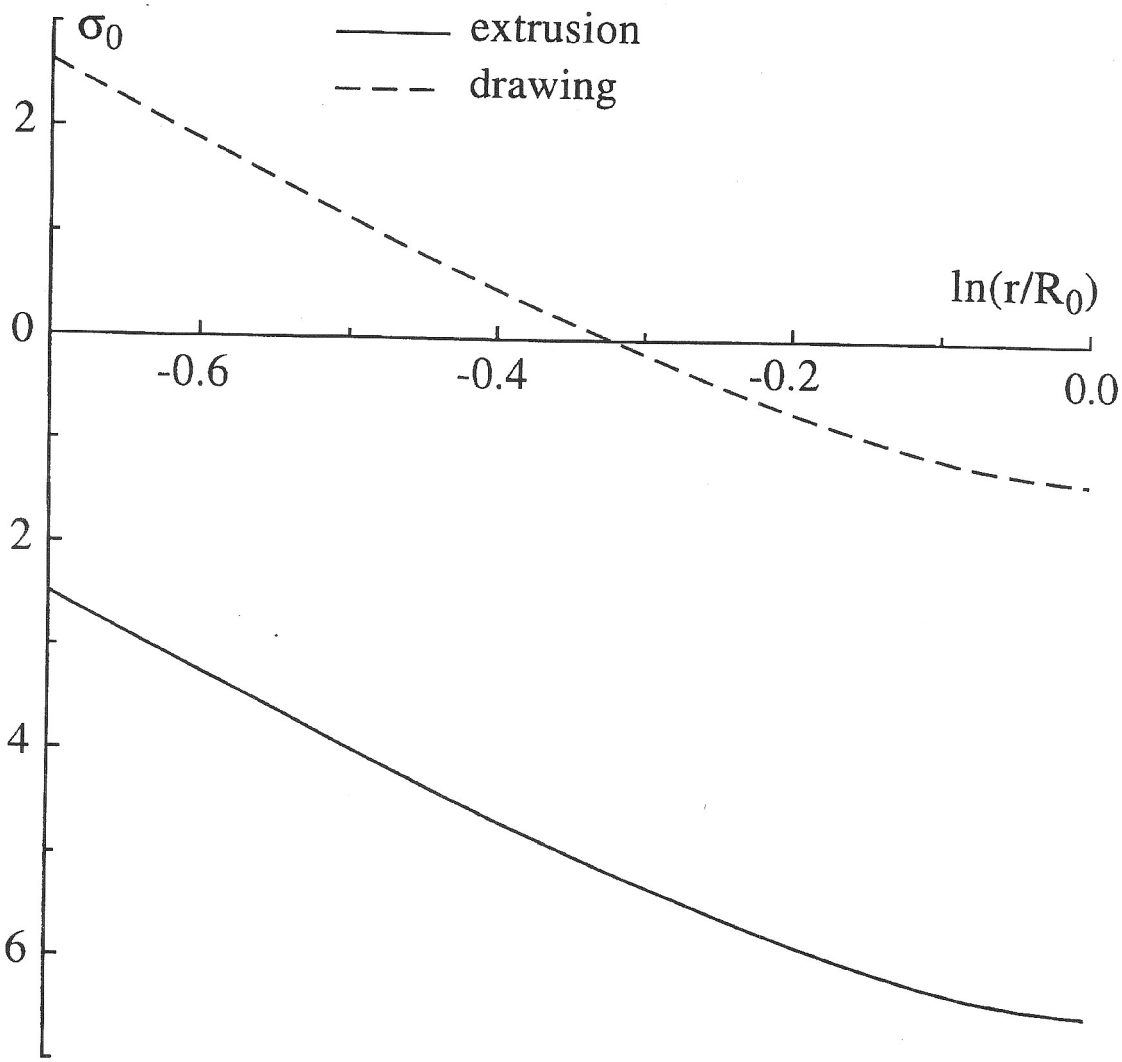


Fig.5. Distribution of the dimensionless hydrostatic stress along the axis of symmetry.

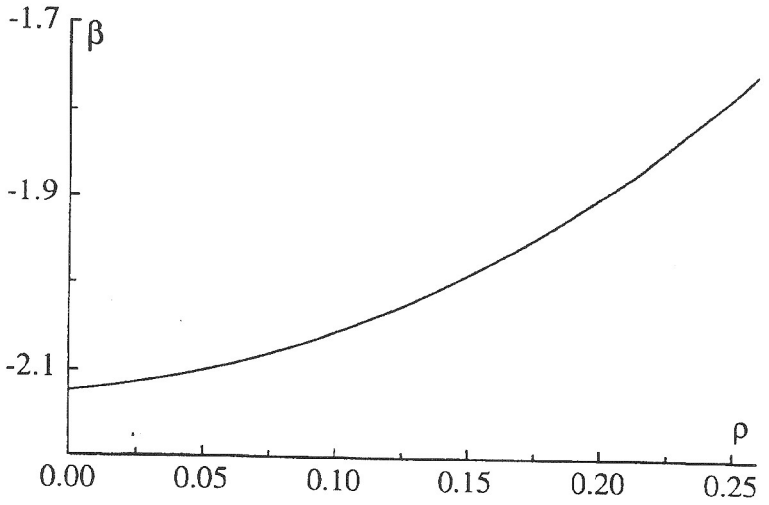


Fig.6[a]. Variation of the triaxiality ratio with ρ in the final product (extrusion).

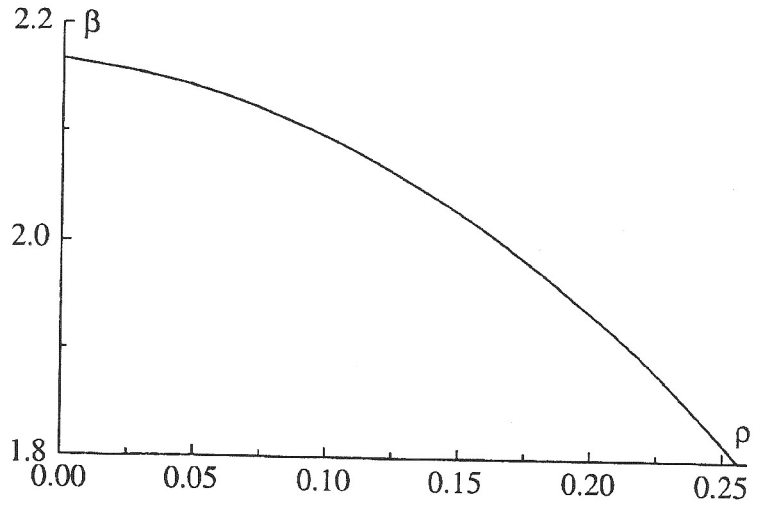


Fig.6[b]. Variation of the triaxiality ratio with ρ in the final product (drawing).

2. Avitzur B. and Choi J.C.: Analysis of Central Bursting Defects in Plane Strain Drawing and Extrusion, *Trans. ASME, J. Engng Ind.*, **108**, 317 (1986).

3. Turczyn S.: The Effect of the Roll-Gap Shape Factor on Internal Defects in Rolling, *J. Mater. Processing Technol.*, **60**, 275 (1996).

4. Alexandrov S. and Goldstein R.: Variational Principle in the Theory of Plastic Flow Taking into Account Formation of Tensile Cracks, *Physics-Doklady, A Journal of the Russian Academy of Sciences*, **40** (6), 297 (1995) [Trans. from Russian].

5. Alexandrov S. and Chicanova N.: Upper Bound of Torsion Moment and Fracture by Rolling of Three Layer Sandwich Sheets, *J. Technol. Plasticity*, **20**, 59 (1995).

6. Alexandrov S.Ye. and Goldstein R.V.: A Rigid-Plastic Analysis of the Limiting Equilibrium of an Edge Cleavage Crack in a Rectangular Plate, *J. Appl. Maths Mechs*, **60** (4), 693 (1996) [Trans. from Russian].

7. Alexandrov S. and Goldstein R.: On Limit Load and Constraint in a Mis-Matched Welded Plate Under Tension. In:*2nd Int. Symp. Mis-Matching of Interfaces and Welds* (eds K.-H. Schwalbe and M.Kocak). GKSS Research Centre Publications, Geesthacht, 759-769 (1997).

8. Gurson A.L.: Continuum Theory of Ductile Rupture by Void Nucleation and Growth: Part 1 - Yield Criteria and Flow Rules for Porous Ductile Media, *Trans. ASME, J. Engng Mater. Technol.*, **99**, 2 (1977).

9. Lemaitre J.: A Continuous Damage Mechanics Model for Ductile Fracture, *Trans. ASME, J. Engng Mater. Technol.*, **109**, 83 (1987).

10. Bonora N.: A Nonlinear CDM Model for Ductile Failure, *Engng Fract. Mech.*, **58** (1/2), 11, (1997),

11. Embury J.D. and LaRoy G.H.: Failure Maps Applied to Metal Deformation Processes. In *Advances in Research on the Strength and Fracture of Materials* (Ed. D.M.R.Taplin), Vol.1. Pergamon Press, New York, 15-41 (1978).

12. Vujovic V. and Shabaik A.H.: A New Workability Criterion for Ductile Metals,*Trans. ASME, J. Engng Mater. Technology*, **108**, 245 (1986).

13. Cristescu N.: Plastic Flow Through Conical Converging Dies, Using a Viscoplastic Constitutive Equation, *Int. J. Mech. Sci.*, **17**, 425 (1975).

14. Malinin N.N.: *Creep in Metal Forming*, Mashinostroenie, Moscow (1986) [in Russian].

15. Alexandrov S. and Vishnayakov L.: Pressing Thin-Walled Tubing from Powdered Material, *Journal Appl. Mech. and Techn. Physics*, **34** (2), 162 (1993) [Trans. from Russian].

16. Druyanov B.: *Technological mechanics of porous bodies*, Clarendon Press, New-York (1993).

17. Vilotic D.: *Ponasanje Celicnih Materijala u Razlicitim Obradnim Sistemima Hladnog Zapreminskog Deformisanja*, Univerzitet u Novom Sadu, Novi Sad (1987) [in Serbian].

18. Alexandrov S., Chikanova N. and Vilotic D.: Compression of a Block Between Cylindrical Dies and Its Application to the Workability Diagram. In *Advanced Methods in Materials Processing Defects* (Eds M.Predeleanu and P.Gilormini). Elsevier, Amsterdam, 247-256 (1997).

19. Korobkhin V.D. and Chudakov P.D.: Energy Rate Dissipation on Velocity Discontinuity Surfaces in Hardening Materials, *Izv. AN SSSR MTT (Mechanika Tverdogo Tela)*, No.3, 158 (1969) [in Russian].

20. Avitzur B.: Study of Flow Through Conical Converging Dies. In *Metal Forming: Interrelation Between Theory and Practice* (Ed. A.L.Hoffmanner). Plenum Press, New York-London, 1-46 (1971).

21. Osakada K. and Niimi Y.: A Study on Radial Flow Field for Extrusion Through Conical Dies, *Int. J. Mech. Sci.*, **17**, 241 (1975).

22. Hill R.: A general method of analysis for metalworking processes, *J. Mech. Phys. Solids*, 11, 305 (1963).

23. Kobayashi S., Oh S.-I. and Altan T.: *Metal Forming and the Finite-Element Method*, Oxford University Press, New-York (1989).

PRIMENA DIJAGRAMA OBRADOVOSTI I POLJA DISKONTINUITETA BRZINA U CILJU ANALIZE NASTANKA PUKOTINA U PROCESIMA OBRADE DEFORMISANJEM

Alexandrov S., Institut za probleme u mehanici, Ruska Akademija Nauka, Moskva Rusija

REZIME

Metoda prezentirana u ovom radu omogućava analizu problema nastanka pukotina u procesima obrade deformisanjem. Metod je baziran na polju diskontinuiteta brzina i dijagramu obradivosti, i primenjuje se za kruto plastične materijale, uz prisustvo pojave deformacionog ojačavanja.

Određivanje nastanka pukotine je sprovedeno uz prikaz dijagrama obradivosti koji predstavljaju zavisnost između troaksijalnih naponskih komponenti (u odnosu na efektivni napon) i deformacionog rada. Korišćenjem deformacionog rada umesto efektivne deformacije omogućuje se određivanje uticaja brzina na površinama diskontinuiteta u procesu nastanka pukotine.

Kao primer primene ove metode analiziran je proces istiskivanja (vučenja).

Journal for Technology of Plasticity, Vol 22 (1997), Number 1-2

THE APPLICATION OF HILL'S METHOD TO THE ANALYSIS OF FORMING PROCESSES WITH DAMAGE EVOLUTION MODELS

Chikanova N., Bauman Moscow State Technical University, Moscow, Russia

ABSTRACT

The paper deals with steady planar flow of a rigid-plastic, hardening material. The evolution of damage is taken into account due to continuum damage mechanics models. An approach based on the Hill method is developed to derive approximating equations which describe the flow between two curvilinear walls of quite arbitrary shape. Any type of friction may be prescribed on the walls. The equations are given in a form which is convenient for users.

1. INTRODUCTION

Significant progress has been made in recent years in the numerical modelling of industrial forming processes such as extrusion, wire drawing and rolling based most of all on the finite element, finite volume, and finite difference methods using high-powered computing facilities. Though a number of finite element codes are commercially available they often fail to meet specific engineering requirements, for example, in simulations of failure processes where the underlying structure of finite element methods is not well suited to the treatment of discontinuities [1-4]. Also, users of finite element software products not seldom complain about an unsatisfactory increase in computer time if contact problems are considered [5,6]. Whilst Lagrangian-based finite element methods are useful for handling the interface between the forming material and the die, the analysis of steady state processes requires many iterations of stepping through the process and in

this case Eulerian reference frame is more natural. On the other hand, Eulerian-based finite element methods require complex numerical schemes to follow the flow path of material particles and to handle boundary conditions [7]. Finite element software products do not satisfy the requirements of the design process well. This problem was fully discussed by Szabo and Actis [8] who gave the comprehensive information about finite element methods in professional practice. Therefore, there is still a need for alternative modelling techniques.

Among most popular analytical approximate approaches to the treatment of metal forming problems are the upper bound method, the slip line field theory, and the slab method. Early theoretical studies of forming processes were limited to very simplified techniques based most of all on the assumptions that (a) the plastic zone is narrow in one direction, and (b) there is a high degree of symmetry reducing the number of independent coordinates to one [9]. To date, a number of shortcomings of these techniques have been overcome. Modifications of the upper bound method, the slip line field theory, and the slab method are widely used for many industrial applications as well as their classical formulations.

Attractive for its simplicity approach for metal forming processes is the upper bound method. It is based on the upper limit load theorem and constitutes for rigid-plastic materials a convenient tool for evaluating the rate of work in forming processes. In view of our interests, namely, steady state of incompressible rigid-plastic hardening materials with a damage variable, this method has at least two groups of drawbacks.

1. The upper bound theorem is not valid for

(a) *Coulomb friction law* [10] and *probably for other types of friction* (for example, a new friction law proposed by Carter [11]), except for Prandtl friction law with a constant friction force. To estimate yield-point loads in the presence of Coulomb friction Collins [12] proposed the generalized upper bound technique in the assumption of constant coefficient of friction and flat tool-workpiece interface. His new upper bound theorem is rather weaker than the usual one so it is necessary to work with 'fictitious' velocity boundary conditions.

(b) *Unprescribed surface configuration.* Lippmann and Takuda [13] considered partially unknown shape of the surface by analyzing plane-strain drawing through wedge-shaped dies for which the shape of the free surface of the strip was determined approximately. This modification to the upper bound method also allows for yield limit to be dependent on internal parameters such as the equivalent strain, temperature, and equivalent rate of shear. However, Azarkhin and Richmond [14] pointed out that the ignoring of restriction of unprescribed surface configuration could lead to the

serious errors and discussed the ways to improve this situation. In [15] Azarkhin and Richmond introduced a modified version of the upper bound method with moving blocks to find the surface configuration on a more rigorous basis. But this question is still open for discussions.

(c) *Materials with the yield stress depending on the history of deformation (hardening, damage and so on).* Extensions of the upper bound method for such materials were proposed by Lippmann and Takuda [13] and by Druynov [16].

2. The upper bound theorem is valid, but some important technological parameters cannot be obtained.

(a) *For combined loading the forces cannot be separated [14].*

(b) *The hydrostatic portion of stress,* which is one of the main parameters responsible for damage or failure, *cannot be determined.* Modification was proposed in [14] where the hydrostatic pressure was found from postprocessing.

However, despite all these modifications the variational principal is strictly required to apply the upper bound method.

Slip line field theory proposes an alternative approach to metal forming process modelling. Plane strain slip line field theory is well developed and is a widely used technique, particular, for the processes with complicated geometries. However, the restrictions to perfectly plastic materials greatly limit its practical value. Most modifications to induce hardening in this theory have been done by perturbation or visioplastic techniques [17]. Collins [18] proposed a procedure for constructing approximate solutions for steady flow processes such as drawing, extrusion or strip rolling involving a small amount of hardening by employing a perturbation technique on perfectly plastic solutions. Another area of difficulty in classical slip line theory is where the governing integral equation is nonlinear, that is, for axisymmetric problems where most the solutions so far obtained are such that the Haar-Karman hypothesis is imposed [19,20]. The numerical/graphical method used for the construction of axisymmetric slip line fields are either tedious or can be applied only to particular problems. In [7] there was an attempt to formulate a finite difference technique of constructing more general axisymmetric slip line fields.

The slab method allows for arbitrary constitutive equations and friction laws. However, the main disadvantage of this method is that it gives no information about thickness distribution of stresses and strains which is important for fracture analysis [21].

A general analytical procedure for analyzing metal forming processes was proposed by Hill [9]. To date his method is considered one of the best due to combining flexibility with rigorous

principles and covering arbitrary material properties, different kinds of friction, and any tool shape. This method allows for constructing approximate equilibrium equations and determining stress and strain fields in the deforming zones. Despite the fact that Hill [9] systematized the details of procedure and illustrated the method by analyzing inhomogeneous compression, bar drawing, and forging, no development on the method has appeared in the literature with few exceptions concerning with adopting it to some particular problems and varifying its validity in this manner [22-24]. In [22] it was pointed out, by considering ring compression with barreling, bar drawing, and tube sinking through a conical die, that the results obtained by the Hill's method were about the same as those by other theories when they were available. It was also mentioned that the solutions obtained were mathematically sound and the formulation was simple and straightforward. The same conclusion follows from [23] where the analysis of circular cylinder in axial compression with friction was performed. The theoretical result was qualitatively well in agreement with experiments. In [24] the Hill's method was applied to predict the density distribution during compacting process of a porous metal ring and showed remarkable result. One can see from this brief review that the Hill's method was applied only to particular problems and no attempts were done to develop and adopt the method for a general class of metal forming processes.

The main task of the paper presented is to develop and adopt the Hill's method for any steady metal forming process for incompressible rigid-plastic, hardening solids with a damage variable under plane strain conditions. The approach proposed is suited for reliable calculations of strains and stresses including the hydrostatic stress. The generalization to axisymmetric flows is obvious and will be presented soon in future papers. Finally, the method can be adopted to fully three-dimensional analysis. The main idea of this approach has been already used in analyzing some nonsteady problems. Nonsteady extrusion of a porous material through a conical die was presented in [25]. The problems of compression, with or without barelling, of a block between cylindrical dies were solved by this method in [26,27].

2. KINEMATICS OF THE PROCESS

Consider an arbitrary shaped converging channel through which plastic material is being forced. The walls of the channel are described by two differentiable functions $x=x_0(y)$ and $x=x_1(y)$ in Cartesian coordinates (x,y). On the walls any type of friction can be induced. In particular case the

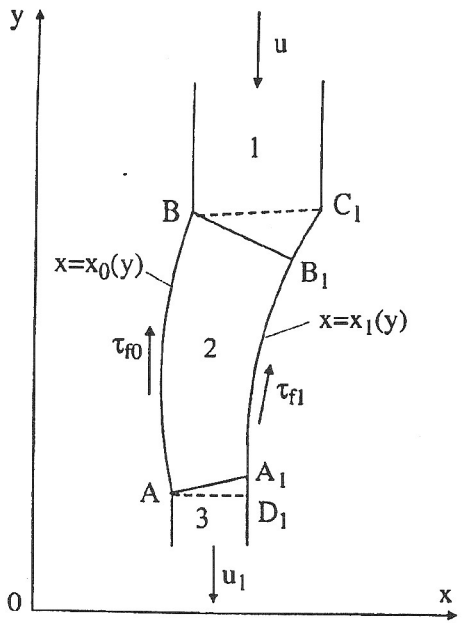


Fig.1[a]. Schematic representation of the process.

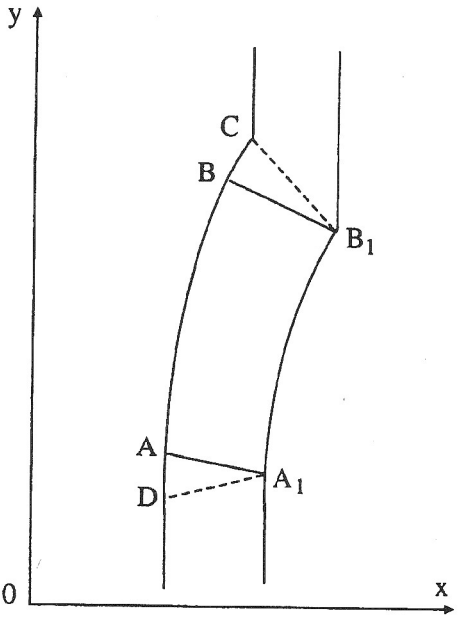


Fig.1[b]. Schematic representation of the deforming zone.

curve $x=x_0(y)$ is the axis of symmetry where, instead of the friction condition, shear stresses are set equal to zero. Since in the present study elastic deformations are disregarded, rigid zones may arise. It is assumed that the motion of rigid zone is a translation along the y-axis. A possible configuration of rigid zones and a plastic zone is shown in Fig.1[a]. The zones 1 and 3 are rigid. The zone 1 moves at the velocity u. In the zone 3 the material has already deformed and undergoes no further deformation. It moves as a rigid body at the velocity u_1. On the rigid-plastic boundaries BB_1 and AA_1 the tangent velocity may suffer discontinuities being allowed for an approximate formulation due to the Hill's method. In the zone 2 an ortogonal curvilinear coordinate system (α,β) with α-lines being coincided with the stream lines is used. The main advantage of this coordinate system is that it fits the tool surfaces exactly. The curvilinear coordinates are defined as functions of the Cartesian coordinates: $\alpha = \alpha(x,y)$ and $\beta = \beta(x,y)$ where the functions are assumed to be smooth, reversible, and single-valued within the zone 2. From the geometrical considerations

$$\partial x/\partial\alpha = h_\alpha \cos\varphi, \quad \partial y/\partial\alpha = h_\alpha \sin\varphi, \quad \partial x/\partial\beta = -h_\beta \sin\varphi, \quad \partial y/\partial\alpha = h_\beta \cos\varphi \tag{1.1}$$

Here h_α and h_β are the Lame parameters and φ is the anticlockwise inclination of the tangent to the α-line to the x-diraction. Substituting (1.1) into equations $\partial^2 x/(\partial\alpha\partial\beta) = \partial^2 x/(\partial\beta\partial\alpha)$ and $\partial^2 y/(\partial\alpha\partial\beta) = \partial^2 y/(\partial\beta\partial\alpha)$ and then rotating the coordinate system xy so that $\varphi = 0$ at some point M (Fig.2), yields

$$\partial h_\alpha/\partial\beta = -h_\beta\,\partial\varphi/\partial\alpha, \quad \partial h_\beta/\partial\alpha = h_\alpha\,\partial\varphi/\partial\beta \tag{1.2}$$

The Christoffel symbols of second kind are given by

$$\Gamma_{11}^1 = \frac{1}{h_\alpha}\frac{\partial h_\alpha}{\partial\alpha}, \quad \Gamma_{22}^2 = \frac{1}{h_\beta}\frac{\partial h_\beta}{\partial\beta}, \quad \Gamma_{12}^1 = \Gamma_{21}^1 = \frac{1}{h_\alpha}\frac{\partial h_\alpha}{\partial\beta},$$
$$\Gamma_{12}^2 = \Gamma_{21}^2 = \frac{1}{h_\beta}\frac{\partial h_\beta}{\partial\alpha}, \quad \Gamma_{11}^2 = -\frac{h_\alpha}{h_\beta^2}\frac{\partial h_\alpha}{\partial\beta}, \quad \Gamma_{22}^1 = -\frac{h_\beta}{h_\alpha^2}\frac{\partial h_\beta}{\partial\alpha} \tag{1.3}$$

The incompressibility condition is written in the form

$$\partial\left(h_\beta v_\alpha\right)/\partial\alpha + \partial\left(h_\alpha v_\beta\right)/\partial\beta = 0 \tag{1.4}$$

where v_α and v_β are the physical components of the velocity vector. Since α-lines are streamlines, $v_\beta=0$. Thus, from (1.4), it follows

$$v = v_0/h_\beta \tag{1.5}$$

with the notation $v_\alpha = v$. Here $v_0 = v_0(\beta)$ is an arbitrary function of β and $v_0 > 0$. The physical

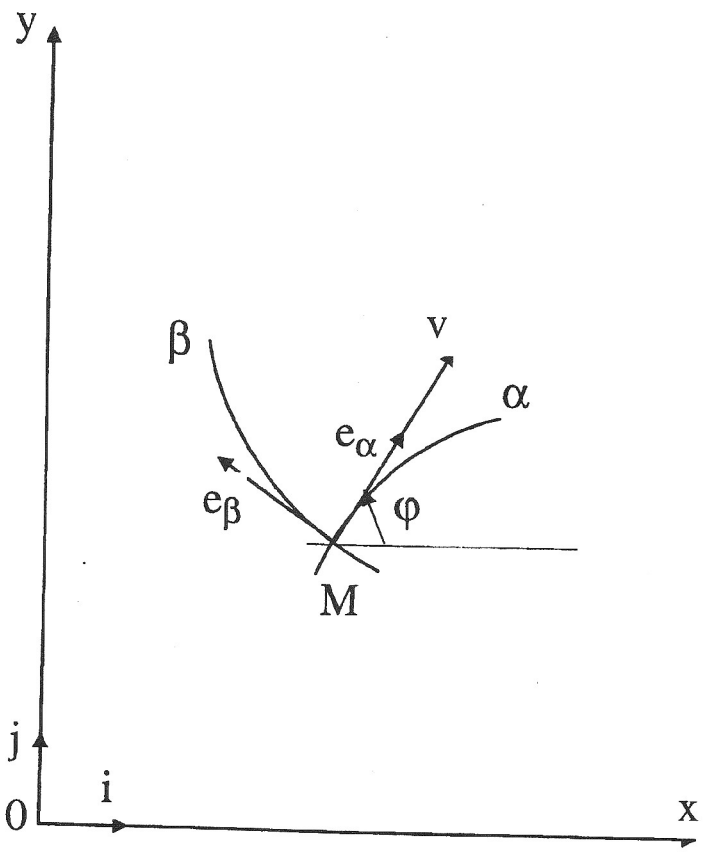


Fig.2. Cartesian and stream line based coordinate systems.

components of the strain-rate tensor, ε_α, ε_β and $\varepsilon_{\alpha\beta}$, can be found by means of tensor analysis with use of (1.5) and (1.1) in the form

$$\varepsilon_\alpha = \frac{1}{h_\alpha}\frac{\partial v}{\partial \alpha} = -\frac{v_0\,\partial\varphi/\partial\beta}{h_\beta^2}, \quad \varepsilon_\beta = \frac{v}{h_\alpha h_\beta}\frac{\partial h_\beta}{\partial \alpha} = -\varepsilon_\alpha$$

$$\varepsilon_{\alpha\beta} = \frac{1}{2h_\beta}\left[\frac{\partial v}{\partial \beta} - \frac{v}{h_\alpha}\frac{\partial h_\alpha}{\partial \beta}\right] = \frac{1}{2h_\beta^2}\left[\frac{dv_0}{d\beta} + v_0\left(\frac{h_\beta}{h_\alpha}\frac{\partial\varphi}{\partial\alpha} - \frac{1}{h_\beta}\frac{\partial h_\beta}{\partial\beta}\right)\right] \tag{1.6}$$

The normal component of the velocity, v_n, must be continuous across the velocity discontinuity lines BB_1 and AA_1 (Fig.1[a]), that gives the following equation

$$[v_n] = 0 \tag{1.7}$$

with the usual square brackets notation for the amount of jump. Let us introduce angle ψ between the α–lines and the tangent to the velocity discontinuity line. Then

$$\mathrm{tg}\psi = h_\beta/h_\alpha\, d\beta/d\alpha \tag{1.8}$$

$$n_\alpha = \mp\sin\psi, \quad n_\beta = \pm\cos\psi \tag{1.9}$$

where the upper sign corresponds to BB_1 with $\psi = \psi_0$ and the lower sign corresponds to AA_1 with $\psi = \psi_1$. By definition, the length element dl is

$$dl = \left|\sqrt{\left(h_\alpha/h_\beta\right)^2\left(d\alpha/d\beta\right)^2 + 1}\; h_\beta d\beta\right| \tag{1.10}$$

Substitution of (1.8) into (1.10) gives

$$dl = h_\beta/\sin\psi\, d\beta \tag{1.11}$$

where $\sin\psi > 0$ and $d\beta > 0$. By definition, $v_n = \mathbf{v}\cdot\mathbf{n}$; $\mathbf{n} = n_x\mathbf{i} + n_y\mathbf{j} = n_\alpha\mathbf{e}_\alpha + n_\beta\mathbf{e}_\beta$. Here $\mathbf{n}$ is the normal vector with its physical components in the Cartesian (n_x, n_y) and curvilinear (n_α, n_β) coordinate systems. $(\mathbf{i}, \mathbf{j})$ and $(\mathbf{e}_\alpha, \mathbf{e}_\beta)$ are the basis vector respectively. It follows from Fig.1[a] that $\mathbf{v} = -u\mathbf{j}$ on the rigid side of the rigid-plastic boundary between the zones 1 and 2 and $\mathbf{v} = v\mathbf{e}_\alpha$ on the plastic side of this boundary. So, equation (1.7) can be rewritten in the form

$$-un_y = vn_\alpha \tag{1.12}$$

From the geometrical consideration (Fig.2), one can find

$$\frac{\partial\alpha}{\partial x} = \frac{\cos\varphi}{h_\alpha}, \quad \frac{\partial\alpha}{\partial y} = \frac{\sin\varphi}{h_\alpha}, \quad \frac{\partial\beta}{\partial x} = -\frac{\sin\varphi}{h_\beta}, \quad \frac{\partial\beta}{\partial y} = \frac{\cos\varphi}{h_\beta} \tag{1.13}$$

Then, due to transformation formulas, one obtains

$$n_y = \sin\varphi n_\alpha + \cos\varphi n_\beta \tag{1.14}$$

Substituting (1.9) and (1.14) into (1.12) leads to the equation

$$tg\psi = u\cos\varphi/(v + u\sin\varphi) \tag{1.15}$$

Equating (1.8) and (1.15), with use of (1.5), yields

$$d\alpha/d\beta = \left(v_0 + h_\beta u\sin\varphi\right)/\left(h_\alpha u\cos\varphi\right) \tag{1.16}$$

Equation (1.16) together with the boundary condition, which must be posed from the geometry, determines the velocity discontinuity curve BB_1. For the curve AA_1 the velocity u should be replaced by u_1 being expressed through the known parameters of the problem and u. The length element for BB_1 is obtained by substitution of (1.16) into (1.10) so as

$$dl = \sqrt{v_0^2 + 2v_0 h_\beta u\sin\varphi + \left(h_\beta u\right)^2}\Big/\left|u\cos\varphi\right| d\beta \tag{1.17}$$

For AA_1, u should be replaced by u_1 in (1.17).

2. APPROXIMATE EQUILIBRIUM EQUATIONS

Let σ_α, σ_β, and $\sigma_{\alpha\beta}$ denote the components of the real stress tensor and s_α, s_β, and $s_{\alpha\beta}$ be the deviatoric components of the stress tensor p_{ij} calculated from the kinematically admissible velocity field and the governing equations of a particular material model. The first group of the components satisfies the equilibrium equations exactly, whilst the second group, in general, does not. If w_α and w_β is an arbitrary differentiable velocity field then the equilibrium equations are equivalent to the equation of virtual work rate

$$\int_S \left(\sigma_\alpha\xi_\alpha + \sigma_\beta\xi_\beta + 2\sigma_{\alpha\beta}\xi_{\alpha\beta}\right)dS = \int_L \left(\sigma_\alpha w_\alpha n_\alpha + \sigma_{\alpha\beta}\left(w_\alpha n_\beta + w_\beta n_\alpha\right) + \sigma_\beta w_\beta n_\beta\right)dl \tag{2.1}$$

Here S is the area of deformation zone; L is the contour bounding this area; ξ_α, ξ_β, and $\xi_{\alpha\beta}$ are the components of the strain-rate tensor being defined by virtue of velocity field w_α and w_β; n_α and n_β are the components of the unit normal vector to the contour L. Due to the Hill's method equation (2.1) should be satisfied approximately, that is, the components of the real stress tensor on the left hand side of (2.1) should be replaced by those calculated from the kinematically admissible velocity field and an arbitrary field w_α and w_β should be replaced by the orthogonalizing motion being connected with the kinematically admissible velocity field. (The number of unknown functions in the kinematically admissible velocity field must be equal to those in the orthogonalizing motion.) Since the hydrostatic pressure $\sigma=(\sigma_1+\sigma_2+\sigma_3)/3$ cannot be obtained from the governing equations for incompressible material, some additional assumptions

about this parameter are required. Let σ be a function of coordinates as it was assumed in [9]

$$\sigma = \sigma_1(\alpha) f_1(\beta) \tag{2.2}$$

where $f_1(\beta)$ is a known function and $\sigma_1(\alpha)$ must be determined from (2.1). The orthogonalizing motion corresponding to (2.2) may be chosen in the form

$$w_\alpha = F(\alpha)/h_\alpha, \quad w_\beta = 0 \tag{2.3}$$

Then, after some transformations and with use of (1.1) and (1.2), equation (2.1) is rewritten as

$$\iint F(\alpha)\left[\frac{h_\beta}{h_\alpha}\left(\frac{\partial s_\alpha}{\partial \alpha}+\frac{\partial \sigma}{\partial \alpha}-2p_{\alpha\beta}\frac{\partial \varphi}{\partial \alpha}\right)+\frac{\partial p_{\alpha\beta}}{\partial \beta}+\left(s_\alpha - s_\beta\right)\frac{\partial \varphi}{\partial \beta}\right]d\alpha d\beta = \tag{2.4}$$

$$= \iint F(\alpha)/h_\alpha\left[\left(p_\alpha - \sigma_\alpha\right)n_\alpha + \left(p_{\alpha\beta} - \sigma_{\alpha\beta}\right)n_\beta\right]dl$$

Integrating the rigid side of (2.4) along the contour AA_1BB_1 (Fig.1[a]) yields

$$\iint F(\alpha)/h_\alpha\left[\left(p_\alpha - \sigma_\alpha\right)n_\alpha + \left(p_{\alpha\beta} - \sigma_{\alpha\beta}\right)n_\beta\right]dl =$$

$$= \int_{\alpha_{B_1}}^{\alpha_{A_1}} F(\alpha)\left(p_{\alpha\beta} + \tau_{f1}\right)_{\perp\beta=\beta_1} d\alpha - \int_{\alpha_B}^{\alpha_A} F(\alpha)\left(p_{\alpha\beta} - \tau_{f0}\right)_{\perp\beta=\beta_0} d\alpha$$

where the following notations are adopted: $\sigma_{\alpha\beta} = \tau_{f0}$, $\sigma_{\alpha\beta} = -\tau_{f1}$ are the friction forces on the curves AB and A_1B_1 respectively; α_{A_1}, α_B, α_{A_1}, α_{B_1} are the α-coordinates of the points A, B, A_1, B_1; $\beta = \beta_0$ and $\beta = \beta_1$ correspond to curves AB and A_1B_1. Hence, (2.4) is equivalent to the following equation

$$\iint F(\alpha)\left[\frac{h_\beta}{h_\alpha}\left(\frac{\partial s_\alpha}{\partial \alpha}+\frac{\partial \sigma}{\partial \alpha}-2p_{\alpha\beta}\frac{\partial \varphi}{\partial \alpha}\right)+\frac{\partial p_{\alpha\beta}}{\partial \beta}+\left(s_\alpha - s_\beta\right)\frac{\partial \varphi}{\partial \beta}\right]d\alpha d\beta = \tag{2.5}$$

$$= \int_{\alpha_{B_1}}^{\alpha_{A_1}} F(\alpha)\left(p_{\alpha\beta} + \tau_{f1}\right)_{\perp\beta=\beta_1} d\alpha - \int_{\alpha_B}^{\alpha_A} F(\alpha)\left(p_{\alpha\beta} - \tau_{f0}\right)_{\perp\beta=\beta_0} d\alpha$$

Let us denote

$$I_1(\alpha,\beta) = h_\beta/h_\alpha\left(\partial s_\alpha/\partial\alpha - 2p_{\alpha\beta}\,\partial\varphi/\partial\alpha\right) + \left(s_\alpha - s_\beta\right)\partial\varphi/\partial\beta \tag{2.6}$$

This value can be calculated from the kinematically admissible velocity field. A specific structure of the differential equations given by (2.5) depends on the shape of rigid-plastic boundaries. In the simplest case, which is often used in practical applications, the rigid-plastic boundaries coincide with curves α = const. Thus, integration with respect to β in (2.5) can be performed with the following result

$$\frac{d\sigma_1(\alpha)}{d\alpha}=\left[r_{\perp\beta=\beta_1}\tau_{f1}+r_{\perp\beta=\beta_0}\tau_{f0}-\int_{\beta_0}^{\beta_1}I_1(\alpha,\beta)d\beta\right]\Bigg/\int_{\beta_0}^{\beta_1}\frac{h_\beta f_1(\beta)}{h_\alpha}d\beta \tag{2.7}$$

In general case, it is necessary to consider separately equations in each zone shown in Fig.1[a]. (Another possible configuration of the deforming zone is shown in Fig.1[b]). In the zone between curves BB_1 and AA_1 the equation (2.7) is still valid. In the zones between curves BB_1 and BC_1 as well as AA_1 and AD_1, from (2.5) it follows

$$\frac{d\sigma_1(\alpha)}{d\alpha}=\left[r_{\perp\beta=\beta_1}\tau_{f1}-\int_{\beta_2}^{\beta_1}I_1(\alpha,\beta)d\beta+\left(p_{\alpha\beta}\right)_{\perp\beta=\beta_2}\right]\Bigg/\int_{\beta_2}^{\beta_1}\frac{h_\beta f_1(\beta)}{h_\alpha}d\beta \tag{2.8}$$

Here $\beta_2=\beta_2(\alpha)$ denotes the curves BC_1 and AD_1 respectively for each of the cases considered. In the zones between curves BB_1 and CB_1 as well as AA_1 and DA_1, from (2.5) it follows

$$\frac{d\sigma_1(\alpha)}{d\alpha}=\left[r_{\perp\beta=\beta_0}\tau_{f0}-\int_{\beta_0}^{\beta_3}I_1(\alpha,\beta)d\beta-\left(p_{\alpha\beta}\right)_{\perp\beta=\beta_3}\right]\Bigg/\int_{\beta_0}^{\beta_3}\frac{h_\beta f_1(\beta)}{h_\alpha}d\beta \tag{2.9}$$

Here $\beta_3=\beta_3(\alpha)$ denotes the curves CB_1 and DA_1 respectively for each of the cases considered. The value σ_1 must be continues on the zone boundaries. Moreover, the boundary conditions are posed on one of the rigid-plastic boundaries. The particular condition is that there are no stresses on the outer surface of this rigid zone. Then, integrating the equilibrium equation over the rigid zone yields

$$\int_{\beta_0}^{\beta_1}v_0\sigma d\beta=\int_{\beta_0}^{\beta_1}\left[uh_\beta\sin\varphi\left(s_\alpha-s_\beta\right)-s_\beta v_0+p_{\alpha\beta}\left(\left(uh_\beta\cos 2\varphi-v_0\sin\varphi\right)/\cos\varphi\right)\right]d\beta \tag{2.10}$$

In particular case, when equation (2.7) is valid in the whole deformation zone, equation (2.10) transforms to the form

$$\sigma_1=\int_{\beta_0}^{\beta_1}\left[uh_\beta\sin\varphi\left(s_\alpha-s_\beta\right)-s_\beta v_0+p_{\alpha\beta}\left(\left(uh_\beta\cos 2\varphi-v_0\sin\varphi\right)/\cos\varphi\right)\right]d\beta\Bigg/\int_{\beta_0}^{\beta_1}v_0f_1(\beta)d\beta \tag{2.11}$$

3. DAMAGE EVOLUTION MODEL

During forming processes failure phenomena are often encountered. In the recent years several approaches have been proposed to describe fracture mechanism and to predict failure. One of them includes the numerical analysis of the forming process employing a proper damage criterion [28] and the other takes into account damage occurrence and its evolution putting damage variables in

the constitutive equations [29-32]. Set of these equations for the damaged material is written by describing a specific micromechanism of failure [33,34]. If we assume that damage is isotropic, i. e. microcracks and microvoids with an orientaion distributed uniformly in all directions, the damage state can be characterized by the scalar value D. The yield criterion under plane strain condition is

$$\left(s_\alpha - s_\beta\right)^2 + 4s_{\alpha\beta}^2 = 4q^2, \quad q = k(1-D) \tag{3.1}$$

where k is the shear yield stress of the virgin material being a function of the equivalent strain e_{eq}. The damage evolution law can be written in the form

$$\dot{D} = F\left(\sigma, D, e_{eq}\right)\dot{e}_{eq} \tag{3.2}$$

A superposed dot denotes material time derivative. Since we consider steady processes, $\dot{D} = v\,\partial D/\partial\alpha$ and equation (3.2) can be rewritten in the form

$$\partial D/\partial\alpha = h_\alpha F\left(\sigma, D, e_{eq}\right)\dot{e}_{eq}/v \tag{3.3}$$

where v is determined from (1.5) and $\dot{e}_{eq}$ from $\dot{e}_{eq} = 2\sqrt{\varepsilon_\alpha^2 + \varepsilon_{\alpha\beta}^2}/\sqrt{3}$ and (1.6). The boundary condition to this equation is usually given in agreement with some experimental observation about an initial amount of damage (or porosity) when an element enters the plastic zone [32]. Applying the associated flow rule to (3.1) and performing some transformations, one obtains $s_\alpha = -s_\beta = 2\varepsilon_\alpha k(1-D)/\left(\sqrt{3}\dot{e}_{eq}\right)$ from which it follows

$$\frac{\partial s_\alpha}{\partial\alpha} = \frac{\partial\varepsilon_\alpha}{\partial\alpha}\frac{2k(1-D)}{\sqrt{3}\dot{e}_{eq}} - \frac{2\sqrt{3}\varepsilon_\alpha}{3\dot{e}_{eq}^2}\left[\frac{\partial\dot{e}_{eq}}{\partial\alpha}k(1-D) - \dot{e}_{eq}\left(\frac{\partial k}{\partial\alpha}(1-D) - k\frac{\partial D}{\partial\alpha}\right)\right] \tag{3.4}$$

Then, substituting (3.4) into (2.6) yields

$$I_1(\alpha,\beta) = \frac{2k(1-D)}{\sqrt{3}\dot{e}_{eq}}\left[\frac{h_\beta}{h_\alpha}\frac{\partial\varepsilon_\alpha}{\partial\alpha} + 2\varepsilon_\alpha\frac{\partial\varphi}{\partial\beta}\right] - \frac{2h_\beta}{h_\alpha}\frac{\partial\varphi}{\partial\alpha}p_{\alpha\beta} - \tag{3.5}$$

$$- \frac{2\sqrt{3}\varepsilon_\alpha h_\beta}{3h_\alpha\dot{e}_{eq}^2}\left[\frac{\partial\dot{e}_{eq}}{\partial\alpha}k(1-D) - \dot{e}_{eq}\left(\frac{\partial k}{\partial\alpha}(1-D) - k\frac{\partial D}{\partial\alpha}\right)\right]$$

Thus, the system of differential equations (2.7), (2.8) or (2.9) and (3.3) where I_1 is determined from (3.5), must be solved simultaneously with respect to σ and D. After that the strain-stress state in the deforming region can be easily obtained.

4. CONCLUSION

A wide class of steady forming processes for plane-strain state has been analyzed analytically by the Hill's general method. The approach proposed has been developed for incompressible, rigid-plastic, hardening solids and handles quite a geneal history-dependent constitutive law for damage variables. The method is ideally suited for reliable calculations of internal stresses and strains. The set of differential equations from which the hydrostatic part of stress and the scalar damage variable can be calculated has been presented.

ACKNOWLEDGEMENT

The author acknowledges the support of the Russian Foundation for Fundamental Research (Grant 96-01-05017).

5. REFERENCES

1. Alexander J.M.: On Problems of Plastic Flow of Metals, *In.: Plasticity Today. Modelling and Applications,* Ed.: A.Sawczuk and G.Bianchi, Elsevier, London, 683, 1985.

2. Belytschko T., Krongauz Y., Organ D., Fleming M. and Krysl P.: Meshless Methods: An Overview and Recent Developments, *Comput. Methods Appl. Mech. Engrg.*, **139**, 3, 1996.

3. Capsoni A. and Corradi L.: A Finite Element Formulation of the Rigid-Plastic Limit Analysis Problem, *Int. J. Numer. Methods Engrg.*, **40**, 2063, 1997.

4. Hwan C.L.: An Upper Bound Finite Element Procedure for Solving Large Plane Strain Deformation, *Int. J. Numer. Methods Engrg.*, **40**, 1909, 1997.

5. Raj K.H., Fourment L., Coupez T. and Chenot J.L.: Simulations of Industrial Forging Of Axisymmetrical Parts, *Eng. Comput.*, **9**, 575, 1992.

6. Parisch H. and Lübbing C.: A Formulation of Arbitrarily Shaped Surface Elements for Three-Dimensional Large Deformation Contact With Friction, *Int. J. Numer. Methods Engrg.*, **40**, 3369, 1997.

7. Hoysan S.F. and Steif P.S.: A Streamline-Based Method for Analyzing Steady State Metal Forming Processes, *Int. J. Mech. Sci.*, **34**, No. 3, 211, 1992.

8. Szabo B.A. and Actis R.L.: Finite Element Analysis in Professional Practice, *Comput. Methods Appl. Mech. Engrg.*, **133**, 209, 1996.

9. Hill R.: A General Method of Analysis for Metalworking Processes, *J. Mech. Phys. Solids.*, **11**, 305, 1963.

10. Drucker D.C.: Coulomb Friction, Plasticity, and Limit Loads, *Trans. ASME J. Appl. Mech.*, 71, 1954.

11. Carter W.T.J.: A Model for Friction in Metal Forming, *Trans. ASME J. Eng. Mater. Techn.*, **116**, 8, 1994.

12. Collins I.F.: The Upper Bound Theorem for Rigid/Plastic Solids Generalized to Include Coulomb Friction, *J. Mech. Phys. Solids*, **17**, 323, 1969.

13. Lippmann H. and Takuda H.: On the Evaluation of the Upper-Bound Approach to Problems of Rigid-Plastic Deformation Under Non-Standard Conditions, *Int. J. Mech. Sci.*, **31**, No. 1, 63, 1989.

14. Azarkhin A. and Richmond O.: Extension of the Upper Bound Method to Include Estimation of Stresses, *Trans. ASME J. Appl. Mech.*, p. 1-6, 1991.

15. Azarkhin A. and Richmond O.: A Model of Ploughing by a Piramidal Indenter - Upper Bound Method for Stress-Free Surfaces, *Wear*, **157**, 409, 1992.

16. Druyanov B.: Technological Mechanics of Porous Bodies, Clarendon Press, New-York, 1993.

17. Collins I.F.: Boundary Value Problems in Plane Strain Plasticity, *In.: Mechanics of Solids*, Ed. H.G. Hopkins and M.J. Sewell, Pergamon Press, New York, 135, 1982.

18. Collins I.F.: The Application of Singular Perturbation Techniques to the Analysis of Forming Processes for Strain-Hardening Materials, *In.: Metal Forming Plasticity*, Ed.: H. Lippmann, Springer-Verlag, Berlin, 227, 1979.

19. Collins I.F.: Slipline Field Analysis of Forming Processes in Plane Strain and Axial Symmetry, *Proceedings of the 1st Int. Conf. on Technology of Plasticity "Advanced Technology of Plasticity"*, Ed.: H. Kudo, Japan Society Techn. Plasticity, Tokio, Vol. 2, 1074, 1984.

20. Chitkara N.R. and Butt M.A.: A General Numerical Method of Construction of Axisymmetric Slip-Line Fields, *Int. J. Mech. Sci.*, **34**, No. 11, 833, 1992.

21. Hosford W.F. and Caddel R.M.: Metal forming: Mechanics and Metallurgy, Prentice-Hall, New York, 1983.

22. Lahoti G.D. and Kobayashi S.:On Hill's General Method of Analysis for Metal-Working Processes, *Int. J. Mech. Sci.*, **16**, 521, 1974.

23. Murota T., Jimma T. and Nagamatsu A.: A Theoretical Analysis of Circular Cylinder in Axial Compression with Friction, *Proceedings of the 16th Japan National Cong. Appl. Mech*, 141,

1966.

24. Doege E. and Bagaviev A.: The Analytical Modelling of the Compacting Process of a Porous Metal Ring, *Int. J. Mech. Sci.*, **39**, No. 10, 1151-1159, 1997.

25. Alexandrov S.E. and Chikanova N.N.: Nonsteady Extrusion of a Porous Material Through a Conical Die, *Proceedings of the 13th Symposium on Engineering Applications of Mechanics "Manufacturing Science and Engineering"*, Ed.: M.A. Elbestawi, McMaster University Press, Ontario,100, 1996.

26. Alexandrov S., Chikanova N. and Vilotic D.: Analysis of Compression With Barrelling of a Block Between Cylindrical Dies, *Proceedings of the 3rd EUROMECH Solid Mechanics Conference*, Stockholm, 123, 1997.

27. Alexandrov S., Chikanova N. and Vilotic D.: Compression of a Block Between Cylindrical Dies and Its Application to the Workability Diagram, *In.: Advanced Methods in Materials Processing Defects*, Ed.: M.Predeleanu, P.Gilormini, Elsevier, Amsterdam, 247, 1997.

28. Avitzur B. and Choi J.C.: Analysis of Central Bursting Defects in Plane Strain Drawing and Extrusion, *Trans. ASME J.Engrg.Industry*, **108**, 317, 1986.

29. Gurson A.L.: Continuum Theory of Ductile Rupture by Void Nucleation and Growth: Part 1 - Yield Criteria and Flow Rules for Porous Ductile Media, *Trans. ASME J. Eng. Mater. Technol.*, **99**, 2, 1977.

30. Tvergaard V.: Influence of Void Nucleation on Ductile Shear Fracture at Free Surface, J. *Mech. Phys. Solids*, **30**, No.6, 339, 1982.

31. Needleman A. and Tvergaard V.: An Analysis of Ductile Rupture in Notched Bars, *J. Mech. Phys. Solids*, **32**, No.6, 461, 1984.

32. Alberti N., Barcellona A., Cannizzaro L. and Micari F.: Prediction of Ductile Fractures in Metal-Forming Processes: an Approach Based on the Damage Mechanics, *Annals of the CIRP*, **43**, 207, 1994.

33. Lemaitre J.: Formulation and Identification of Damage Kinetic Constitutive Equations, *In.: Continuum Damage Mechanics*, Ed.: D.Krajcinovic and Lemaitre, Springer-Verlag, Wien, 37, 1987.

34. Bonora N.: A Nonlinear CDM Model for Ductile Failure, *Engrg. Fract. Mech.*, **58**, No.1-2, 11, 1997.

PRIMENA HILOVE METODE U ANALIZI PROCESA DEFORMISANJA SA MODELOM RAZVOJA PUKOTINE

Chikanova N., Baumanov Dražavni Tehnički Univerzitet u Moskvi, Rusija

REZIME

U radu se analizira stacionarno ravansko tečenje kruto plastičnog tela sa ojačanjem. Razvoj pukotine je uzet u obzir preko modela oštećenja kontinuuma. Razvijen je jedan pristup uz pomoć Hill-ove metode u cilju dobijanja aproksimativnih jednačina koje opisuju tečenje između dve ploče. Moguće je primeniti bilo koji zakon tečenja.

Jenačine su date u obliku koji se relativno jednostavno može primeniti na konkretne slučajeve deformisanja. Metod predstavlja pouzdani način za izračunavanje unutrašnjih napona i deformacija. Prikazan je i set diferencijalnih jednačina koje omogućavaju izračunavanje hidrostatičke komponente naponskog stanja.

INSTRUCTION FOR CONTRIBUTORS

Instruction for the preparation of camera-ready papers to be published in the **Journal for Technology of Plasticity**

1. The language of the Journal is English

2. Only original papers will be accepted

3. The structure of the paper should be as follows:

- Title of paper
- Author(s) name and affiliation
- Abstract of 100-150 words
- Introduction
- Body of the paper structured in sequential headings
- Conclusion
- References

For the Yugoslav authors the summary (Rezime) in Serbian language of 400 - 600 words on separate page is required.
Summary in Serbian language for the non-Yugoslav authors will be prepared by editor.

4. SI units should be used.

The material designation should be given in American (AISI) or English standards.

5. The paper should not exceed 10 pages of A4 size (210x297 mm)

6. Format

Margins of the manuscript **must** be:

a) first page

- top 9cm
- bottom 5cm
- left and right 3.5 cm

b) other pages

- top and bottom 5cm
- left and right 3.5cm

7. Typing

a) Points:

Title of paper - **POINTS 15, BOLD, CAPITAL LETERS**

Author(s) name and abstract - *POINTS 10, ITALIC*

Headings 1 - **POINTS 12, BOLD, CAPITAL LETTERS**

Headings 2, 3 .. - **POINTS 10, BOLD, SMALL LETTERS**

Text - POINTS 10

b) Fonts:

It is required to use **TIMES NEW ROMAN**

c) Spacing

It is required to use **1.0 (single)** line spacing

8. Printing

The paper will be reproduced directly from the submitted original manuscript. It **must** be typed on a A4 paper format (210x297 mm) using a computer and a laser printer.

9. The original + one copy + a copy of the manuscript on diskette (3.5'') should be send to the following address:

Prof. Miroslav Plančak, Phd, MEng.
Univerzitet u Novom Sadu
FTN - Institut za proizvodno mašinstvo
Trg Dositeja Obradovića 6
21000 NOVI SAD
YUGOSLAVIA

Tel: ++381 21 35 01 22 ext. 250
Fax: ++381 21 54 495
E-mail: plancak@uns.ns.ac.yu
plancak@Eunet.yu